VOLATILE FUEL & ORGANIC COMPOUND PRODUCTION BY *ASCOCORYNE SARCOIDES*: EXPLORATION OF ENVIRONMENTAL VARIABLES AND ANALYTICAL METHODS

by

Natasha Dawn Mallette

A dissertation submitted in partial fulfillment
of the requirements for the degree

of

Doctor of Philosophy

in

Chemical Engineering

MONTANA STATE UNIVERSITY
Bozeman, Montana

August 2013

APPROVAL

of a dissertation submitted by

Natasha Dawn Mallette

This dissertation has been read by each member of the dissertation committee and has been found to be satisfactory regarding content, English usage, format, citation, bibliographic style, and consistency and is ready for submission to The Graduate School.

Dr. Brent M. Peyton

Approved for the Department of Chemical & Biological Engineering

Dr. Jeffrey Heys

Approved for The Graduate School

Dr. Ronald W. Larsen

STATEMENT OF PERMISSION TO USE

In presenting this dissertation in partial fulfillment of the requirements for a doctoral degree at Montana State University, I agree that the Library shall make it available to borrowers under rules of the Library. I further agree that copying of this dissertation is allowable only for scholarly purposes, consistent with "fair use" as prescribed in the U.S. Copyright Law. Requests for extensive copying or reproduction of this dissertation should be referred to ProQuest Information and Learning, 300 North Zeeb Road, Ann Arbor, Michigan 48106, to whom I have granted "the right to reproduce and distribute my dissertation in and from microform along with the non-exclusive right to reproduce and distribute my abstract in any format in whole or in part."

Natasha Dawn Mallette

August 2013

ACKNOWLEDGEMENTS

The completion of this dissertation would have not been possible without the funding I received from primarily two sources at the National Science Foundation, the Integrative Graduate Education and Research Traineeship (IGERT) program and Emerging Frontiers in Research and Innovation (EFRI), Grant No. 0937613. Also, the following people, in addition to my Bozeman family and friends, were instrumental in my graduate tenure, organized by association (past or present).

My research group members: Elle Pankratz, Dr. Robert Gardner, Dr. Brandy Stewart, Dr. Dana Skorupa, Ari Staven, Kristopher Hunt, Dr. James Folsom, Reed Taffs, Karen Moll, Hans Bernstein, Trevor Zuroff.

My colleagues in the Department of Chemical & Biological Engineering: Drs. Brent Peyton, Ross Carlson, Dr. Phil Stewart, Dr. Abigail Richards, Shelley Thomas, Jill Brenden, Dr. Jennifer Hornemann, James Conolly, Egan Lohman.

My colleagues at the Center for Biofilm Engineering: John Neuman, Smita Sutrave, Laura Bickle, Betsey Pitts, Ann Willis, Dr. Darla Goeres, Carol Leist, Tara Gunsch, Margie Hansen, Cole Kimball, Peg Dirckx, Austin Jacobs, Coltran Hophan-Nicolas, Dr. Albert Parker, Dr. Erin Field, Dr. Warren Jones, Adie Phillips, Dr. Jacob Valenzuela, Dr. Kristen Brileya, Dr. Laura Jennings, Dr. Pat Secor, Dr. Kara Bowen-DeLeon, Chris Allen, Stephen Markwardt, Dr. Mark Burr, Dr. Anne Camper.

My colleagues across campus: Dr. Gary Strobel, Eric Booth, Dr. Berk Knighton, Dr. Scott Busse, Dr. Valerie Copie, Dr. Jared Bowen, Dr. Jonathan Hilmer, Jesse Thomas.

TABLE OF CONTENTS

TABLE OF CONTENTS-CONTINUED

TABLE OF CONTENTS-CONTINUED

LIST OF TABLES

LIST OF TABLES - CONTINUED

Table Page

LIST OF TABLES - CONTINUED

Table Page

LIST OF TABLES - CONTINUED

Table Page

LIST OF TABLES - CONTINUED

Table Page

LIST OF FIGURES

LIST OF FIGURES - CONTINUED

LIST OF FIGURES - CONTINUED

LIST OF FIGURES - CONTINUED

Figure Page

LIST OF FIGURES - CONTINUED

Figure Page

LIST OF FIGURES - CONTINUED

Figure Page

ABSTRACT

Ascocoryne sarcoides is an endophytic filamentous fungus isolated from Northern Patagonia that can produce petroleum-like fuel compounds directly from cellulose (Strobel et al., 2008). The aim of this project was to study volatile organic compound production by *A. sarcoides*. The project is different from many other cellulosic biofuel projects that explore alcohol production from pre-treated biomass fermentation. It focuses on the ability of *A. sarcoides* to convert cellulose and related simple sugars to fuel-related hydrocarbons. The influence of environmental conditions on the growth characteristics and compounds produced from normal metabolic processes was explored.

Quantification of volatile production from growth on glucose showed the major compounds were ethanol and acetaldehyde, with the remainder of volatiles near 2 ppm from a continuously aerated culture. These volatiles included compounds of fuel-interest such as benzaldehyde, nonanal, 1-octen-3-ol and 1-butanol, 3-methyl-. Notable compounds with fuel related properties included isopentane, d-limonene, and cyclopropane, propyl-. These compounds all have octane ratings greater than 90 and enthalpies of combustion greater than 3200 kJ mol^{-1}. Oxygen availability influenced the type and number of volatile compounds produced. For example, growth on a soluble cellulose substrate produced greater numbers of volatile compounds at oxygen limited concentrations and more alcohols, alkanes, aromatics, ketones, and esters were identified from mass spectrometry data. In addition, the oxygen availability influenced growth characteristics with a starting oxygen concentration of 7% was low enough to greatly inhibit growth. The growth substrate had a marked influence on the volatile compounds produced. *A. sarcoides* growth on microcrystalline cellulose produced a greater variety of hydrocarbon compounds compared to growth on glucose, and the highest yield of volatile organics was estimated at 105 mg (g biomass)$^{-1}$ from the cellulose substrate.

The fungus *A. sarcoides* demonstrated production of valuable fuel compounds on multiple carbon sources. Further work should carry on the analysis of culturing conditions and include evaluation of hydrocarbon yields on pre-treated cellulosic biomass. Studies of this nature should continue to advance knowledge of fungal biological potential for industrial processes.

CHAPTER 1

PROJECT INTRODUCTION & GOALS

Significance

Ascocoryne sarcoides (NRRL 50072) is a cellulolytic fungal endophyte capable of converting cellulosic materials to fuel-related hydrocarbon compounds such as alkanes, alcohols and aromatics (Figure 1.1) (Griffin et al., 2010; Strobel et al., 2008). Some of the volatile organic compounds (VOC) produced are equivalent to compounds in diesel fuel such as 1,3 dimethyl benzene, 1-octene and 3-methyl nonane (Mallette et al., 2012). Therefore, the volatiles from *A. sarcoides* have been termed Mycodiesel® (Strobel et al., 2008). The ability of *A. sarcoides* to produce such compounds on a variety of substrate sources including cellulose has been demonstrated (Griffin et al., 2010; Strobel et al., 2008).

The vision for *A. sarocoides* and other similar organisms is the consolidated conversion of cellulosic materials to fuel-related hydrocarbon compounds such as alkanes, alcohols and aromatics (Griffin et al., 2010; Strobel et al., 2008). Ideally, a sustainable process for producing drop-in replacement transportation fuels for diesel and/or gasoline could become a reality with the help of studies on fungi like *A. sarcoides*.

This project sought to understand some of the factors which influence VOC production by *A. sarcoides*, not in the hope of direct commercialization, but to improve the knowledge of fungal VOC and to gain insight into possible solutions for producing biofuels. Potentially, the knowledge and methods developed could be applied to other

fungal strains. The main goal of this project was to gain fundamental bioprocess knowledge about VOC production by *A. sarcoides*. As a direct result, analytical techniques previously employed to study these systems were found to have major limitations for this type of work. Hence, analytical improvements were made, and new methods for analyzing the data were developed to obtain more accurate and applicable information about the fungal system and VOC production.

Figure 1.1. *A. sarcoides* colonizing a saw-dust flake from a pine beetle-killed conifer tree. The image was taken at the Imaging and Chemical Analysis Laboratory (ICAL) at Montana State University using SE-FEM with iridium coating and a SE2 detector at a magnification of 5000X.

Background

Energy Market

In 2010, 72% of the world's energy came from fossil fuels, including coal, crude oil and natural gas. The remainder originates from industrial and municipal wastes, biofuels, geothermal, nuclear, hydroelectric, wind and solar sources. The great majority of U.S. transportation fuels comes from oil and accounted for 62% of the total world oil usage in 2010 (International Energy Agency, 2012). At the end of 2012, the U.S. used an average of 13 million barrels of petroleum per day for transportation fuels. This number has been increasing steadily since the 1970's (U.S. Energy Information Administration, 2013).

The increased use of petroleum has negative implications for human health from air and water contamination and environmental stability due to increased carbon dioxide emissions, as well as geopolitical stability issues around the world. The U.S. Energy, Independence and Security Act (EISA) of 2007 set a goal of increasing biofuels added to gasoline to 36 billion gallons per year by 2022, and specifically 250 million gallons per year of cellulosic biofuel by 2022 (Yacobucci and Schnepf, 2007).

Biofuels

Biofuels are fuels created from biological material with or without biological processes. Organisms can convert renewable carbon into fuel or fuel precursors through many strategies. An example is photoautotrophic organisms reducing CO_2 with energy from light, such as algae and plants. Heterotrophic organisms, such as bacteria, yeast, and

fungi, catabolize organic carbon, often from photoautotrophs, through fermentative or aerobic respiration processes.

Producing biofuels on a scale that will influence global markets is a major challenge. Ethanol, despite its relatively low energy density, was once thought to be able to meet demand for local and sustainable fuel, but that is now considered unrealistic (Wald, 2007). Biofuels that are a direct replacement for current petroleum fuels will have higher energy density and other advantages over ethanol, which cannot be used in existing distribution networks or current engine designs. Sometimes called "green" gasoline (or "green diesel"), these fuels can often preserve the fuel efficiency of existing engine designs (Regalbuto, 2009). Therefore, finding methods to create drop-in replacement fuels is paramount. A well-studied strategy for green gasoline is biodiesel from algal lipids, and a promising possibility is to create a bioprocess to convert cellulose directly to fuel compounds using organisms such as *A. sarcoides*.

Cellulosic Biofuels

Large volumes of sustainable biofuels with low cost will likely use cellulosic biomass as feedstock (Dale and Ong, 2012; Perlack et al., 2005), essentially converting atmospheric carbon from CO_2 sequestered while the biomass was growing into fuel hydrocarbons. Use of local feedstocks would reduce the dependence of our nation on imported petroleum for liquid fuel and also reduce the total amount of carbon being released into the atmosphere (Carroll and Somerville, 2009; Xu et al., 2009). Therefore, finding a process which can use local cellulosic biomass feedstocks for regional fuel

production is invaluable to bringing the U.S. closer to the production goals of EISA. An illustration of such a potential process is shown in Figure 1.1, where *A. sarcoides* has colonized a saw-dust particle from a local conifer tree.

Currently, commercial hydrocarbon yields from cellulosic feedstocks are achieved through chemical, not biological, processes such as Fischer-Tropsch synthesis, gasification, and hydrotreating (Regalbuto, 2009). Advances in genetic annotation, synthetic biology and metabolic engineering have given us new tools for achieving production goals and improving yields of valuable metabolites and by-products. The discovery or construction of biofuel synthesis pathways is one of the first tasks required to make biofuels economically viable (Lee et al., 2008). An efficient way to gain insight into how metabolic engineering could improve yields of by-products is mathematical modeling of metabolic adaptations to environmental stressors through metabolic pathway construction (Carlson and Taffs, 2010). Laboratory scale studies record microbial responses to environmental conditions such as pH, temperature, and limited nutrients, allowing stoichiometric models of metabolism to be built. Model inputs can be adjusted to learn how metabolic resources are allocated among the microbial reactions.

The Role of Fungi

Fungi are universal in the environment and possess biochemical pathways to convert a plethora of nutrient sources to secondary metabolites. These metabolites can be life-saving such as in the case of penicillin or they can have fuel potential, such as the isoprenoid farnesene produced by *Saccharomyces cerevisiae* (Keller et al., 2005; Rude

and Schirmer, 2009). Fungi are known to produce medium to long chain hydrocarbons, and the prevalence of these compounds is in the C_{19}-C_{30} chain length (Ladygina et al., 2006). The variety of biochemical pathways in the fungal kingdom gives fungi great potential for applications in biotechnology.

A. sarcoides was first isolated by Professor Gary Strobel from *Eucryphia cordifolia*, a tree known locally as ulmo in Northern Patagonia. As an endophyte, *A. sarcoides* lives within the intracellular tissue of its host. It is theorized that endophytes grow in symbiosis within their hosts, and the compounds they produce serve the host by defending it from pathogenic strains of bacteria or fungi. The unique properties of endophytes make them of interest for applications in antimicrobials, amino acids and other industrial relevant products (Stinson et al., 2003; Suryanarayanan et al., 2009; Zhi-Lin et al., 2012).

Submerged cultivation of fungi has been used by the agriculture, food and medical industries. Most large-scale systems operate with submerged cultures, so this method is a natural extension for exploring characteristics of *A. sarcoides*. Within submerged cultures, careful study of pH should be undertaken with fungi, as it can impact enzyme systems and surface metabolic reactions (Cochrane, 1963). Temperature studies are also important as temperature impacts all of the organism's activities, such as growth, spore germination and reproduction (Cochrane, 1963). Fungi generally have a necessary but low oxygen demand for growth. Most fungi are obligate aerobes, but many exceptions have been discovered which are able to function as facultative anaerobes (Griffin, 1994).

Microbial utilization of cellulose as a carbon source requires production of cellulase enzymes. The genes responsible for cellulases in *A. sarcoides* were expressed when grown on cellobiose and cellulose but not when grown on a non-cellulose medium (Gianoulis et al., 2012). The production of cellulases in liquid culture by other filamentous fungi like *Aspergillus fumigatus* can be influenced by carbon source, pH, and temperature (Stewart and Parry, 1981). These environmental factors can influence gene expression and metabolic pathways, impacting the final products from growth. Therefore, this project investigated how environmental factors influenced the production of volatiles on cellulose substrates. A visualization of *A. sarcoides* growing on microcrystalline cellulose is shown by Figure 1.2; the particles are well-integrated with the fungal hyphae improving the proximity of released cellulose enzymes and cellulosic substrate.

Analytical Methods & Considerations

Previous studies have identified a variety of compounds produced by *A. sarcoides* on different media (Griffin et al., 2010; Strobel et al., 2008). The methods inlcuded using discrete solid phase microextraction (SPME) fibers to sample the headspace of cultures and then measure the adsorbed compounds with gas chromatography-mass spectrometry (GC-MS). To accurately measure the volatiles produced by *A. sarcoides*; multifaceted analytical methods were needed. The SPME technique was introduced in the 1990's (Arthur and Pawliszyn, 1990), and SPME fibers have been used to identify and quantify

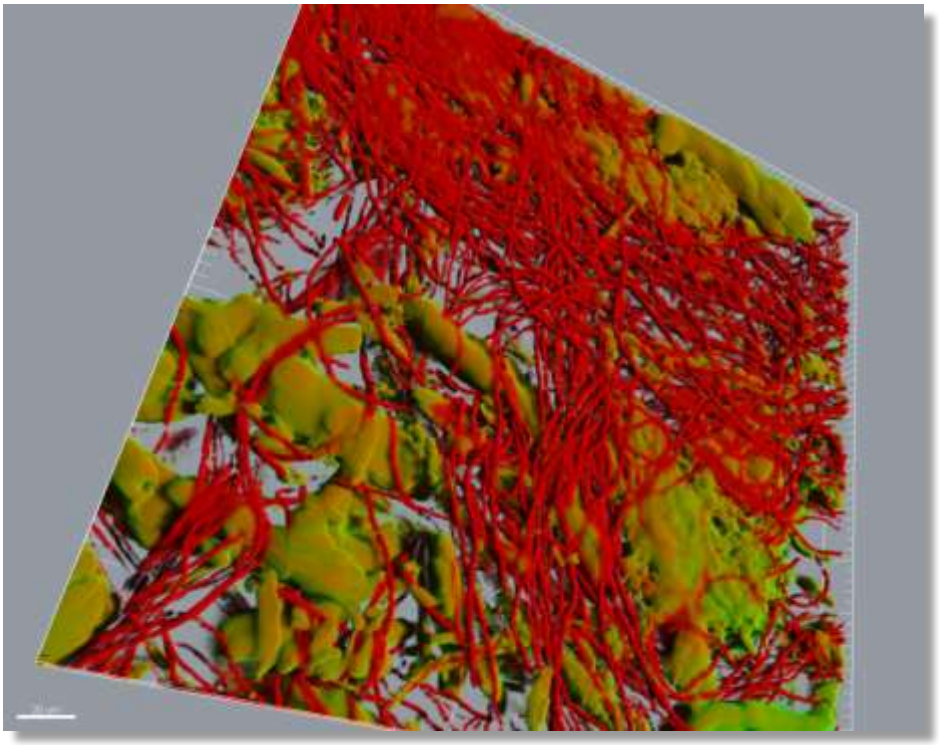

Figure 1.2. *Ascocoryne sarcoides* (red), a filamentous fungus, growing on microcrystalline cellulose (green), imaged with confocal scanning laser microscopy. Sample was taken from aerobic shake flask with liquid medium. Hyphae tangle and confine cellulose particles while consuming them to produce fuel-like hydrocarbon compounds.

complex volatile mixtures, including hydrocarbons from water, soil, food and wine (Langenfeld et al., 1996; Mallouchos et al., 2002; Parkerton et al., 2000; Robinson et al., 2011). The advantages of the method include minimizing systematic errors with extraction of volatiles, eliminating the need for solvents (Wercinski, 1999), and being simple, fast and relatively sensitive (Pawliszyn and Smith, 1999). However, several studies have revealed quantification errors with this method (Brás et al., 2011; Weldegergis et al., 2011; Zeng and Noblet, 2002), so further evaluation of the quantitative use of the method for volatile mixtures from *A. sarcoides* was tested.

The analytical method proton transfer reaction-mass spectrometry (PTR-MS) has been used to monitor volatile organic compounds (VOCs) emitted from plants, bacteria and subterranean fungi (Aprea et al., 2007; Aprea et al., 2009; Bäck et al., 2010; Bunge et al., 2008; Ezra et al., 2004; Insam and Seewald, 2010; Kai et al., 2010; Maleknia et al., 2007; Ramirez et al., 2009; Steeghs, 2004; Tomsheck et al., 2010). These studies often employed solid substrata, rarely included submerged liquid fungal cultivation (Bäck et al., 2010), and collected data at discrete time points. An advantage of PTR-MS is that it can be run in real time to continuously collect data on the concentrations of specific compounds (Ezra et al., 2004; Lindinger et al., 1998; Tomsheck et al., 2010). PTR-MS is primarily a quantitative tool and generally requires a detailed knowledge of the components present to be successfully employed. Ion mass (as measured by a quadrupole mass spectrometer) is not a unique indicator of chemical composition. For instance, an ion at m/z 107 can represent either $C_8H_{10}H^+$ (ethylbenzene or xylene isomer) or $C_7H_6OH^+$ (benzaldehyde). Beyond the identification of a few small molecules, such as acetaldehyde and methanol, interpretation of the PTR-MS measurements of complex VOC mixtures benefits from the support of another separation technique to provide identification of components.

SPME GC-MS has been combined with PTR-MS to better elucidate VOCs from plants (Aprea et al., 2009; Bouvier-Brown et al., 2007; Ruth et al., 2005) and human lungs (Bajtarevic et al., 2009; King et al., 2010). These studies showed the combined techniques allowed for both qualitative and quantitative determinations of VOCs. The use of SPME in conjunction with PTR-MS added qualitative value to the interpretation of the

PTR-MS data and strengthened the information obtained from experimentation, particularly as it applied to biological metabolic processes. The knowledge of compounds present obtained by SPME allowed elucidation of the most probable sources assigned to ions measured by the PTR-MS.

Volatile sampling with external adsorbents is a technique similar to SPME, but generally, the volume of adsorbent is larger. The method can be used passively (no air flow) as with typical household radon detection kits, or actively with a flow of gas. Passive sampling of this type has been used to measure the volatiles from many fungal species including *Penicillium* spp., *Aspergillus* spp. and *Cladosporium cladosporoides* (Matysik et al., 2009). Booth et al. (2011) demonstrated an active use of this technique for 1,8-cineole collection from *Hypoxylon* sp fungal cultures using Carbotrap adsorbent materials (Supelco, Bellefonte, PA). The Carbotrap adsorbents are graphitized carbon black materials which are non-porous and exhibit hydrophobic surfaces; therefore, water adsorption is low. Surface interactions of volatiles with the material depend upon dispersion or London forces allowing volatiles to be effectively trapped in high humidity systems. Carbotrap B is designed for lower molecular weight volatiles from C_4-C_{14} in carbon length, and Carbotrap C is designed for higher molecular weight volatiles from C_8-C_{20} (Hewitt, 1998).

Nuclear magnetic resonance (NMR) is a robust analytical method with many applications. It has been used to characterize many fractions of petroleum crude oils, coal and shale-derived distillate fuels (Silva et al., 2011). The technique can be used to distinguish the structures of molecules, determine the molar content of constituents, and

the number of carbon atoms per molecule. NMR has been successfully used to study 3-octanone and related octane derivatives from *Myrothecium inundatum*, a fungal endophyte (Banerjee et al., 2010).

Extractions of liquids to measure volatile components are time-honored techniques with many established standardized methods published by the U.S. Environmental Protection Agency including 550, 3510C, 3520C (Treybal, 1959). However, the method requires large volumes of culture liquid on the order of a liter per sample, is time intensive and requires significant volumes of solvent to implement.

Volatile Fuel Properties

Ignition testing is used to evaluate fuel characteristics of petroleum fuels. The ignition properties of petroleum fuel are characterized by the research octane number (RON) and the cetane number (CN) for gasoline and diesel fuel, respectively. The RON simulates fuel performance under low severity engine operation and is governed by a standard from the American Society for Testing and Materials (ASTM), ASTM D-2699, IP 237. While another fuel indicator, motor octane number (MON) simulates more severe operation that might be incurred at high speed or high load and is governed by ASTM D-2700, ASTM D-2885, IP 236 (Speight, 2002). The octane number (ON) of gasoline at the pump is generally reported as the average of the RON and MON. A compound with a high ON tends to have a low cetane number. The scales of each generally range from zero to 100 (Nag, 2008). For gasoline, straight chained hydrocarbons without branching have a low RON, but high CN if they have long enough carbon length, around 12

carbons. For example, a straight chained HC with 16 carbons has a CN of 100. The CN is determined by a standard engine test (ASTM D613) which measure the ignition quality of the fuel (Ghosh and Jaffe, 2005). In general, increased methyl branching of an alkane or carbon double bonding increases a compound's ON (Lee et al., 2008). Many compounds found in petroleum fuel do not have published experimental data for ON or CN, so models have been developed to estimate values based on chain length and structures (Ghosh et al., 2005; Ghosh and Jaffe, 2005).

The amount of energy contained by a gasoline fuel can be quantified by the heat or enthalpy of combustion (ΔH_{comb}). This property impacts the economics of engine performance. Fuel requirements are a compromise between maximum fuel availability and good fuel consumption characteristics (Speight, 2002). Therefore, both ONs and heats of combustion will be combined to estimate the fuel potential of identified volatile compounds.

Summary

Replacing petroleum fuels with biofuels is a large undertaking, one whose success is dependent upon the efficient use of cellulosic biomass. Fungi have potential to use the sugars in cellulosic biomass and convert them to petroleum-like fuels. Studying *A. sarcoides* and its ability to produce petroleum-like compounds have yielded insights that could contribute to the eventual replacement of petroleum fuels. Analyzing the methods to apply to this new field of fungal biofuels is a valuable component that streamlines other research in the field.

Dissertation Summary and Outline

The following chapters of this dissertation describe work completed to characterize the factors which influence volatile production by *A. sarcoides* and include an in-depth analysis of the methods used to measure and quantify the VOC. A brief summary of each chapter's technical content is listed below.

Chapter 2: Resolution of volatile fuel compound profiles from *Ascocoryne sarcoides*: a comparison by proton transfer reaction-mass spectrometry and solid phase microextraction gas chromatography-mass spectrometry. This chapter addresses the existing technology used for reporting VOC production by fungi and yeasts. Before accurate VOC quantification could be undertaken, the applicability of HS-SPME to the system was determined. Although HS-SPME is frequently used to quantify volatiles from complex systems such as fungi like *A. sarcoides* (Ahamed and Ahring, 2011; Aulakh et al., 2005; Strobel et al., 2008), Chapter 2 clearly shows that higher molecular weight compounds are in general preferentially adsorbed and quantified by this method therefore overpredicts their abundance. For alcohols in the fungal headspace environment, there was a reasonable correlation with PTR-MS measurements. Chapter 2 quantified many of the volatile compounds produced by *A. sarcoides* and determined that when grown on glucose under the given conditions, ethanol and acetaldehyde were the dominate volatiles produced. The effectiveness and limitations of HS-SPME for the headspace of *A. sarcoides* cultures were demonstrated.

Chapter 3: Evaluation of cellulose as a substrate for hydrocarbon fuel production by *Ascocoryne sarcoides* (NRRL 50072). Specifically, Chapter 3 shows an in depth comparison of VOC production based on growth substrate and culturing conditions. Gasoline, aviation and diesel fuel relevant hydrocarbons were produced on all substrates tested. The culture's medium concentration and headspace oxygen concentration had an impact on VOC production, but a significant impact was not seen with temperature, pH or age of the culture. An interesting metabolic shift was seen in late stationary phase whereby conversion of non-oxygenated VOC (i.e. 1-heptene, 6-methyl-) to their oxidized form (i.e. 2-heptanone, 6-methyl-) was observed. It is theorized that this process is thermodynamically favorable to the organism because it generates electrons. The compounds with fuel potential were numerous, and included alcohols, ketones and aromatics, which can be directly used or refined for use in fuel blends. Additional analysis of VOC applicability to hydrocarbon fuel showed *A. sarcoides* produced relevant fuel-related hydrocarbons on cellulose with an average research octane number of 66 for the non-oxygenated hydrocarbons. These compounds included isopentane, 3,3-dimethyl hexane and d-limonene. Quantification of the overall capacity of *A. sarcoides* cultures for gasoline range organics (GRO) and diesel range organics (DRO) was achieved by liquid-liquid extractions and the highest results were 1.1 mg GRO per g biomass for glucose medium growth and 45 mg DRO per g biomass for cellulose medium growth. An image of *A. sarcoides* growth on microcrystalline cellulose particles is seen in Figure 1.2. This chapter demonstrates the effectiveness of combining multiple analytical techniques to the analysis of VOC produced by *A. sarcoides*.

Chapter 4: Oxygen availability and the impact on fuel-related hydrocarbon and lipid production by *Ascocoryne sarcoides*. This chapter exhibits a detailed study on the impact of headspace oxygen concentration on VOC production by *A. sarcoides* and also explores the lipid biofuel potential of the final fungal culture. The oxygen available to *A. sarcoides* impacted the type and distribution of VOC detected as well as growth. For sealed batch growth, the lowest starting oxygen concentration, 7%, had the highest number of alkanes and alcohols despite having the lowest final biomass density. Starting the oxygen concentrations below 21% had around three times more VOC of interest than at the 21% oxygen concentration. Variations in lipid composition based on starting oxygen concentrations were seen. The 10% oxygen concentration had nearly double the level of total neutral lipids and fatty acid methyl esters than 21% starting oxygen concentration. This led to a total biofuel production potential of 7.5±0.9% g lipid per g biomass at 10% starting oxygen concentration compared to 4.1±0.3% g lipid per g biomass at 21% starting oxygen concentration. There was also a fermentative metabolic shift observed under limited oxygen conditions which produced acetate and ethanol concentrations not found in the 21% starting oxygen concentration environment.

The bulk of this dissertation was supported by the studies highlighted in Appendix A, Preliminary Methods Development with *Ascocoryne sarcoides*. These studies were not published but formed the foundation for work in the main body of the dissertation, by allowing consistent laboratory growth to be achieved and reasonable biomass levels for analytic methods. Studies highlighted in Appendix A include extensive medium development for liquid cultures of *A. sarcoides* on a variety of carbon sources,

exploration of additional nutrients and pH buffers and the impact of light on the growth of *A. sarcoides*. The information gained about *A. sarcoides* respiration from larger-scale reactor studies like the ones included in Chapter 2 is also discussed in the Appendix. The Appendix also expands upon glucose and cellulose growth kinetics included in the main body of the dissertation. In addition, a carbon balance on an *A. sarcoides* system is discussed and shows the variations measured among reactor runs. The specific oxygen consumption rates are highlighted as they indicate oxygen limitation stress for *A. sarcoides* at low pH values near 3.

Each chapter in this dissertation addresses a different aspect of this project and has improved the knowledge of the field in a unique way. The technical chapters are composed of an abstract, introduction, methods, discussion of results and conclusion sections. A conclusion chapter follows the technical chapters, and then a final reference list combines the references from all chapters. The Appendices include relevant results which were obtained in support of the technical chapters and the overall goals of the project (Appendix A) as well as tabulated data of technical chapter figures (Appendix B).

CHAPTER 2

RESOLUTION OF VOLATILE FUEL COMPOUND PROFILES FROM *ASCOCORYNE SARCOIDES*: A COMPARISON BY PROTON TRANSFER REACTION-MASS SPECTROMETRY AND SOLID PHASE MICROEXTRACTION GAS CHROMATOGRAPHY-MASS SPECTROMETRY

Contribution of Authors and Co-Authors

Manuscript in Chapter 2

Author: Natasha D. Mallette

Contributions: Designed the study, collected and analyzed data, and wrote the manuscript.

Co-author: W. Berk Knighton

Contributions: Collected and analyzed data, assisted with study design, discussed the results, commented and edited the manuscript.

Co-author: Gary A. Strobel

Contributions: Assisted with study design and edited the manuscript.

Co-author: Ross P. Carlson

Contributions: Assisted with study design and edited the manuscript.

Co-author: Brent M. Peyton

Contributions: Designed the study, discussed the results and implications, and edited the manuscript.

Manuscript Information Page

Natasha Mallette[1,2], W. Berk Knighton[3], Gary A. Strobel[4], Ross P. Carlson[1,2], Brent M. Peyton[1,2#]

Journal Name: AMB Express (SpringerOpen)
Status of Manuscript:
____Prepared for submission to a peer-reviewed journal
____Officially submitted to a peer-reviewed journal
____Accepted by a peer-reviewed journal
__x_Published in a peer-reviewed journal
Published online 05 April 2012

[1]Department of Chemical and Biological Engineering, Montana State University, Bozeman, MT 59717, USA
[2]Center for Biofilm Engineering, Montana State University, Bozeman, MT 59717, USA
[3]Department of Chemistry and Biochemistry, Montana State University, Bozeman, MT 59717, USA
[4]Department of Plant Sciences, Montana State University, Bozeman, Montana 59717, USA.

[#]Corresponding author: BPeyton@coe.montana.edu

Abstract

Volatile hydrocarbon production by *Ascocoryne sacroides* was studied over its growth cycle. Gas-phase compounds were measured continuously with a proton transfer reaction-mass spectrometry (PTR-MS) and at distinct time points with gas chromatography-mass spectrometry (GC-MS) using head space solid phase microextraction (SPME). The PTR-MS ion signal permitted temporal resolution of the volatile production while the SPME results revealed distinct compound identities. The quantitative PTR-MS results showed the volatile production was dominated by ethanol and acetaldehyde, while the concentration of the remainder of volatiles consistently reached 2,000 ppbv. The measurement of alcohols from the fungal culture by the two techniques correlated well. Notable compounds of fuel interest included nonanal, 1-octen-3-ol, 1-butanol, 3-methyl- and benzaldehyde. Abiotic comparison of the two techniques demonstrated SPME fiber bias toward higher molecular weight compounds, making quantitative efforts with SPME impractical. Together, PTR-MS and SPME GC-MS were shown as valuable tools for characterizing volatile fuel compound production from microbiological sources.

Keywords

biofuel, solid phase microextraction, proton transfer reaction-mass spectrometry, volatile organic compounds, fungal hydrocarbons, gas chromatography-mass spectrometry

Introduction

Ascocoryne sarcoides is an endophytic fungus recently isolated from Northern Patagonia and has the potential to produce a petroleum-like fuel (Mycodiesel®) directly from a cellulose fermentation process (Strobel et al., 2008). Fungi produce medium to long chain hydrocarbons, and the prevalence of these compounds is in the C_{19}-C_{30} chain length (Ladygina et al., 2006). In contrast, *Ascocoryne sarcoides* (NRRL 50072) has been reported to produce a series of straight chained and branched medium chain-length hydrocarbons of C_5-C_{10} chain length, in the range of gasoline fuel, including heptane, 2-pentene, octane, 1-methyl-cyclohexene, 3,5-octadiene, and cyclodecene (Griffin et al., 2010; Solomons and Fryhle, 2002). This interesting metabolism requires further work to characterize growth patterns and develop the organism for potential biofuel applications.

Recent studies have identified a variety of compounds produced by *A. sarcoides* on different media using headspace GC-MS on discrete solid phase microextraction (SPME) fiber samples (Griffin et al., 2010; Strobel et al., 2008). The SPME technique was introduced in the 1990's (Arthur and Pawliszyn, 1990), and SPME fibers have been used to identify and quantify complex volatile mixtures including hydrocarbons from water, soil, food and wine (Langenfeld et al., 1996; Mallouchos et al., 2002; Parkerton et al., 2000; Robinson et al., 2011). Its advantages include minimizing systematic errors with extraction of volatiles, eliminating the need for solvents (Wercinski, 1999), and being simple, fast and relatively sensitive (Pawliszyn and Smith, 1999). However, several studies have revealed instabilities with quantification by this method (Brás et al., 2011;

Weldegergis et al., 2011; Zeng and Noblet, 2002), so further evaluation of the quantitative use of the method for volatile mixtures from *A. sarcoides* was tested.

Another analytical method with potential for analyzing biofuels, proton transfer reaction-mass spectrometry (PTR-MS) has been used to monitor volatile organic compounds (VOCs) emitted from plants, bacteria and subterranean fungi (Aprea et al., 2007; Aprea et al., 2009; Bäck et al., 2010; Bunge et al., 2008; Ezra et al., 2004; Insam and Seewald, 2010; Kai et al., 2010; Maleknia et al., 2007; Ramirez et al., 2009; Steeghs, 2004; Tomsheck et al., 2010). These studies often employed solid substrata, rarely included submerged liquid fungal cultivation (Bäck et al., 2010), and collected data in discrete time points. To our knowledge, however, no studies have used PTR-MS to investigate the continuous evolution of volatile organic fuel compounds from a submerged liquid fungal culture over its entire growth cycle.

An advantage of PTR-MS is that it can be run in real time to continuously collect data on the concentrations of specific compounds (Ezra et al., 2004; Lindinger et al., 1998; Tomsheck et al., 2010). PTR-MS is primarily a quantitative tool and generally requires a detailed knowledge of the components present to be successfully employed. Ion mass (as measured by a quadrupole mass spectrometer) is not a unique indicator of chemical composition. For instance, an ion at m/z 107 can represent either $C_8H_{10}H^+$ (ethylbenzene or xylene isomer) or $C_7H_6OH^+$ (benzaldehyde). Beyond the identification of a few small molecules, such as acetaldehyde and methanol, interpretation of the PTR-MS measurements of complex VOC mixtures benefits from the support of another separation technique to provide identification of components.

SPME GC-MS has been combined with PTR-MS to better elucidate VOCs from plants (Aprea et al., 2009; Bouvier-Brown et al., 2007; Ruth et al., 2005) and human lungs (Bajtarevic et al., 2009; King et al., 2010). These studies showed the combined techniques allowed for both qualitative and quantitative determinations of VOCs. The use of SPME in conjunction with PTR-MS added qualitative value to the interpretation of the PTR-MS data and strengthened the information obtained from experimentation, particularly as it applied to biological metabolic processes. The knowledge of compounds present obtained by SPME allowed elucidation of the most probable sources assigned to ions measured by the PTR-MS.

Here, PTR-MS was combined with headspace SPME GC-MS to explore the applicability of both methods for time-course resolution and quantification of volatiles emitted over the culture cycle of *A. sarcoides*. We present the results of the continuous PTR-MS method as compared with those of discrete headspace SPME GC-MS for monitoring the activity of a novel fungal culture and show both the benefits and shortcomings of each technique.

Materials and Methods

Culture Medium and Conditions

Ascocoryne sarcoides (NRRL 50072) was provided by Dr. Gary Strobel and grown in a Biostat B Twin Plus 5-liter jacketed reactor (Sartorius Stedim Biotech) on a minimal medium consisting of (per liter): glucose (20 g), ammonium chloride (5 g), $NaH_2PO_4 \cdot 2H_2O$ (2.75 g), $MgSO_4 \cdot 7H_2O$ (0.86 g), $Ca(NO_3)_2 \cdot 4H_2O$ (.28 g), yeast extract

(0.05 g), and trace salts: KCl (60 mg), KNO_3 (80 mg), $FeCl_3$ (2 mg), $MnCl_2$ (5 mg), $ZnSO_4$ (2.5 mg), H_3BO_3 (1.4 mg), and KI (0.7 mg). The minimal medium was used, in contrast to a more nutrient rich one, to minimize the amount of volatile compounds originating from the medium. An un-inoculated control reactor was run to account for background VOCs resulting from the medium constituents or air supply. Both vessels were sparged with air from compressed air cylinders at 1.5 L/min. This sparge air was humidified prior to introduction into the Biostat to minimize evaporative losses. The pH was controlled at 4.5 with 2 M HCl, 2 M NaOH and was continuously monitored by an internal Hamiltion Easyferm Plus probe. In addition, the stir rate (250 rpm) and temperature (23^{o}C) were held constant by the Biostat control system. The reactor gaseous effluent was sent to the PTR-MS and an off-gas analyzer for O_2 and CO_2 measurements.

Accumulation of *A. sarcoides* was analyzed through daily samples of cell dry weight, where samples were filtered onto glass fiber filters (Whatman GF/F), rinsed, and dried overnight in an oven at 80^{o}C. Once removed from the oven, filters were allowed to equilibrate at room temperature in a desiccator and then weighed. Daily glucose concentrations were measured by High Performance Liquid Chromatography (HPLC), Agilent 1200 using an Aminex HPX-87H ion exclusion column at 45^{o}C with 0.005 M H_2SO_4 eluent.

Quantification of Volatiles by PTR-MS

Proton transfer reaction-mass spectrometry (PTR-MS) was used to quantify a selected set of volatile compounds produced by *A. sarcoides* by constantly monitoring the

gaseous effluent from the cultured reactor into the stationary phase of growth. The PTR-MS instrument ionized organic molecules in the gas phase through their reaction with H_3O^+, forming protonated molecules (MH^+, where M is the neutral organic molecule) and fragment ions ,which were detected by a standard quadrupole mass spectrometer. This process can be used with volatiles in air with or without dilution, since the primary constituents of air (nitrogen, oxygen, argon and carbon dioxide) have a proton affinity less than water and thus are not ionized. Most organic molecules (excepting alkanes) have a proton affinity greater than water and are therefore ionized and detected (Lindinger et al., 1998).

The cultured and un-inoculated controls were analyzed by diverting a portion of the reactor effluent gas to the PTR-MS. Measurements were made from the initial inoculation until 18.5 days. At times, the gas stream was diluted with additional air to prevent premature degradation of the MS detector and keep measurements within the linear dynamic range of the PTR-MS. During dilution periods, the dilution stream was added to the reactor effluent stream and balanced with the effluent flow rate using flow controllers. Sample lines were constructed from PFA Teflon tubing and stainless steel fittings. Mass spectral scans were acquired from 20 to 220 amu at 0.5 sec/amu.

The absolute concentration of constituents in a sample were quantified directly from the measured ion intensities using the known reaction time and the theoretical reaction rate constant for the proton transfer reaction (Lindinger et al., 1998). Concentrations reported within were derived from the PTR-MS measurements and calculated using equations derived from reaction kinetics, assuming a reaction rate

coefficient of 2×10^{-9} ml s^{-1} which is appropriate for the measured compounds (Ezra et al., 2004; Lindinger et al., 1998). This method provided a means by which the measured ion intensity at any mass can be expressed as an equivalent estimate of concentration.

The total VOC concentration produced by the fungal culture is taken as the difference between the fungal culture and the control measurements. This total reflects only the contribution from those species having proton affinities greater than that of water, which is assumed to represent the majority of the VOCs produced.

Volatile Analysis with SPME GC-MS

Solid phase microextraction (SPME) was used to identify gaseous compounds as described previously (Griffin et al., 2010), but a brief description of the relevant details is provided here. Throughout the growth period, 12 mL of *A. sarcoides* culture was aseptically removed, sealed, centrifuged at 4,000 rpm for 4 minutes, then 10 mL of supernatant was added to a GC vial and stored at 4°C until analysis. For analysis, the SPME fiber (divinylbenzene/Carboxen on polydimethylsiloxane by Supelco) (Bellefonte, PA) was exposed to the vial headspace while the sample was stirred for 45 minutes. The fiber was inserted into the injection port of the GC at 240°C. The GC temperature was held at 40°C for 2 minutes, and then ramped to 230°C at 5°C min^{-1}. The mass spectrometer was tuned to meet EPA Method 8260 BFB tuning criteria. The relative amount of identified compounds was estimated by comparison with a 4-bromofluorobenzene internal standard calibration curve delivered in methanol over the concentration range of 2 to 75 µg/mL.

The quantities of volatiles desorbed from the fiber were calculated from the peak area of the total ion current measured by the mass spectrometer. This method assumed that fungal VOCs and the internal standard have the same gas-liquid partitioning, efficiency of adsorption to the fiber, and response in the GC-MS system as that of the internal standard. As will be shown later, all of these conditions are not met, and the quantities obtained are estimates. Nevertheless, the use of the internal standard allowed for a relative quantitative comparison between samples from the same culture across a time period. Data acquisition and data processing were performed on Hewlett Packard ChemStation software system. The identification of compounds produced by *A. sarcoides* was made via library comparison using the National Institute of Standards and Technology (NIST) database, and all chemical compounds described in this report use the NIST Chemistry WebBook terminology (Linstrom and Mallard 2011). When the library identified multiple compounds as matches, careful consideration of the spectra yielded one with much higher similarity or a determination of "unknown" was made.

Henry's Law Constants

To characterize the headspace concentration response to a specific set of compounds at known initial concentrations using the PTR-MS and the SPME technique, a known mixture (Table 2.1) was introduced into the Biostat reactor system. The reactor was sparged with humidified air at 1.5 L/min, equivalent to that employed for the culturing conditions. Temperature (23^{o}C) and stir rate (250 rpm) were held constant by the Biostat control system. A portion of the gaseous reactor effluent was diverted to the

PTR-MS to measure effluent volatile concentrations over a time period of 48 hours to determine the Henry's Law constants for each volatile compound. Liquid aliquots were removed from the reactor at 0, 1, 2, 3, 6, 12, 24, and 48 hours for analysis by headspace SPME GC-MS.

Table 2.1. Initial concentrations and Henry's Law constants for compounds run as standards in the abiotic experiment.

		Henry's Law Constants[a]		
Standard Compound	C_o[b] (+/-)	NIST[c]	Yaws[d]	Experimental
Acetaldehyde	2242 (415)	14	10.3	13.9
Benzaldehyde	2239 (23)	39	39.6	38.9
Ethanol	2822 (546)	120	121.7	173
Nonanal	2032 (851)	0.7	1.5	1.2
1-Octen-3-ol	1489 (653)	62[e]	39.4[e]	25.2
1-Butanol, 3-methyl	1294 (45)		73.8	77.6

[a] All values in mol/kg*bar
[b] Initial headspace concentration based on Henry's Law constants in ppbv with standard deviation in parenthesis
[c] Sander, R (2011).
[d] Yaws, CL (1999).
[e] 1-Octanol value, value for 1-Octen-3-ol not available

The relationship governing the equilibrium concentration in the liquid in relation to the headspace is defined by Henry's Law:

$$p_A = \frac{C_{A_{liq}}}{H_A} \qquad \text{(eqn. 2.1)}$$

Where ρ_A is the partial pressure of compound A, C_{Aliq}, is its concentration in the liquid, and H_A is the Henry's Law constant for A. Henry's Law constants were evaluated from the PTR-MS measurements following the methodology of Karl et al. (2003) and compared with literature values (Table 2.1) (Linstrom and Mallard, 2011; Yaws, 1998). Experimentally determined Henry's Law constants were evaluated from the slope of the natural log of concentration versus time, and the initial substrate concentration was taken as the intercept. As the concentration of each compound decreases in the liquid, the headspace gaseous concentration in equilibrium with the liquid can be calculated from the first-order rate equation using the initial headspace concentration and the Henry's Law constant.

$$C_A(t) = C_{Ao} \exp\left[\frac{-F}{H_A V R T} * t\right] \qquad \text{(eqn. 2.2)}$$

Where C_A is the gaseous concentration of A, F is the flow rate of gas, V is the volume of liquid containing A, R is the ideal gas constant, and T is the temperature.

Initial concentration of compound A added to the reactor can be measured by PTR-MS and confirmed by calculations based on the volume of compound A added, V_A.

$$C_{Ao} = \frac{V_A \rho_A}{MW_A H_A P V} \qquad \text{(eqn. 2.3)}$$

Where ρ_A is the density of A, MW_A is the molecular weight of A, and P is the pressure of the reactor headspace. The initial concentration for each standard from equation 2.3 is listed in Table 1.

Results

Abiotic Results

Abiotic results were obtained from known concentrations of six standard compounds in the reactor system under a set of controlled conditions that closely mimicked the fungal reactor system to better understand how the measurements of the PTR-MS and SPME GC/MS compare. All of the compounds were added at a level to achieve an initial headspace concentration of 2000 ppbv. The concentration profiles versus time for each of the standards as measured by the PTR-MS and the SPME fiber are shown in Figure 2.1. The headspace concentration of each measured standard decreased in an exponential fashion as predicted by equation 2.2. Henry's Law, as an equilibrium relation, dictates that the concentration of each standard in the gas phase will decrease proportionally with time as the liquid phase concentration decreases due to sparging. The rate of decrease is determined by the air sparge rate and the system mass balance and is inversely related to the Henry's Law constant. For example, nonanal has the smallest Henry's Law constant reported in Table 2.1 and its headspace concentration decreased the fastest of all the analyzed compounds. Henry's law constants for each of the standards can be obtained by plotting the time series data from Figure 2.1 as the natural log of concentration versus time, yielding a linear relationship (not shown) where the slope of the line is related to the Henry's Law constant (Karl et al., 2003). The Henry's Law constants calculated from the PTR data are consistent with those reported previously in the literature (Table 2.1), which indicates that the ions monitored are free

from any interferences and the response of the PTR-MS is within the linear dynamic range of the instrument. The SPME results agree less favorably quantitatively and are discussed below. Qualitatively, the PTR-MS and SPME agree on the identification of the standard compounds with the exception of ethanol which was not detected by the SPME.

The SPME results in Figure 2.1 show that the divinylbenzene/Carboxen on polydimethylsiloxane fiber is inefficient at trapping acetaldehyde and ethanol. This result is not totally unexpected, as the fiber is not specified for the analysis of C2 compounds. It appears that the SPME fiber did not provide results proportional to the amount of acetaldehyde or ethanol present. Additionally, the SPME measurements of 1-butanol, 3-methyl- had a contradictory trend to the PTR-MS measurements and did not decrease in concentration over time. The SPME results for the higher molecular weight components appear to more closely follow the anticipated Henry's law behavior and are fairly consistent with the PTR-MS results with correlation coefficients above 0.8.

A better means of accessing the correlation between the PTR-MS and SPME data can be made by collecting the concentration data at the same discrete time points. The PTR-MS and SPME time point concentrations have been plotted against each other in Figure 2.2 with the corresponding correlation factors. Note that ethanol was not included in Figure 2.2, as there was no ethanol peak detected in the SPME GC-MS technique.

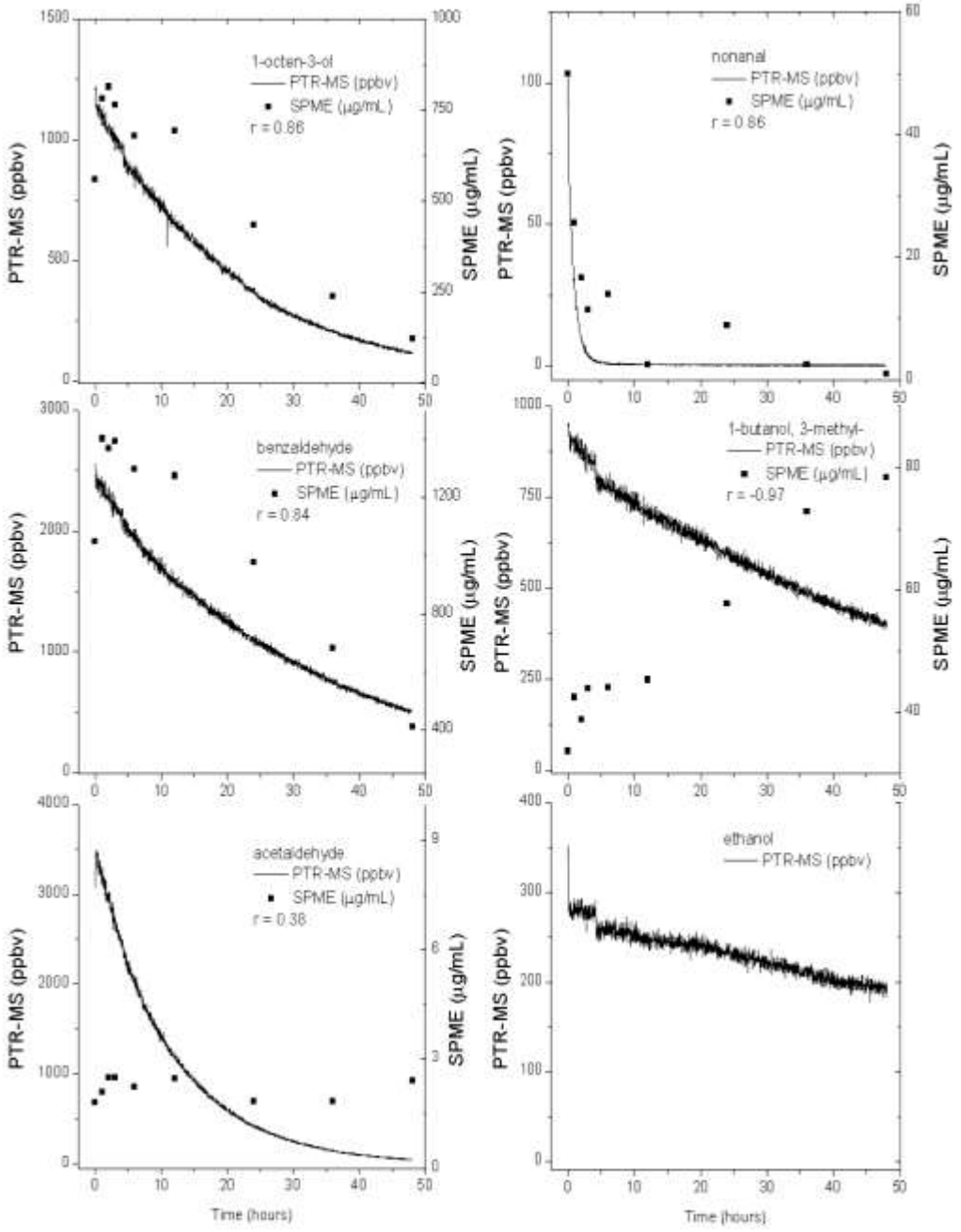

Figure 2.1. Abiotic concentration profiles of standard compounds as measured by PTR-MS and SPME GC-MS. PTR-MS response in parts per billion volume (ppbv) was monitored continuously over 48 hour time period. HS-SPME samples were removed at 0, 1, 2, 3, 6, 12, 24, 36 and 48 hours with correlation coefficients corresponding to six minute PTR-MS averages.

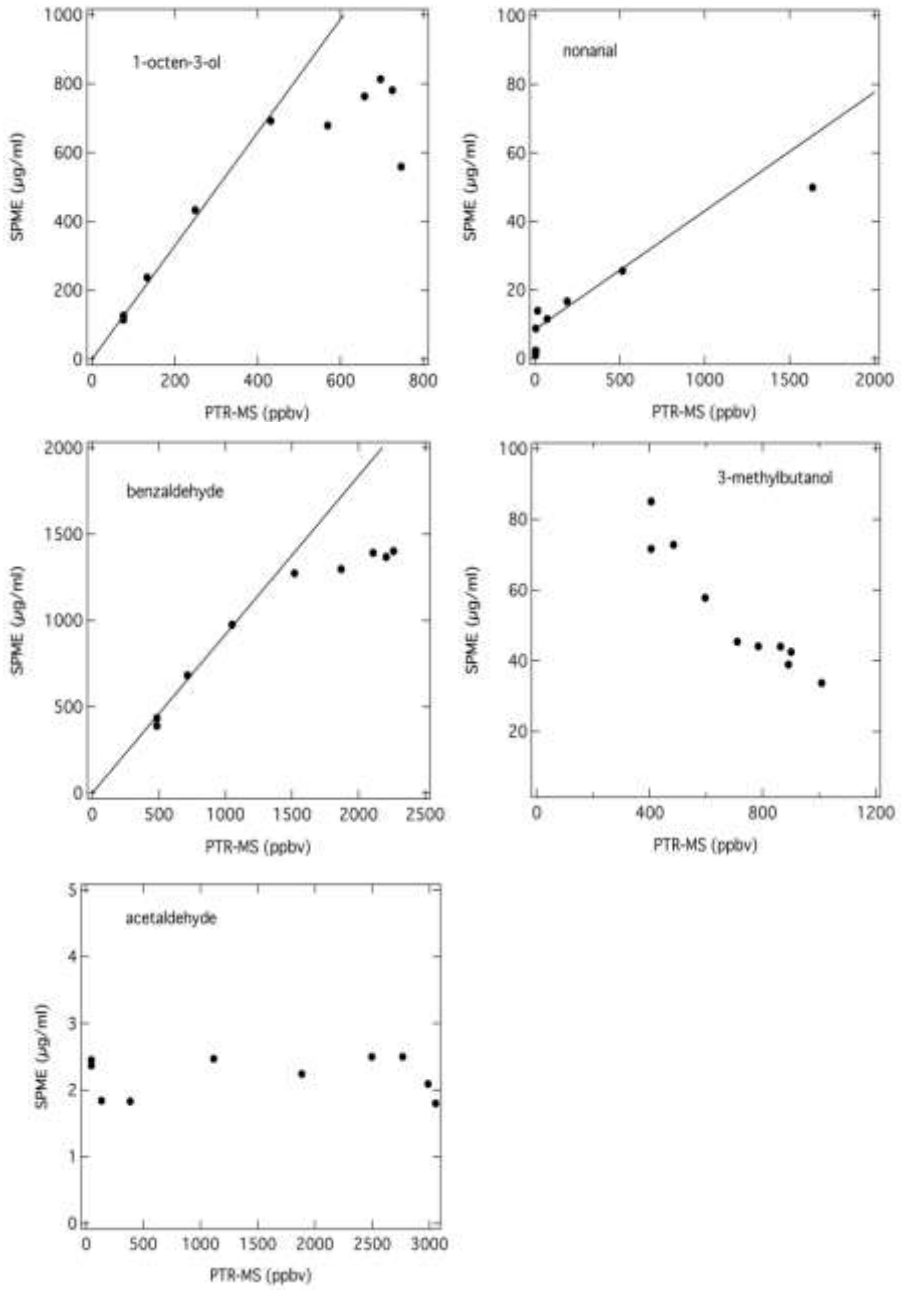

Figure 2.2 Abiotic correlation of standard compound concentrations. Correlation of relative concentration measurements for PTR-MS and the SPME GC-MS technique for all compounds with abiotic measurements except for ethanol, which had a non-detect response by SPME GC-MS. PTR-MS values are centered at SPME sample collection times and are six minute averages. Lines indicate linear correlation at low concentrations with divergence at high concentrations while correlation coefficients include all data points.

While it is apparent in both Figures 2.1 and 2.2 that the measurement of acetaldehyde and 1-butanol, 3-methyl- by the two techniques do not correlate well, Figure 2.2 shows that the degree of correlation for benzaldehyde and 1-octen-3-ol is concentration dependent. The PTR-MS and SPME measurements appear to track one another at the lower concentrations. At the higher concentrations, the SPME results appear to saturate, which suggests that the adsorption capacity of the fiber may have been exceeded. The nonanal results appear to be similarly affected, but the comparison is less definitive due to rapid removal of nonanal from solution and the appearance of the non-zero intercept. The contradictory trend for 1-butanol, 3-methyl- suggests that the adsorption process is competitive, because the 1-butanol, 3-methyl- concentration, as measured by SPME, increases as the stronger adsorbing species decrease in concentration as they are removed from solution. These results indicate that the concentrations measured by the SPME technique are strongly dependent not only on the type of mixture constituents, but also on the relative concentrations of those components. Thus even in relatively simple systems such as this, some care must be exercised in deducing quantitative information from the SPME data.

Quantification of Volatile Products of *A. sarcoides*

Applying these techniques to the biological system, Figure 2.3 shows the time series of the total VOC signal (sum of all the ions from m/z 40-205) as measured by the PTR-MS along with a measure of *A. sarcoides* biological growth expressed as biomass density. The initial variation in the VOC signal is due to inoculation of the reactor with

an active culture, and the initial peak decays away due to the sparging process. The culture demonstrated a lag phase until day 3 before entering an exponential growth phase. The total VOC concentration increased as the fungus entered exponential phase indicating growth associated product synthesis. The flow rate of gas supplied to the reactor was constant such that increasing concentrations demonstrates increased metabolic production of VOCs. The maximum ion concentration of VOCs measured was 10,000 ppbv at 284 hours (near 12 days). The cell concentration began to stabilize on day 12 around 4.5 g/L indicating the culture's entry into stationary phase. Once the stationary phase was reached after day 12, the total VOC signal stabilized, and then dropped rapidly around 380 hours. Throughout stationary phase, the PTR-MS measured the VOCs excluding acetaldehyde and ethanol at 2,000 ppbv. The very sharp transitions in the VOC signal are due to variations in the sparge flow and should not be interpreted as specific metabolic changes.

Continuous monitoring by the PTR-MS revealed that two ions (m/z 45 (acetaldehyde) and m/z 47 (ethanol)) comprised the majority of the ion signal from the *A. sarcoides* culture. Excluding m/z 45 and m/z 47, the remaining ion intensity measured was between 1,000 and 2,000 ppbv in concentration for the majority of the time (Figure 2.3). The remaining ions account for ~ 14% of the total VOC signal. A listing of all of the ions whose intensity exceeded 1 ppbv is tabulated in Table 2.2 along with their signal intensity at discrete time points. Ions of the carbon 13 isotopes are not included, i.e m/z 72 which is 5.5% of m/z 71. Total production of compounds in Table 2.2 increased to over 2,000 ppbv at 280 hours and leveled off as the fungus entered stationary phase after

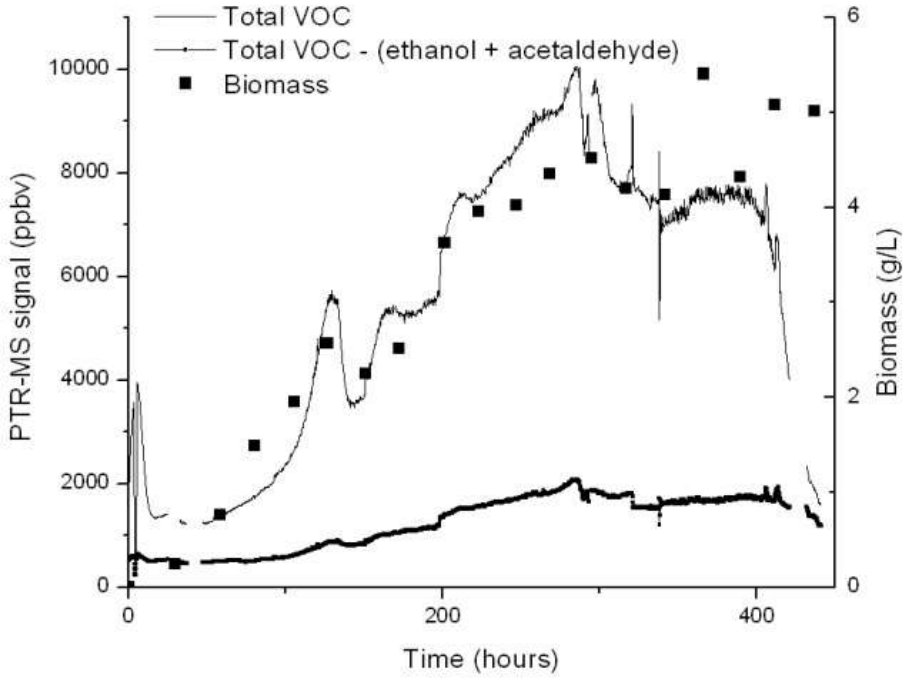

Figure 2.3. Total VOCs in sparged air from *A. sarcoides* culture as measured by PTR-MS. The total VOCs excluding the signals from ethanol and acetaldehyde were near 2000 ppbv at their maximum. Biomass was measured by dry weight.

day 12. The majority of these compounds were composed of 4 and 5 carbon alcohols, acetic acid or acetate esters and compounds producing m/z 59 (acetone and/or propanal). The PTR-MS signal from 1-butanol, 3-methyl- was over 1% of the total VOCs. Notable compounds of fuel interest included 1-octen-3-ol, nonanal, 1-butanol, 3-methyl- and benzaldehyde (Figure 2.4). The PTR-MS signals of the alcohols in Figure 2.4 increased steadily until near the end of the growth cycle with a peak around 275 hours at the end of the exponential growth phase. The benzaldehyde signal reached a maximum around 210 hours before halving just before 300 hours and remained there for the stationary growth

phase of *A. sarcoides*. The SPME measured concentration profiles correspond well with the PTR-MS results for the higher molecular weight alcohols (correlation coefficients > 0.8), but not for ethanol or benzaldehyde (correlation coefficients < 0.7). An increase in the concentration of a compound should elicit a relative increase in the measured response of each technique. Figure 2.4 and Table 2.2 clearly show that there are compounds for which the SPME response to a change in VOC concentration does not scale with the corresponding PTR-MS signal change. The differences in response show the confounding effects of SPME fiber selectivity.

The total ion signal was consistent with *A. sarcoides* biomass concentration; meaning VOC production was closely related with growth (Figure 2.3). The VOC concentration profiles vary by compound as shown in Figure 2.4 with some being associated with growth. The compounds with the highest concentrations were acetaldehyde and ethanol. The major ion signatures, m/z 101, m/z 119, and m/z 159 found in the Strobel et al. (2008) experiment on oatmeal agar were not observed in this study. This change in product composition is most likely due to different carbon source and experimental conditions.

Identification of Volatile Products of *A. sarcoides*

The qualitative information provided by the SPME technique identifies specific VOCs, thereby allowing better ion assignments to be made with the PTR-MS. Most of the compounds positively identified by the SPME technique were also detected with PTR-MS, though the relative amounts of the identified compounds differed significantly

Table 2.2. Select ion signals in the dynamic headspace of *A. sarcoides* culture measured by PTR-MS.

Mass (amu)[a,b]	Signal Intensity (ppbv) at given age in days[c]						
	2	**5**	**9**	**11**	**13**	**15**	**17**
33 [methanol]	1.0	3.6	6.8	9.1	11.1	10.6	12.8
41	6.3	12.7	27.1	40.8	48.8	49.7	52.2
43	36.6	87.8	198	264	251	260	269
57	11.1	44.7	129	180	187	201	234
59 [C_3H_6O]	17.0	71.9	198	264	251	260	269
61	7.6	23.2	69.6	87.7	60.4	54.8	52.5
69	1.7	3.5	5.9	7.5	6.6	7.3	8.6
71 [1-butanol, 3-methyl-]	12.9	24.0	76.4	99.1	98.6	111	127
73 [C_4H_8O]	4.4	39.8	38.6	41.3	43.8	44.1	38.2
75	0.2	0.5	1.9	2.3	1.4	1.5	1.6
87 [$C_5H_{10}O$]	1.0	2.2	4.0	4.9	7.4	10.0	8.0
89 [ethyl acetate]	5.3	14.1	47.9	53.4	32.0	31.0	31.6
91	0.3	0.8	2.0	2.6	2.0	2.1	2.0
93	0.2	0.2	0.9	1.1	0.6	0.8	0.9
105	0.2	0.5	1.8	2.4	2.1	2.2	2.6
107 [benzaldehyde]	0.2	6.3	7.5	6.9	3.5	3.4	3.3
111 [1-octen-3-ol]	0.1	0.5	2.5	3.4	2.6	3.8	4.4
115	0.0	0.5	1.8	1.8	0.9	0.5	0.7
117	0.2	0.4	1.5	2.1	2.0	3.0	4.2
129	0.1	0.4	0.9	1.3	1.2	1.2	1.5
143 [nonanal]	0.1	0.6	0.6	0.7	0.2	0.4	0.5
SUM	106	338	847	1086	1013	1063	1153

[a] Acetaldehyde (45), ethanol (47) and minor ion signals are excluded.
[b] Tentative assignments to the ion are given in brackets.
[c] Signal intensity denoted as 4 hour averages associated with the data in Table 2.3.

between the two techniques. In some instances, the ions detected by PTR-MS were not unique and reflect the collective signal from more than one compound; often the case for lower mass ions. A total of twenty-seven distinct peaks were found using SPME GC-MS, with eight being unidentifiable (Table 2.3). Of the identified compounds, there was a mixture of (in order of descending frequency) organic acids and esters, alcohols,

aldehydes, aromatics and alkanes. Two alkanes were identified by the SPME GC-MS (pentane and 4-methyl-heptane). The branched 8 carbon alkane, 4-methyl-heptane, was produced from Day 2 to Day 15. Physical property information for Table 2.3 compounds is listed in Table 2.4.

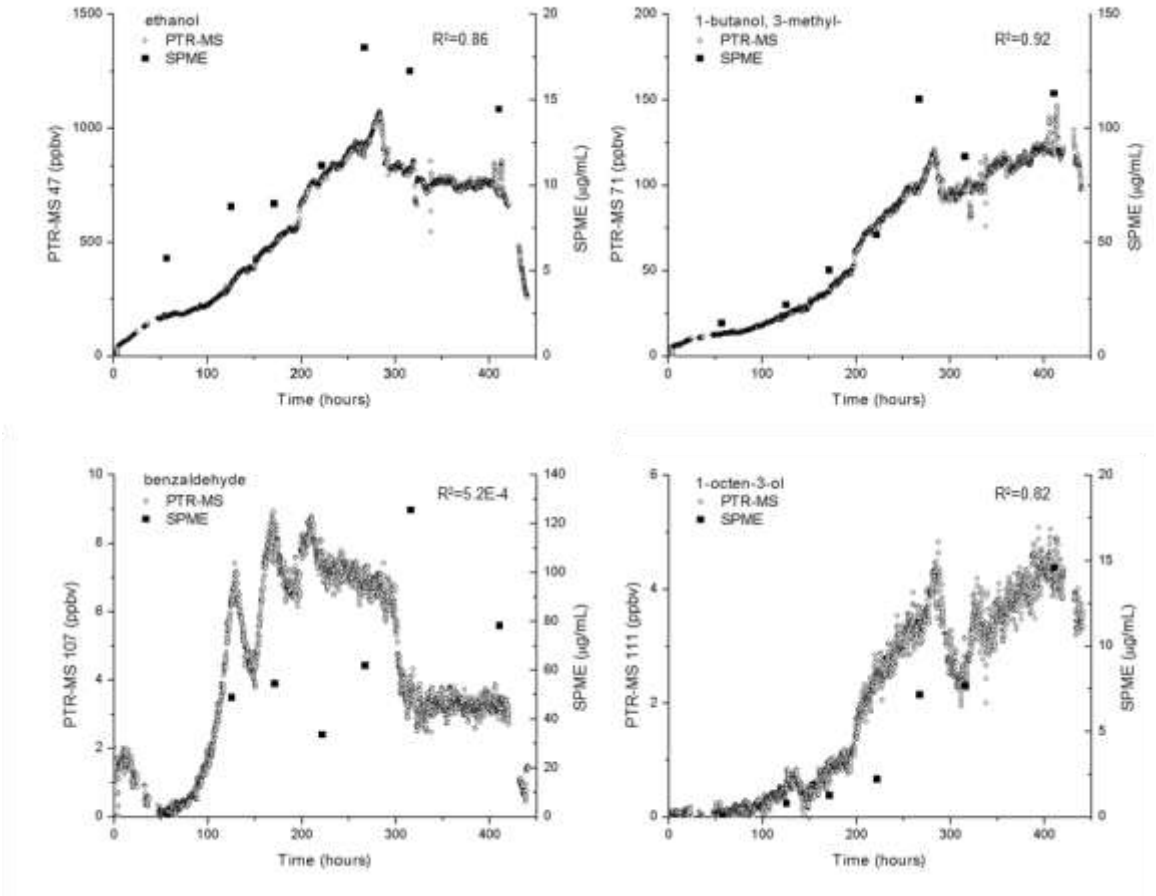

Figure 2.4. Measured concentrations of ethanol, 1-butanol, 3-methyl-, benzaldehyde and 1-octen-3-ol over the course of the growth period as measured by PTR-MS and HS-SPME GC-MS including correlation coefficient, r.

As noted in Table 2.3, twelve compounds identified in this study were also detected by Griffin et al. (2010) on various media including cellulose. Although there

were major differences in the volatile constituents identified, this was not surprising due to the very different experimental conditions of this study. For example, acetic acid, heptyl ester was reported (Strobel et al., 2008) as one of most abundant compounds, but it was not identified by SPME in these results. However, many minor compounds identified by Strobel et al. (2008) on oatmeal agar were identified in this study despite conservative identification changes later made (Strobel et al., 2010). These compounds are noted in Table 2.3 and include heptane, 2-methyl-; acetic acid, decyl ester; ethanol; 1-propanol, 2-methyl-; phenylethyl alcohol; 1-butanol, 3-methyl-; and an isomer of 3-octen-2-ol (1-octen-3-ol).

Of the compounds identified by SPME GC-MS, the concentration profiles of several correlated with the PTR-MS measured concentrations with correlation coefficient exceeding 0.80 (Tables 2.2 and 2.3). These compounds include acetic acid, ethyl ester (89) and the alcohols: 1-butanol, 3-methyl- (71), 1-octen-3-ol (111) (Figure 2.4). The concentration profile of 1-butanol, 3-methyl- as indicated by SPME correlated well with the PTR-MS measurements of ion 71 (Figure 2.4) with a correlation coefficient of 0.93, despite the negative correlation found by the abiotic results (Figures 2.1 and 2.2). A possible explanation for this is the concentrations of other compounds in the fungal gas phase were small and did not preferentially displace 1-butanol, 3-methyl- from the fiber, while in the abiotic results, this was not the case. The concentration profiles for 1-octen-3-ol were strikingly similar despite the relatively low concentration of this product. This was also the case for butanoic acid, 3-methyl- and nonanal whose PTR-MS measured concentrations were less than 1 ppbv. Like 1-butanol, 3-methyl-, their measured

concentrations steadily increased through the majority of the time points. The variance in reported signals is seen in Table 2.2 and 2.3 and Figure 2.4.

The SPME measurements of compounds that did not correlate well with the PTR-MS signal included benzaldehyde (107) and 1-propanol, 2-methyl- (57). For benzaldehyde, the first SPME data point matches the PTR-MS signal, but afterwards, the measured SPME concentrations are out of step with PTR-MS concentrations (Figure 2.4). There was a similar incongruity with the 1-propanol, 2-methyl- measurements. The PTR-MS measurement of 1-propanol, 2-methyl- is made by monitoring the m/z 57 ion. The m/z 57 ion, however, is not unique to 1-propanol, 2-methyl-, and it is probable that the lack of agreement between the PTR-MS and SPME results may be due to signal interference in the PTR-MS measurement. While perturbations in the PTR-MS signal for benzaldehyde could be similarly explained by signal interference, but the abiotic results for benzaldehyde showed no interference, eliminating this possibility.

Discussion

Taken together, the results of the PTR-MS and SPME GC-MS techniques provide a more definitive description of the VOCs produced by *A. sarcoides* for product (e.g. biofuel) development. However, the challenges associated with the quantitative and qualitative analysis of complex VOC mixtures in an aqueous solution are non-trivial, and neither method had the ability to both identify and quantify the breadth of compound diversity synthesized by this complex fungal system.

Table 2.3. GC-MS head-space analysis of VOCs produced by *A. sarcoides* culture collected with a SPME fiber.

Retention Time (min)	**Possible Compound[a] (Molecular mass (Da))**	**Peak Area at given age in days[b]**				
		2	**5**	**9**	**15**	**17**
1.34	Unknown (56)	17.8	13.0	ND	ND	ND
1.38	Pentane (72)[c]	ND	12.6	38.7	22.6	31.8
2.01	Heptane, 4-methyl- (114)[d]	12.9	12.6	11.1	15.6	ND
2.09	Unknown (118)	10.2	9.1	7.3	8.8	6.7
3.26	Ethyl acetate (88)[c]	10.1	19.5	52.9	51.8	44.8
3.89	Ethanol (46)[d]	79.3	121.8	157.3	223.5	188.2
6.07	Unknown (114)	ND	16.1	27.5	45.2	ND
6.40	1-Propanol, 2-methyl- (74)[c,d]	10.1	20.1	17.7	74.9	52.8
7.70	Unknown	11.7	11.0	7.7	11.0	23.7
8.19	1-Butanol, 3-methyl- (impure) (88)[c,d]	88.6	139.7	334.1	665.5	667.6
9.15	Unknown (134)	8.0	10.7	12.8	ND	ND
9.56	Unknown (159 or 88)	ND	11.7	18.7	35.8	ND
11.65	1-Octen-3-ol (128)[c,d(isomer)]	ND	7.6	22.8	80.3	84.5
12.02	Acetic acid, octyl ester (172)[c]	15.6	7.8	3.4	2.6	4.4
12.95	Benzaldehyde (106)	5.2	302.8	211.3	679.7	453.5
13.33	Acetic acid, nonyl ester (186)[c]	33.9	32.8	7.5	5.5	ND
13.99	Unknown (122)	10.9	32.8	1.7	ND	ND
14.58	Acetic acid, n-decyl ester (200)[c,d]	19.3	9.1	ND	ND	ND
14.86	$C_{15}H_{24}$, sesquiterpene (204)[c]	19.3	8.1	5.4	4.1	ND
15.95	Nonanal (142)	15.1	12.1	12.3	17.6	46.7
16.99	Benzyl alcohol (108)[c,d]	ND	5.1	39.3	39.1	34.9
18.37	Unknown (126)	4.4	5.1	10.0	17.0	26.8
18.71	Decanal (156)	ND	ND	ND	24.7	60.8
23.27	Butanoic acid, 3-methyl- (102)[c]	ND	ND	ND	8.9	20.3
24.83	Oxime-, methoxy-phenyl- (151)	ND	ND	ND	39.8	35.7
26.30	Acetic acid, 2-phenylethyl ester (164)[c]	ND	ND	ND	24.5	24.0
28.33	Phenylethyl alcohol (122)[c,d]	ND	ND	ND	37.6	36.6

[a] Unknown compounds represent those whose assignment is uncertain. However, probable molecular masses are included when consistent.
[b] Peak areas listed as 10^6; ND = signal not detected
[c] identified by Griffin et al. 2010 (12)
[d] identified by Strobel et al. 2008 (32, 33)

Table 2.4. PTR-MS ions including fractions, Henry's Law constant, boiling point and vapor pressure for selected compounds from Table 2.3.

Compound	[+]Boiling Point (^{o}C)	[+]Vapor pressure (mmHg at 25^{o}C)	[*]Henry's Law Constant (mol/kg*bar)	PTR-MS ions (fractions)
pentane	36	527	$7.8x10^{-4}$	No Reaction
4-methy-heptane	117	20.5	$2.7x10^{-4}$	No Reaction
acetic acid, ethyl ester	77	112	8.9	[a]43(34), 61(43), 89(24)
ethanol	79	[#]58.7	120	[a]29, 47
2-methyl-1-propanol	108	[#]10.3	100	[a]57(100)
1-butanol, 3-methyl	131	4.76	81	[a]41(11), 43(35), 71(37)
1-octen-3-ol	[+]174	.513	39	[b]41(4), 57(3), 69(45), 111(42), 129(6)
acetic acid, octyl ester	210	.194		[b1]43, 61
benzaldehyde	179	1.27	[e] 39	[c]107(100)
acetic acid, nonyl ester	227	.197		[b1]43, 61
acetic acid, decyl ester	244	.031		[b1]43,61
alpha amorphene	[+]271	.0107		[a1]81, 95, 109, 123, 135, 149, 205
nonanal	191	.532	0.69	[d]69(21), 83(10), 125(18), 143(51)
benzene methanol	205	.094	9000	[d]79(15), 91(85)
decanal	209	.207		[d1]157
3-methyl-butanoic acid	175	.554	1200	Not measured
Methoxy-phenyl-oxime	254	~.023		Not measured
acetic acid, 2-phenylethyl ester	239	.0564		[a]43(37), 61(63)
phenylethyl alcohol	219	.074	[#]349.5	[a]105(100)

[*] Sander, R (2011); [+]http://www.thegoodscentscompany.com/data/rw1024051.html; [#] Yaws 1999; [a] Ezra et al. 2004; [a1] ions observed for the sesquiterpene carophyllene; [b]Buhr et al. 2002; [b1]predicted ions based data reported for smaller acetate esters; [c]Warneke et al.; [d]This study; [d1]insufficient ion intensity to identify fragment ions; [e] 1-Octanol value

The *A. sarcoides* culture consistently produced numerous VOCs. There was little quantitative agreement in VOC concentrations between the SPME technique and the PTR-MS for the suite of compounds produced by *A. sarcoides*. Both techniques have advantages for exploring potential fuel products from fungal or other cultures. SPME effectively identifies a range of compounds produced by the culture, and at modest concentrations, has adequate fiber capacity for many relevant compounds. The use of PTR-MS gives quantitative data on the evolution of volatiles permitting temporal resolution of microbial volatile production. These data can be used to help elucidate real-time metabolism shifts of an organism for product applications (excluding alkanes) and metabolic modeling. The PTR-MS results may also be valuable in guiding genetic engineering efforts to improve production rates of specific compounds.

To effectively use PTR-MS and SPME GC-MS, the inherent differences in signal acquistion must be considered. Foremost, PTR-MS is a continuous measurement of VOCs in the gaseous stream stripped from an aqueous culture; SPME is a measurement of the headspace compounds that develop above a liquid aliquot after a 45 minute exposure and equilibration period. However, SPME is not truly an equilibrium measurement, because the concentration of the headspace is potentially being depleted by compounds adsorbing to the fiber, lowering their vapor pressure and thereby constantly shifting the headspace composition (eqn. 2.1) (Zeng and Noblet, 2002). SPME adsorbs VOCs from the headspace then estimates a liquid concentration based on one internal standard. Therefore, we anticipate differences in distribution of VOCs detected by the two methods (Figures 2.1 and 2.2). The measurement variability that exists between the

two techniques should decrease if the gaseous effluent measured by the PTR-MS is at or near equilibrium with the compounds in the liquid. Based on the abiotic experimental results with a known mixture of VOC standards, equilibrium was assumed for the experimental reactor system.

A limitation of PTR-MS is that alkanes are not ionized by H_3O^+ and therefore are not detectable making it unsuitable for some biofuel applications. Additional quantitative complications can arise due to the presence of fragment ions (decomposition products of the protonated molecule). While ionization via proton transfer with H_3O^+ is considered to be a relatively soft ionization method, many of the components produced by *A. sarcoides* fragment extensively. Most notable are the alcohols that, except for methanol, fragment by the elimination of H_2O from the protonated molecule (Buhr et al., 2002). Thus, the alcohols are detected as an ion corresponding to $(M\text{-}OH)^+$. Despite these considerations, the results clearly demonstrate the applicability of the PTR-MS for time series resolution of volatiles from biological cultures.

SPME analysis should reflect the chemical composition and capacity on the SPME fiber if possible. However, not all compounds adsorb to the fiber material with equal affinities or at equal rates, such that the use of one internal standard is not sufficient to determine all constituent concentrations (Pawliszyn, 1997). The preferential adsorption by some compounds appears to be further exacerbated if the capacity of the fiber is exceeded. The least volatile, highest affinity compounds will be extracted from the headspace-liquid matrix last, therefore adequate extraction times must be observed (Pawliszyn and Smith, 1999). Therefore, drawing conclusions about the concentration of

constituents in complex mixtures is very difficult due to fiber selectivity and saturation characteristics. In general, the SPME fiber appeared to preferentially adsorb the higher molecular weight compounds and therefore over predicts their abundance (Table 2.3). While these ions may have been detected by the PTR-MS, signals were low in concentration either because their headspace concentrations were low or because of possible adsorptive losses in the sample lines and therefore were not included in Table 2.2. An outcome of this preferential adsorption was seen in the 1-butanol, 3-methyl- data. In the fungal culture, the SPME data correlated well with the PTR-MS signal (Figure 2.4), but not in the abiotic data (Figure 2.1) because the culture headspace environment was dominated by lower molecular weight compounds. The negative trend seen in the abiotic results was most likely because the higher molecular weight compounds were preferentially adsorbed by the SPME fiber, leaving few adsorption sites for the other compounds (Figure 2.1). The extent of fiber bias for the lower volatility, higher molecular weight compounds is not easily predicted or measured for complex mixtures. However, SPME appears to be more applicable in the fungal headspace environment than in conditions where higher concentrations of higher molecular weight compounds were present, such as in the abiotic system.

The PTR-MS and SPME results demonstrated the quantitative limits of the SPME technique even when an internal standard was used. However, use of SPME to estimate relative concentrations of higher molecular weight compounds may be reasonable if application is restricted to qualitative temporal trends and not individual quantitative time points. A possibility for improving the SPME technique is to use replicate samples with

additional fiber types to better capture and characterize the breadth of compounds present.

This study shows that despite their shortcomings, the combined use of PTR-MS with a qualitative technique such as GC-MS by headspace SPME is a valuable method for obtaining more detailed analysis of the VOCs produced by microbial systems and can be applied to biofuel product development. However, when quantifying compounds as produced by metabolic processes, especially when those compounds are in a complex mixture, the combination of multiple techniques is warranted until a single more robust qualitative and quantitative analytical method is developed.

Acknowledgements

The authors would like to thank Elle Pankratz for her general laboratory assistance and continuous hard work. This work was supported by the National Science Foundation (NSF) Emerging Frontiers in Research and Innovation (EFRI), Grant No. 0937613 and Chemical, Bioengineering, Environmental and Transport Systems (CBET), Grant No. 0802666. Additional funding for Natasha Mallette was provided by the NSF Integrated Graduate and Education Research Traineeship (IGERT) Program. Manuscript preparation was supported by the National Science Foundation (NSF) Emerging Frontiers in Research and Innovation (EFRI), Grant No. 0937613

CHAPTER 3

EVALUATION OF CELLULOSE AS A SUBSTRATE FOR HYDROCARBON FUEL PRODUCTION BY *ASCOCORYNE SARCOIDES* (NRRL 50072)

Contribution of Authors and Co-Authors

Manuscript in Chapter 3

Author: Natasha D. Mallette

Contributions: Designed the study, collected and analyzed data, and wrote the manuscript.

Co-author: Elle M. Pankratz

Contributions: Collected and analyzed data, discussed the results, commented and edited the manuscript.

Co-author: Albert E. Parker

Contributions: Designed the study, assisted with statistical analysis and interpretation of results.

Co-author: Scott C. Busse

Contributions: Collected and analyzed data, edited the manuscript.

Co-author: Gary A. Strobel

Contributions: Assisted with study design, provided laboratory equipment and edited the manuscript.

Co-author: Ross P. Carlson

Contributions: Assisted with study design and edited the manuscript.

Co-author: Brent M. Peyton

Contributions: Designed the study, discussed the results and implications, and edited the manuscript.

Manuscript Information Page

Natasha Mallette[1,2], Elle M. Pankratz[1,2], Albert E. Parker[2,3], Gary A. Strobel[4], Scott C. Busse[5], Ross P. Carlson[1,2], Brent M. Peyton[1,2#]

Journal Name: Journal of Sustainable Bioenergy Systems
Status of Manuscript:
_x__Prepared for submission to a peer-reviewed journal
____Officially submitted to a peer-reviewed journal
____Accepted by a peer-reviewed journal
____Published in a peer-reviewed journal

[1]Department of Chemical and Biological Engineering, Montana State University, Bozeman, MT 59717, USA
[2]Center for Biofilm Engineering, Montana State University, Bozeman, MT
[3]Department of Mathematical Sciences, Montana State University, Bozeman, MT
[4]Department of Plant Sciences, Montana State University, Bozeman, MT
[5]Department of Chemistry and Biochemistry, Montana State University, Bozeman, MT

[#]Corresponding author: BPeyton@coe.montana.edu

Abstract

When grown on cellulose as the sole reduced carbon substrate , *Ascocoryne sarcoides* produced aviation, gasoline and diesel relevant hydrocarbons. The type and quantity of hydrocarbons produced by *A. sarcoides* were impacted by substrate, growth stage, and culturing conditions: medium concentration and pH. Numerous non-oxygenated hydrocarbons were produced on cellulose such as isopentane, 3,3-dimethyl hexane and d-limonene. Growth on cellulose at 23^{o}C and pH 5.8 produced the overall highest yield of total fuel range organics at 105 mg·g biomass^{-1}. A change in carbon metabolism was seen in late stationary phase from growth on cellulose to production of more oxygenated compounds with longer carbon chain length and fewer fuel-related HCs possibly from the oxidation of hydrocarbons to gain energy.

Introduction

Many strategies are being explored to produce replacements for liquid petroleum fuel from cellulosic feedstocks. These include microbial conversion of cellulosic sugars after extensive pretreatment, as well as chemical and thermal conversion technologies (Carroll and Somerville, 2009). Cellulose and related polymers are the most abundant organic compounds on the planet. When combined with the ability of bacterial and yeast strains to produce biofuel from sugars (Dien et al., 2003), this near carbon-neutral feedstock is a good candidate for producing biofuels for our future needs (Ragauskas et

al., 2006). In the United States, over 1.3 billion tons of cellulose are available yearly from non-food crop production (Perlack et al., 2005).

Ascocoryne sarcoides (NRRL 50072) is a cellulolytic fungal endophyte capable of direct conversion of cellulosic materials to fuel-related hydrocarbon compounds such as alkanes, alcohols and aromatics (Griffin et al., 2010; Strobel et al., 2008). The vision for *A. sarcoides*, and other organisms like it, is the consolidated conversion of sugars in cellulosic materials into fuel with little pre-treatment. This technology is still in its infancy with yields far below industrially relevant levels (Mallette et al., 2012). However, *A. sarcoides* was one of the first discovered endophytic fungi with fuel-related compound production in the C_5-C_{10} carbon chain length range, and its productivity levels are not in the range of being economically feasible. So, it is improbable that it is the organism with the highest potential. In fact, similar organisms that produce fuel-related volatile organic compounds are being discovered every year (Mends et al., 2012; Morath et al., 2012; Zhi-Lin et al., 2012). Therefore, research exploring the factors which influence organisms such as *A. sarcoides* to produce volatile organics and hydrocarbons are relevant.

Microbial utilization of cellulose as a carbon source requires production of cellulase enzymes. The genes responsible for cellulases in *A. sarcoides* were expressed when grown on cellobiose and cellulose, and not when grown on a non-cellulose medium (Gianoulis et al., 2012). The production of cellulases by *Aspergillus fumigatus* in liquid culture can be influenced by carbon source, pH, temperature as well as other factors (Stewart and Parry, 1981). These environmental factors can influence gene expression

and metabolic pathways, also impacting the final products from growth. Therefore, studies exploring volatile hydrocarbon (VHC) production under varying environmental conditions were performed. In addition, previous studies reporting volatile fuel compound production by *A. sarcoides* on cellulose as a substrate were conducted primarily on agar-based medium or in nutrient rich liquid medium with a single pH condition, so in this work, a minimal defined medium was used for the majority of the cultures (Ahamed and Ahring, 2011; Gianoulis et al., 2012; Griffin et al., 2010; Strobel et al., 2008). The carbon source of the medium was varied to explore the impact of substrate on VHC production.

Here we report the results of assessing the effects of pH, growth medium, and temperature on fuel-related hydrocarbon production by the fungus and show hydrocarbon production with cellulose as a substrate by measuring fuel compounds in both the gas and liquid phases of *A. sarcoides* cultures. Multiple methods of analyzing VHC were used to identify and quantify the compounds produced. This work demonstrates the potential of *A. sarcoides* to produce a variety of VHC compounds with fuel potential and provides guidance for efforts being made on other organisms having this capability.

Materials and Methods

Culture Medium and Conditions:

Flask and Bottle Tests

A. sarcoides (NRRL 50072) was grown in 250 mL baffled flasks or bottles on a minimal cellulose medium (CM) consisting of (per liter): 50 µm microcrystalline

cellulose (20 g) (Acros Organics), ammonium chloride (5 g) (Fisher Chemical), $NaH_2PO_4 \cdot 2H_2O$ (2.75 g) (Fisher Chemical), $MgSO_4 \cdot 7H_2O$ (0.86 g) (Fisher Chemical), $Ca(NO_3)_2 \cdot 4H_2O$ (0.28 g) (Fisher Chemical, yeast extract (0.05 g) (Fisher BioReagents), and trace salts: KCl (60 mg), KNO_3 (80 mg), $FeCl_3$ (2 mg), $MnCl_2$ (5 mg), $ZnSO_4$ (2.5 mg), H_3BO_3 (1.4 mg), and KI (0.7 mg). 100 mmol KH_2PO_4 was added as a buffer. CM was modified with glucose (Fisher Chemical) in place of cellulose for glucose medium (GM), and with 90,000 average molecular weight sodium carboxymethyl cellulose (CMC) (Sigma Aldrich) in place of cellulose for CMC medium. To test the impact of nutrient limitation, the GM recipe listed above was increased three fold for all components except calcium and magnesium compounds. Initial pH was adjusted to 3.5, 5.0, 5.6 and 6.5 with 2 M NaOH or HCl.

Response surface design is a method that reduces the total number of experiments in an optimization study by using mathematical modeling to determine the minimum number of experiments necessary. Response surface design and analysis has been used for efficient optimization of fungal systems (Dagbagli and Goksungur, 2008). Therefore, an experimental design matrix developed using response design was used to determine culture conditions with previous experimental results used as boundaries. The experimental matrix is shown in Table 3.1.

Temperature was controlled at 13, 20 and 28^{o}C. Three different oxygen conditions were used for the smaller scale flasks/bottles: aerobic, sealed batch, and anoxic. Cultures covered with permeable cloth were considered aerobic; those sealed with stoppers containing ambient air in the headspace were denoted sealed batch; those

sparged with N_2 then sealed with oxygen impermeable stoppers were denoted anoxic. Cultures were shaken in temperature controlled incubators at 150 rpm. All cultures were inoculated with a 7-day culture prepared with Microbank^{TM} Bead frozen stocks (-80^{o}C) and grown in CM with cellulose replaced with 0.5 g cellobiose and 0.45 g yeast extract.

Biomass Analysis: Flask and Bottle Tests

Biomass was determined by cell dry weight as described previously (Mallette et al., 2012) and by a modified Bradford method (Bio-Rad, Hercules, CA). On soluble substrates, fungal growth curves were monitored by optical density at 600 nm with a GENESYS spectrophotometer (Thermo Scientific).

Volatile Hydrocarbon Analysis by Nuclear Magnetic Microscopy: Flask and Bottle Tests

Throughout the growth period, samples of culture liquid were collected ranging from 7 to 14 days for glucose cultures and up to 60 days for sealed cellulose cultures. The liquid samples were centrifuged to remove cells, and the cell-free culture liquid added to a Nuclear Magnetic Microscopy (NMR) tube with 10% deuterium oxide (D_2O) by volume. Proton NMR was run on a Bruker DRX600 spectrometer operating at a proton frequency of 600.13 MHz. Data were collected using a 1D Nuclear Overhauser Effect Spectroscopy (NOSEY) experiment with 100 ms mixing time and 2 second presaturation of the water signal. A total of 32,000 data points were collected, with a sweepwidth of 7183.91 Hz. The 64 scans were averaged for each data set with a total recycle time of 4.28 seconds. All data sets were collected with the same receiver gain, so the intensity of the signals could be directly compared.

The data were processed using an exponential window with a 0.5 Hz line broadening and a final size of 16,000 real points. All results were corrected for background with un-inoculated controls. This technique measures signal of protons (H+) on the liquid bound compounds and is therefore quantitative on a molecular level. The signal peaks and areas are grouped based on structure and elemental compositions and compared with control samples. The peak spectra were grouped by aromatics, non-oxygenated hydrocarbons and sugars. Oxygenated hydrocarbons are included in the sugars peak, so cannot be differentiated with this technique. The results are non-specific as far as carbon length, but can indicate structure (e.g. branching).

Statistical analysis of VHC data from NMR spectra was completed using linear mixed effects (*lme*) models in the *lme4* package (Bates et al., 2013) in the free statistical and graphing program *R* (R Core Team, 2013). Results from three models are reported here; an overall model including both substrates and individual models for each substrate. Initially models were fit with all two-way interactions among co-variates. If none of the two-way interactions were significant, interactions were not included in the model used for statistical inference. In addition, the validity of the models was confirmed with discrete models built for each variable. For the overall model with all samples and the glucose model, covariate inputs were pH, temperature, and age of the culture at the sampling time; no two-way interactions were statistically significant. Headspace oxygen condition, e.g. anoxic, substrate and medium concentration were input as fixed effects with crossed random effects from start date of the experiment and the date measured on the NMR equipment. The cellulose model has the same inputs as the others with one

exception. Medium strength was not included in the final model, because all experiments were conducted at one medium concentration. A model was fit with all two-way interactions among covariates, but none of the interactions were statistically significant. Therefore, two-way interactions were not included in the model used for statistical inference. For the cellulose data, two outliers were identified, and it was determined that they had a large influence on the results. Therefore, they were removed from the reported analysis.

Culture Medium and Conditions:
Gas-purged Reactors

A. sarcoides (NRRL 50072) was grown in 10 L bottles with 4 L of media CM, GM, both at three fold concentration, and Potato Dextrose Broth (PDB) at 24 g/L. CM and GM were brought to pH 5.8 with 2 M NaOH. Continuous house air supply at 1 liter per minute passed through the bottle headspace, and the cultures were incubated at 23^{o}C with shaking at 100 rpm. At the conclusion of the experiments, biomass was determined by cell dry weight as described previously (Mallette et al., 2012) or by a modified Bradford method (Bio-Rad, Hercules, CA) for cellulose substrate.

Volatile Hydrocarbon Collection:
Gas-purged Reactors

The air passing through the bottle headspace was routed with teflon tubing to an external column containing 10 g of Carbotrap^{TM} B and 10 g of Carbotrap^{TM} C (Supelco, Bellefonte, PA). Carbotrap^{TM} B collects compounds with a carbon range of C_5-C_{12} and Carbotrap^{TM} C collects compounds from C_{12}-C_{20}. Volatiles were collected on one column

from day 5 to day 17 of growth and for cellulose, on another from day 17 to day 32. Volatiles were also collected from un-inoculated controls and subtracted from culture results. Carbotrap™ columns were conditioned before collection as described previously (Booth et al., 2011). The combination of multiple materials allowed for collection of volatiles over a large range of carbon compounds. This method concentrated the compounds produced by the culture, allowing greater resolution of products, especially those produced at a low rate (Booth et al., 2011).

Volatile Hydrocarbon Analysis by GC-MS: Gas-purged Reactors

Liquid from the 4 L cultures was extracted using the U.S. Environmental Protection Agency (EPA) method 3510. The extracted liquid was analyzed by GC-MS by Pace Analytical Labs (Billings, MT) for gasoline range organics (GRO) by EPA method 8015/8021 and for diesel range organics (DRO) by EPA 8015 modified. Peak areas were used to quantify total DRO and GRO, correcting for un-inoculated controls. DRO and GRO are reported separately from the external column collection and desorption described below.

Volatile compounds collected on the external Carbotrap column were desorbed and analyzed as described previously with only slight modifications (Booth et al., 2011). The column was conditioned with a dry purge at 30^{o}C with ultra-high purity nitrogen for one hour, followed by desorption of the column at 180^{o}C for one hour at 0.7 L min^{-1}. The column effluent gas was externally condensed with liquid nitrogen in a solid phase microextraction (SPME) compatible 30 mL vial. The vial was stored frozen or on ice

before measurement by SPME GC-MS. In brief, a SPME fiber (divinylbenzene/Carboxen on polydimethylsiloxane by Supelco, Bellefonte, PA) was exposed to the vial headspace while heating to 30^{o}C for 45 minutes. The fiber was inserted into the injection port of the GC at 240^{o}C. The GC column temperature was held at 40^{o}C for 2 minutes, and then ramped to 230^{o}C at 5^{o}C min^{-1}. The relative amount of identified compounds was estimated by comparison with a 4-bromofluorobenzene (BFB) internal standard calibration curve delivered in methanol over the concentration range of 2 - 75 μg mL^{-1}. The GC was interfaced with a Hewlett Packard 5973 mass spectrometer which was tuned to meet EPA Method 8260 BFB tuning criteria. In addition, the vial headspace was sampled and analyzed. The vial was heated to 30^{o}C to volatilize components and 50 μL of the headspace was removed and directly injected into the GC.

Data processing was performed with MassHunter Pro B.04.00 and Mass Profiler Pro B.04.00 (Agilent Technologies, Santa Clara, CA). Cross-comparison of spectra across all substrates was completed before compound identification to eliminate errors associated with database searches and identity allocation. Spectra from the un-inoculated controls were compared with samples in Mass Profiler Pro to subtract peaks similar to control peaks. The software compared peak spectra with similar retention times, so slight differences in retention time did not impact the results. A fold change of 10,000 was used to report spectra values, though a fold change of 10 gave the same results. The reported mass spectra were compared to library spectra from the National Institute of Standards and Technology (NIST) Standard Reference Database, 2.0f. A quality match cutoff of 75% reported database matches with 75% or greater similarity. The library match process

was repeated and when the library identified multiple compounds as matches for a single compound, visual comparison of the sample spectra determined the final identification. Sample spectra that could not be rectified with the library spectra were considered "unknown" even if the library considered it to have a quality match above 75%. All identified compounds are listed in the NIST Chemistry WebBook terminology (Linstrom and Mallard, 2011).

The quantities of volatiles desorbed from the fiber were calculated from the peak area of the total ion current measured by the mass spectrometer minus the peak area from un-inoculated controls. As previously shown (Mallette et al., 2012), the fungal volatile hydrocarbons (HC) and the internal standard do not have the same gas-liquid partitioning, efficiency of adsorption to the fiber, or response in the GC-MS system, so the quantities obtained are therefore estimates. Nevertheless, the use of the internal standard allowed for a relative comparison between samples from the same culture across a time period.

Results and Discussion

Analytical results from liquid and gas-phase measurements are summarized for both small-scale flask and bottles tests and larger-scale gas-purged reactors. Small-scale batch cultures allowed for a greater matrix of variables to be tested but non-specific VHC results (Table 3.1). The larger-scale gas-purged batch reactor experiments were used to expand upon the knowledge of VHC identities and distributions. These analyses differ from previously reported results due to the experimental and analytical methods used and therefore the results presented here reflect quantitative data not possible with HS-SPME

and show a new technique for reporting HS-SPME GC-MS results using an external column as described by Booth et al. (2011).

Table 3.1. Experimental design matrix used for small-scale batch cultures to explore effects of the variables on VHC production by *A. sarcoides* growth on glucose and cellulose. A. Experimental variables, B. Combination of variables.

A.

Value	Medium Nutrient Level	pH	Temperature (^{o}C)
-1	1x	3.5	13
0	2x	5	20
1	3x	6.5	28

B.

Medium Nutrient Level	Temperature (^{o}C)	pH	Run Order
-1	1	1	1
0	0	0	3
1	-1	-1	2
-1	-1	-1	2
0	0	0	3
0	0	0	3
1	1	1	1
1	-1	1	2
-1	-1	1	2
-1	1	-1	1
1	1	-1	1

Environmental Factors for
VHC: Flask and Bottle Tests

VHC production by the fungus can be significantly influenced by the environment in which it is grown. The samples were measured by NMR and the resulting peak areas analyzed to determine which variables were statistically significant. NMR spectra from a 15 day old culture grown at 20^{o}C and pH 5 showed distinct HC peaks between 1 and 2

ppm, but culture-free cellulose medium samples had none (Figure 3.1). The peak area was proportional to the amount of HC present. HC were measured at a pH ranging from 3.5-6.5 and at temperatures 13, 20 and 28^{o}C. A limitation of NMR was the oxygenated hydrocarbons, e.g. alcohols and aldehydes were not quantified, because it was not possible to distinguish them accurately with this technique from other oxygenated compounds such as the carbohydrate substrates, acids or esters. Nevertheless, the NMR technique did show the presence of a distinct resonance in the upfield region indicative of hydrocarbon protons.

The linear mixed effects model compiled from the 125 samples showed the greatest impact on HC was due to the carbon source with glucose cultures having on average 28 times more HC production than cellulose cultures with a p-value of 4E-7. Therefore, individual substrate models for HC production were completed to assess the impact of environmental conditions. There was a statistically significant impact on HC production by pH for CM cultures, but not GM cultures, with slightly increasing NMR measured HC with increasing pH up to 6.5 (p-value 9.7E-3). For growth on glucose, the medium strength had a significant effect on HC production. For example, for every doubling of medium component concentrations, the cultures grown had 1.6 fold more total NMR detected HC with a p-value at 2.2E-8. There were small impacts from temperature and culture age on HC production from both CM and GM cultures after accounting for all other environmental effects. However, the statistical analysis resulted in no significant difference with all p-values greater than 0.05. For example, statistically similar HC levels were reached for cultures grown at 13, 20 and 28^{o}C.

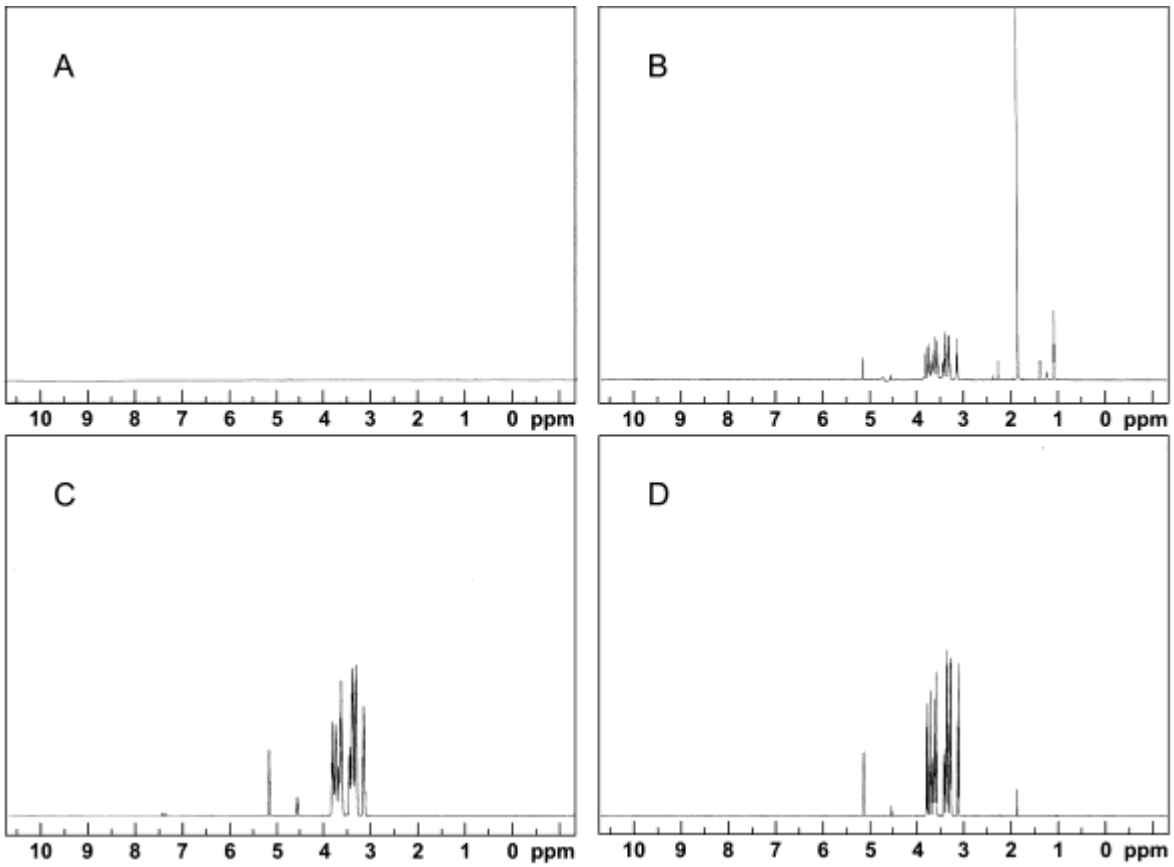

Figure 3.1. NMR spectra for A. Cellulose control medium, B. *A. sarcoides* culture grown on cellulose medium at 20^{o}C and at pH 5 for 15 days. C. Glucose control medium, D. *A. sarcoides* culture grown on glucose medium at 20^{o}C and at pH 5 for 15 days. Peaks between 1-2 ppm indicate non-oxygenated hydrocarbons, and peaks between 4 and 5 show sugars from the breakdown of the cellulose substrate and oxygenated products such as acids and alcohols.

The HC levels of *A. sarcoides* cultures were measured with varying headspace oxygen values to understand the impact of oxygen availability on HC metabolism. Overall, there was a was not a significant impact of oxygen availability on HC yields with respect to biomass concentration in GM. Building on these results, larger scale batch reactor experiments were conducted to compare volatile and liquid HC production on

three different substrates with three fold medium concentrations, starting with a pH of 5.8, and aerobic headspaces (Gas-purged reactors section below).

Environmental Factors for Growth: Flask and Bottle Tests

Medium substrate and headspace oxygen concentration were important factors for the growth rate of *A. sarcoides* in the liquid media tested. Growth rates and final biomass concentrations were calculated for CMC and GM in aerobic conditions and for CM, CMC, and GM in sealed batch conditions (data not shown). Lower oxygen values in sealed batch cultures showed slower specific growth rates on CMC (0.038 +/- 0.006 hr^{-1}), but not on GM (both ~0.02 hr^{-1}) which had a similar rate to CM (0.017 +/- .01 hr^{-1}). However, despite comparable growth rates, a higher final biomass concentration on GM (0.871 +/- 0.033 g L^{-1}) was reached under sealed batch conditions as compared to 0.503 +/- 0.009 g L^{-1} under aerobic conditions. Growth on CM achieved maximum biomass (0.797 +/- 0.062 g L^{-1}) under aerobic conditions.

Substrate Effects: Gas-purged Reactors

Substrate had a marked impact on HC production type and frequency. Growth on cellulose (CM) and potato dextrose broth (PDB) showed more than twice the number of compounds as growth on glucose (GM). This is not surprising due to the differences in initial substrate complexity. Figure 3.2 shows CM cultures had 10 compounds in common with GM. CM showed increased product diversity from GM, with 50 compounds distinct from GM, and 16 in common with PDB. The majority of compounds produced on GM were also produced on either PDB or CM. Many unique compounds

were produced, 38 for CM and 41 for PDB, indicating the diverse metabolic capability of the organism to produce different compounds on complex substrates. The most diverse variety of hydrocarbons (Table 3.2) and the most numerous at 66 (Figure 3.2) was produced on the undefined substrate, PDB. This was not surprising as PDB contained the most complex substrates, though CM was similar with 60 compounds.

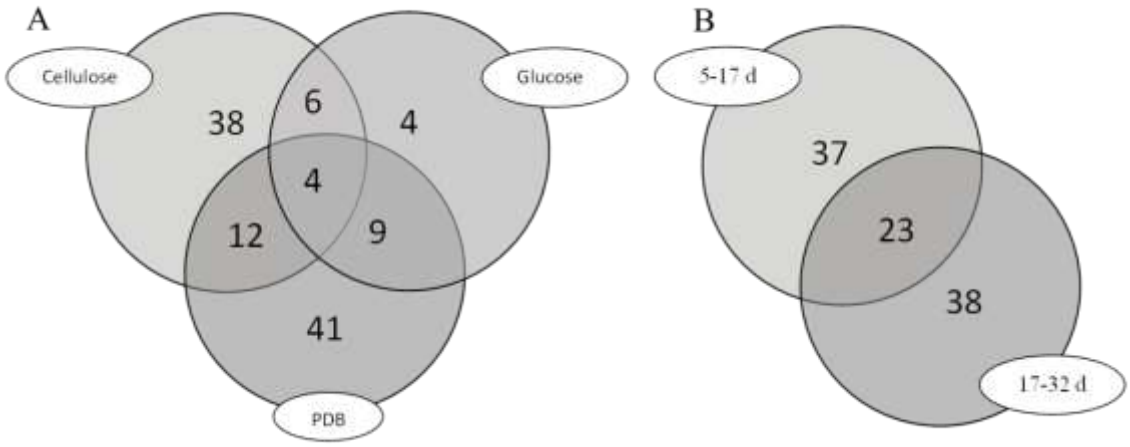

Figure 3.2. A.VENN diagram of HC product similarity based on media type. Cultures were grown at room temperature and 1 L min^{-1} air flow. All HCs were collected between 5-17 days of growth. B. HC product similarity based on age of cellulose growth for 5-17 days of growth and 17-32 days of growth.

After compound identification by GC-MS (64 of the 114 compounds were identifiable based on a conservative quality match cutoff of 75%), the compounds were sorted into classes based on structure: alkane, alkene, aldehyde, ketone, aromatic, alcohol, acid, and ester. Compounds with non-aromatic ring structures were classified

Table 3.2. Identified compounds produced by *A. sarcoides* on three substrates: CM (cellulose), GM (glucose) and PDB (potato dextrose broth. Samples were measured by HS-SPME GC/MS. Manual matching of spectra to the NIST library was assisted by a 75% quality match cutoff. MW indicates the molecular weight of the compound. Presence of the compound from the headspace of the culture is abbreviated in the Media Present column to C1 C2 for CM at two different time points, G for GM, and P for PDB media. An empty cell indicates the compound was not detected. *VHC compounds detected previously from *A. sarcoides*; (iso) = isomer detected (Griffin et al., 2010; Mallette et al., 2012; Stinson et al., 2003; Strobel et al., 2008).

						Percent of Total Area			
RT	Compound Identification	Industrial Category	MW	Quality Match	Media Present	CM(1)	CM(2)	GM	PDB
	ALKANE								
7.6	Dodecane, 2,6,10-trimethyl-	Isoparaffin	212.4	79.6	C1,C2	0.72	1.32		
8.0	Butane, 2-methyl-	Isoparaffin	72.2	80.0	ALL	0.71	1.00	3.69	0.69
9.5	Nonane, 4,5-dimethyl-	Isoparaffin	156.3	82.3	C1	0.61			
9.9	Undecane, 3-methyl-	Isoparaffin	170.3	85.4	C1,C2,P	1.17	1.06		0.51
10.6	Dodecane	Paraffin	170.3	87.0	C1	0.58			
11.6	Oxetane, 3-(1-methylethyl)-	Cycloparaffin	100.2	87.5	G,P			44.6	14.0
13.3	Nonadecane	Paraffin	268.5	76.4	C1	0.78			
13.8	Hexane, 3-methyl-	Isoparaffin	100.2	80.9	C1	0.36			
14.3	Cyclopropane, propyl-	Naphthene	84.2	89.0	C1,G,P	0.50		0.59	0.47
21.3	Cyclohexane, 1-ethenyl-1-methyl-2,4-bis(1-methylethenyl)-	Naphthene	204.4	82.8	G,P			0.52	0.18
22.2	n-Propylidenecyclohexane	Isocyclic	154.3	78.8	C2		0.68		
23.7	(+)-Cycloisosativene	Tricycloparaffin	204.4	93.4	G,P			0.63	0.53
	ALKENE								
10.7	1,5-Cyclooctadiene, 1,5-dimethyl-	Cyclic olefin	136.2	87.0	C1	0.54			
15.3	1-Heptene, 6-methyl-	Olefin	112.2	87.4	C1,C2	0.76	7.98		
16.9	Cyclohexene, 4-methyl-*$^{(iso)}$	Cyclic olefin	96.2	83.8	P				2.87
17.1	1,3-Hexadiene, 3-ethyl-2-methyl-	Olefin	124.2	84.5	C2		0.89		
19.1	1,4-Hexadiene, 3-ethyl-	Olefin	110.2	83.6	C2		0.34		

Table 3.2 Continued

19.6	1H-Cycloprop[e]azulene, 1a,2,3,4,4a,5,6,7b-octahydro-1,1,4,7-tetramethyl-, [1aR-	Bicycloparaffin	204.4	87.3	G,P			0.63	0.41
21.4	Azulene, 1,2,3,5,6,7,8,8a-octahydro-1,4-dimethyl-7-(1-	Cyclic olefin	204.4	89.8	G,P			1.04	0.91
24.1	1,6-Cyclodecadiene, 1-methyl-5-methylene-8-(1-methylethyl)-, [s-(E,E)]-	Cyclic olefin	204.4	96.2	G			0.56	
	AROMATIC								
10.5	p-Xylene	Aromatic	106.2	92.9	P				0.15
10.9	D-Limonene	Aromatic	136.2	91.5	C1,P	0.93			1.84
11.7	Benzene, 1-ethyl-2-methyl-	Aromatic	120.2	86.0	P				0.27
12.0	Furan, 2-pentyl-*	Aromatic	138.2	77.5	C1,C2,P	0.57	3.90		0.30
12.9	Benzene, 1-methyl-2-(1-	Aromatic	134.2	82.7	P				0.19
14.7	α-Methylstyrene	Aromatic	118.2	96.4	P				0.30
15.2	Benzene, 2-ethyl-1,4-dimethyl-	Aromatic	134.2	87.8	P				0.14
17.5	Benzene, 1,2,4,5-tetramethyl-	Aromatic	134.2	83.5	C1,P	0.24			0.18
17.7	Benzene, 1,3-dichloro-	Aromatic (Cl)	147.0	85.2	C1,P	0.24			0.19
19.2	Benzene, 2-ethenyl-1,4-dimethyl-	Aromatic	132.2	89.4	P				0.15
19.9	Benzene, 1-ethyl-4-methoxy-	Aromatic	136.2	78.7	P				0.57
19.9	Benzaldehyde*	Aromatic	106.1	82.0	P				0.84
21.9	Benzonitrile*	Aromatic (N)	103.1	94.2	C1,G	0.45		2.13	
22.9	Acetophenone	Aromatic	120.2	94.8	P				1.55
25.0	1H-Indene, 1-methylene-	Indene	128.2	96.0	G			0.54	
25.3	Benzenemethanol,- (1-methyl-2-	Aromatic (OH)	176.3	79.6	P				0.15
28.0	Benzyl Alcohol*	Aromatic (OH)	108.1	95.1	C2		0.29		
28.7	Phenylethyl Alcohol*	Aromatic (OH)	122.2	93.4	C1,C2	4.02	7.78		

Table 3.2 Continued

	KETONE							
10.6	2-Hexanone, 4-methyl-*(iso)	114.2	76.8	C2		0.31		
12.1	2-Heptanone, 6-methyl-*(iso)	128.2	83.4	C2		0.68		
12.6	3-Octanone*	128.2	78.6	C1,C2	0.52	0.67		
16.2	2-Nonanone*	142.2	87.6	C1, P	0.65			0.48
22.0	2-Undecanone*	170.3	86.0	C2		0.86		
22.2	2(3H)-Furanone, dihydro-4-	100.1	83.6	P				0.21
	ALDEHYDE							
4.0	Butanal, 3-methyl-	86.1	76.3	C1	0.66			
10.6	Heptanal	114.2	76.6	C2		0.48		
15.1	4,4-Dimethylpent-2-enal	112.2	80.5	C2		0.31		
20.2	2-Nonenal, (E)-	140.2	86.5	C2		0.43		
24.0	2,4-Nonadienal, (E,E)-	138.2	87.6	C2		0.50		
25.0	2-Undecenal	168.3	80.7	C2		0.33		
	ALCOHOL							
11.4	1-Butanol, 3-methyl-*	88.2	86.5	C2		4.98		
11.7	1-Hexanol*(and iso)	102.2	84.5	C2		1.91		
11.8	1-Hexanol, 5-methyl-2-(1-	158.3	83.7	C1	0.85			
12.5	1-Pentanol*	88.2	75.7	C1,C2	0.97	0.57		
17.8	1-Octen-3-ol*	128.2	86.8	ALL	0.57	2.66	0.55	1.36
20.3	1,6-Octadien-3-ol, 3,7-dimethyl-	154.3	77.8	P				0.21
	ACID							
17.9	Acetic acid*	60.1	92.5	C1,C2,G	16.97	23.2	9.74	
21.0	Propanoic acid, 2-methyl-	88.1	76.7	ALL	4.94	6.34	10.2	3.21
22.7	Butanoic acid	88.1	81.2	C1,C2	0.34	0.43		
23.4	Butanoic acid, 3-methyl-*	102.1	77.6	C1,G	13.8		6.54	
27.5	Hexanoic acid*	116.2	91.2	C2		0.74		

Table 3.2 Continued

	ESTER							
5.9	Butanoic acid, 2-methyl-, methyl	116.2	83.0	P				0.58
5.9	Acetic acid, 2-methylpropyl ester*	116.2	80.9	G			0.88	
8.8	1-Butanol, 3-methyl-, acetate*	130.2	81.4	C1,C2,P	7.46	0.73		2.88
12.6	Hexanoic acid, 2-ethyl-, methyl ester*(iso)	158.2	87.8	P				0.76
13.0	Acetic acid, hexyl ester*	144.2	85.5	C2,P		1.90		3.48
13.6	Pentanoic acid, pentyl ester	172.3	83.3	C1,C2	1.53	1.92		
13.9	Trichloroacetic acid, tridecyl ester	345.7	79.8	C2		0.25		
14.0	3-Hexen-1-ol, acetate, (Z)-	142.2	78.5	P				0.29
14.2	4-Hexen-1-ol, acetate, (Z)-	142.2	83.0	P				0.62
15.8	Acetic acid, heptyl ester*	158.2	91.7	C1,C2	0.36	1.65		
18.1	Formic acid, heptyl ester	144.2	83.8	C2		1.97		
18.5	Acetic acid, octyl ester*	172.3	92.1	C1,C2,G	1.18	4.56	0.67	
19.3	3-Octen-1-ol, acetate, (Z)-	170.3	76.6	C1,C2,P	0.53	0.92		0.31
19.8	2-Hydroxyisocaproic acid, methyl ester	146.2	89.3	C1,C2,G	0.29	0.63	0.75	
19.8	Z-7-Decen-1-yl acetate	198.3	75.3	P				0.16
20.1	2-Furanmethanol, acetate	140.1	80.6	P				0.14
20.9	Acetic acid, nonyl ester*	186.3	86.8	C1,C2	0.31	1.25		
23.8	5-Decen-1-ol, acetate, (E)-	198.3	87.6	C2		0.43		
24.7	Acetic acid, phenylmethyl ester	150.2	96.1	C2		0.40		
25.4	Benzeneacetic acid, methyl ester	150.2	88.9	C1	0.41			
26.0	Benzeneacetic acid, 2-phenylethyl ester	240.3	90.0	C2		0.92		
26.6	Acetic acid, 2-phenylethyl ester*	164.2	93.8	C1,C2	2.36	3.07		
	UNKNOWNS			ALL	32.2	9.11	14.8	57.9

based on bonding in the ring (e.g. a double carbon bond was put in the alkene class). Comparing the results from days 5-17 (See Culture Age Effect Section for discussion on multiple cellulose time points), Figure 3.3 shows PDB cultures had a total of 37 compounds which could be identified; CM had a total of 35 and GM, 17. CM or PDB cultures had the highest number of compounds in all classes except alkene (which had low numbers for every substrate). There was similar production of alkanes, alkenes, and ketones from growth on PDB and CM. Growth on CM showed the only detected

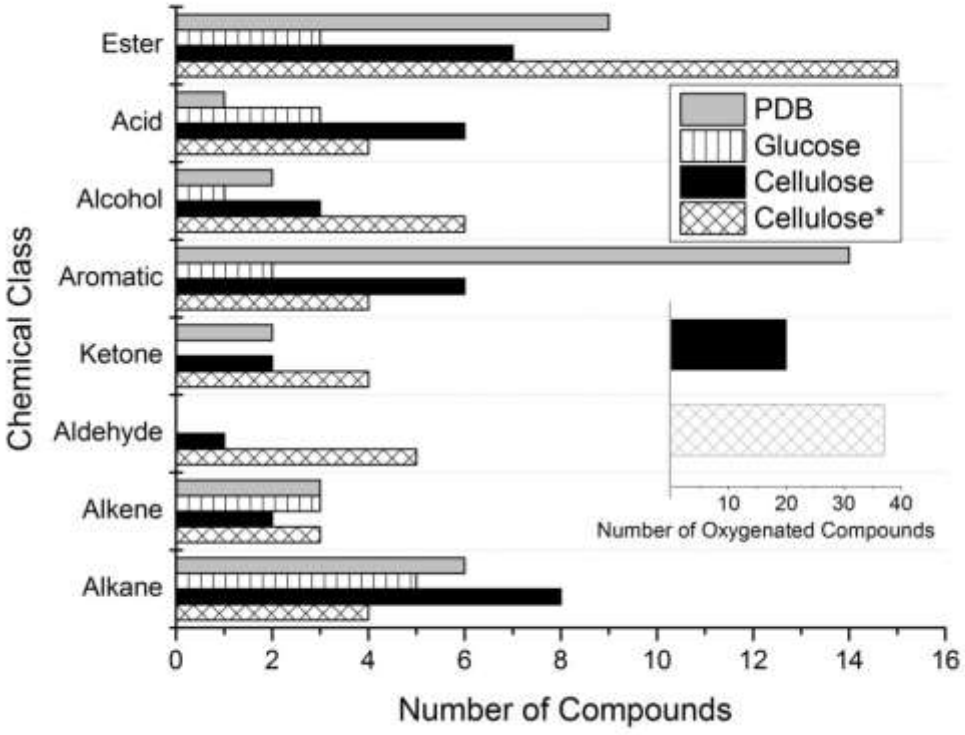

Figure 3.3. Compound diversity by class for hydrocarbon compounds produced by *A. sarcoides* on three substrates from day 5-17 of growth. Cellulose* = 17-32 days of growth. Inset: Total number of compounds containing the element oxygen for the cellulose substrate.

aldehyde compounds and had higher production of acids and alcohols than either PDB or GM. Growth on PDB had the highest production of aromatics (14 vs. 6) for CM growth and 2 for GM growth. HC production from CM as compared to GM showed greater numbers of almost all chemical classes at day 17 including aromatic compounds, 6 vs. 2, and alkanes, 8 vs. 5. The only exception to this observation was that there was one more alkene identified from growth on GM. The largest diversity of compounds produced by all three substrates were the aromatics and esters (Figure 3.3). Overall, the greatest diversity of compounds in every class except aromatics was produced with cellulose as the growth substrate.

The quantity of HC being produced is crucial to evaluating cellulose as an appropriate substrate for fuel production. Looking at the overall modest yields of fuel-range organic HC in Table 3.3, the highest yields of HC in the liquid cultures were diesel range organics (DRO), with a maximum at 45 mg*g biomass^{-1} from CM while GM and PDB grown cultures were much lower at 8.6 mg*g biomass^{-1} and 1.8 mg*g biomass^{-1}, respectively (Table 3.3). The gasoline range organics (GRO) showed an opposite trend, with glucose at 1.08 mg*g biomass^{-1}, with an order of magnitude lower result for the cellulose at 0.12 mg*g biomass^{-1}. Interestingly, the PDB culture had low yield results for both GRO and DRO, though PDB was the substrate from which the production of valuable HCs was first determined (Stinson et al., 2003). The greater DRO (C_9-C_{36}) yield compared with the more volatile GRO (C_5-C_{12}) (Table 3.3) for all cultures is an indication of the way the cultures were grown and does not capture the GRO potential of a culture grown with a sealed headspace environment. The total weight of volatile

hydrocarbons (VHC) adsorbed onto the external column excluding water weight are given, normalized to biomass concentration, in Table 3.3. When the HC recovered from the liquid and gas phases were added, the yield of HC from growth on CM was significantly higher per gram biomass than from growth on GM or PDB. This is a significant indication that *A. sarcoides* can more effectively utilize cellulose over simpler carbon sources for HC production.

Table 3.3. Yield of fuel-range organic HC from *A. sarcoides*. Gasoline Range Organics (GRO) and Diesel Range Organics (DRO) were liquid (l) bound products from growth of *A. sarcoides* on three substrates, which volatile hydrocarbons (VHC) were desorbed from external column collecting from the culture headspace gas (g). Cultures were grown at room temperature and aerobically with 1 liter/min air flow. Concentration measured by extraction and normalized to volume or grams of biomass in the liquid culture. Cellulose harvested at 32 days; glucose and potato dextrose broth harvested at 17 days.

		Medium		
HC Recovered	Phase	CM	GM	PDB
GRO (mg/L)	l	0.024	2.12	~0
GRO (mg/g biomass)	l	0.12	1.08	0.002
DRO (mg/L)	l	9	16.9	10.4
DRO (mg/g biomass)	l	45	8.6	3.2
VHC desorbed (mg/g biomass)	g	60.2	14.2	5.9
SUM (mg/g biomass)		105.3	23.9	9.1

The total fuel-range HC production yields shown in Table 3.3 also indicate cellulose as the most efficient substrate with a total yield of 105 mg of fuel-range organic HC per mg biomass, while the results for GM and PDB were respectively 24 and 9 mg of fuel-range organic HC per mg biomass. However, the total amount of HC collected was not impressive. The total from the liquid extractions were quite modest (< 20 mg/L) for all substrates with a maximum of 16.9 mg/L of on GM, and the highest yield of VHC collected from the headspace was 60.2 mg per g biomass. Other strains such as *Hypoxylon* sp. have shown potential for higher yields of HCs (Ul-Hassan et al., 2012), so this study also elucidates methods that can be applied to characterize the hydrocarbon production of other fungal strains. Overall, the substrate and product data indicate that diverse metabolic pathways may be used by *A. sarcoides* for different substrates.

Culture Age Effect: Gas-purged Reactors

Two time points for the 4 L cellulose culture were taken to assess the importance of sampling time on the HC results. Significant changes were seen in the VHC composition between the two time points. The number of compounds detected was nearly constant before (60 total) and after day 17 (61 total) (Figure 3.2B). However, the type of compounds varied significantly, with more unique compounds detected than similar ones: 23 compounds were consistent between time periods, with 37 being unique to days 5-17, and 38 unique to days 17-32.

Of the identifiable compounds, there was a significant change in speciation of the HC produced for the different time periods. Figure 3.3 shows that after day 17,

corresponding to late stationary phase of growth, there was a shift from aromatic and alkane production to more oxygenated compounds as represented by the ester, ketone, aldehyde and alcohol classes. The number of aromatic compounds detected decreased from 6 to 4, and the number of alkane compounds decreased from 8 to 4, while the ester compounds increased from 7 to 12 and the aldehydes increased from 1 to 5 compounds. This resulted in a significant increase in the total number of oxygenated compounds (Figure 3.3 inset) from 20 to 37 after day 17. The shift indicated there was a change in the metabolism of *A. sarcoides* near or during stationary phase which caused the unique speciation of compounds produced. During the increase in oxygenated compound production from days 17-32, there were many unique esters, aldehydes and alcohols detected. Aldehydes produced in stationary phase had increased carbon chain length, ranging from C_7-C_{11}, while the only aldehyde produced during the first time period, butanal, 3-methyl-, was a C_5 (Table 3.3). In addition, the longest chained esters, C_{15} and C_{16}, were produced during the second time period (Figure 3.4). In contrast, four unique alcohols, C_5 and C_6, were detected after stationary phase; shorter as a whole than the alcohols of first time period: C_5, C_8, and C_{10}. The total number of acids did not change significantly with age, and the same acids were produced in both time periods with only a few exceptions. Butanoic acid, 3-methyl-, C_7, was only detected from days 5-17. Hexanoic acid (C_6) and the longest acid at C_{12}, 5-decen-1-ol, acetate, were only observed from days 17-32.

A possible metabolism change in stationary phase is the oxidation of non-oxygenated HC to gain electrons. For example, 2-heptanone, 6-methyl- was only present

during the second time period and could have been oxidized from the alkene, 1-heptene, 6-methyl- (Table 3.3). Another compound only present during the second time period, 1-butanol, 3-methyl-, could have resulted from the oxidation of butane, 2-methyl- through the aldehyde intermediate butanal, 3-methyl-, also present during the first time period (Table 3.3). This potential conversion is consistent with biochemical oxidation of an alkane to an alcohol through an aldehyde intermediate. Further work is needed to track individual compounds through the entire growth cycle.

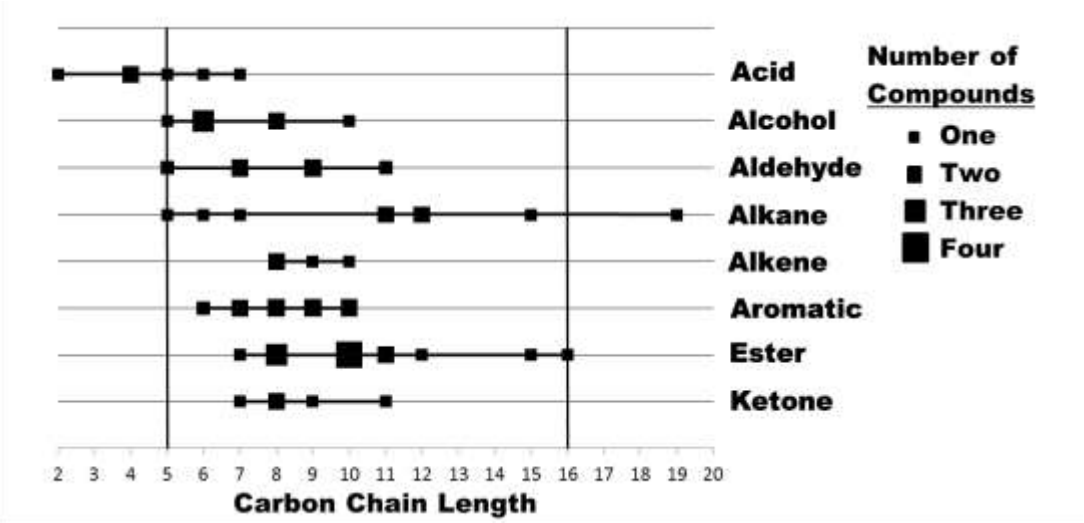

Figure 3.4. Identified HCs produced by *A. sarcoides* on cellulose grouped based on carbon chain length and sorted by class. Vertical lines denote the carbon chain length range including gasoline (C_5-C_{12}) and aviation fuel (C_8-C_{16}).

Identified VHC with Fuel
Potential: Gas-purged Reactors

Many of the compounds identified in this work have fuel potential, such as hexane, 3-methyl- and cyclopropane, propyl- (Table 3.2). Table 3.4 provides some non-oxygenated compounds along with their chemical properties. The non-oxygenated compounds for

Table 3.4. Octane ratings and enthalpies of combustion (ΔH_{comb}) for select non-oxygenated fuel compounds found from growth on cellulose which fit the carbon chain length and boiling point (T_b) requirements for gasoline fuel. The C_8 and higher compounds also could be applied to aviation fuel. All compounds were identified by GC-MS. Boiling points measured at 760 torr and enthalpies measured at standard conditions. Octane ratings are the average of Motor Octane Number and Research Octane Number (Ghosh and Jaffe, 2005). Source for boiling points and enthalpies from Yaws' Handbook (Yaws, 2003). N/A = no value available.

Compound Identification	**Formula**	**Fuel Class**	**Octane Rating**	**T_b (^oC)**	**ΔH_{comb} (kJ/mol)**	**CAS #**
Butane, 2-methyl-	C_5H_{12}	Isoparaffin	91	28	3240	78-78-4
Cyclopropane, propyl-	C_6H_{12}	Cycloparaffin	92	69	3765	2415-72-7
Hexane, 3-methyl-	C_7H_{16}	Isoparaffin	75	92	4466	589-34-4
1,4-Hexadiene, 3-ethyl-	C_8H_{14}	Olefin	84	109	N/A	2080-89-9
1-Heptene, 6-methyl-	C_8H_{16}	Olefin	84	113	4959	5026-76-6
Hexane, 3,3-dimethyl-	C_8H_{18}	Isoparaffin	72	112	5072	563-16-6
Benzene, 1,2,4,5-	$C_{10}H_{14}$	Aromatic	104	197	5520	95-93-2
d-Limonene	$C_{10}H_{16}$	Aromatic	104	177	5824	138-86-3
Nonane, 4,5-dimethyl-	$C_{11}H_{24}$	Isoparaffin	55	182	6916	17302-23-7
Undecane, 3-methyl-	$C_{12}H_{26}$	Isoparaffin	5	210	7528	1002-43-3
Dodecane	$C_{12}H_{26}$	Paraffin	-40	216	7530	112-40-3

which enthalpy of combustion values (ΔH^{o}_{comb}) were available included four isoparaffins, two olefins, and two aromatic compounds. The compounds' carbon lengths ranged from C_5-C_{12} and boiling points from 28 to 216^{o}C. The boiling point for all compounds falls within the boiling point requirement (25-230^{o}C) and carbon chain length, C_5-C_{12}, range for gasoline fuel, while the majority fit the boiling point requirement (126-287^{o}C) and carbon chain length, C_8-C_{16}, for aviation fuel (Figure 3.3) (Speight, 2002; Yoon and Lee, 2012). Only 7% (4 out of 61 total) of the compounds identified were outside of these ranges. In addition, *A. sarcoides* produced 38 unidentified compounds which were most likely of similar carbon length based on NIST MS spectra matches. However, these compounds did not meet the strict 75% quality match cutoff and identifications were not reported.

Aviation fuel is composed of 70-85% paraffins including isoparaffins, cycloparaffins and naphthenes (Blakey et al., 2011). In general, paraffins including isoparaffins compose 50% or more of refined naptha, the fraction used for commercial gasoline (Ciapetta and Wallace, 1972). The isoparaffins in Table 3.4 have the highest enthalpies of combustion by class with undecane, 3-methyl- at 7528 kJ mol^{-1} and nonane, 4,5-dimethyl- at 6916 kJ mol^{-1} and also the lowest octane ratings, a standard indicator of fuel combustion properties. The lowest octane rating at -40 comes from the paraffin, dodecane, with the highest enthalpy of combustion at 7530 kJ mol^{-1}. Since paraffins including isoparaffins compose such a large fraction of commercial gasoline, a negative or low octane rating does not preclude the use of a compound in a fuel mixture. The

aromatic compounds have the highest octane ratings by class with benzene, 1,2,4,5-tetramethyl- and d-limonene at 104.

In addition, other non-oxygenated compounds (one cycloparaffin, one olefin and one cyclo-olefin) were observed for which boiling points, octane ratings and/or enthalpies of combustion were not readily available in the literature: 1,3-hexadiene, 3-ethyl-2-methyl-; cyclohexane, propylidene-; and 1,5-cyclooctadiene, 1,5-dimethyl-. However, these compounds have the correct carbon chain length and branching properties for gasoline fuel. Compounds produced which were more suited for kerosene or diesel fuel included an isoparaffin: dodecane, 2,6,10-trimethyl- at a boiling point of 253^{o}C and a paraffin: nonadecane at 330^{o}C.

The compounds with fuel potential in Table 3.2also include numerous oxygenated compounds, such as alcohols, ketones and aromatics which can be further refined for use in fuel blends. It is clear that *A. sarcoides* produces compounds with gasoline fuel potential using cellulose as a feedstock (Table 3.2 and 3.4). The high numbers of alkanes and aromatics produced by *A. sarcoides* indicate that if overall yields can be significantly improved, refinement of the produced mixture could result in a high-octane fuel.

Conclusions

The diverse metabolic capability of *A. sarcoides* to utilize multiple carbon sources to produce gasoline, diesel and aviation range organics was demonstrated. The use of multiple analytical methods to assess HC production by *A. sarcoides* cultures in both the liquid and gas phases yielded a wealth of information. HC production variability was

observed with carbon source, medium concentration and pH of the culture indicating the potential to further optimize production by varying process and growth parameters. Both gasoline range (C_5-C_{12}) and diesel range (C_9-C_{36}) organics were detected in all cultured media. The highest levels of recovered HCs were measured from growth on cellulose at a pH of 5.8 and 23^{o}C. Cellulose stood out as the preferable substrate for HC production and fuel-related compounds based on the quantity and variety of fuel compounds produced. There was a pronounced shift to more oxygenated compounds, longer carbon chain length, and fewer fuel-related HCs as the cellulose culture progressed in stationary phase indicative of a change in carbon metabolism. Future refinement of production mechanisms by *A. sarcoides* and other similar fungi is warranted to increase HC yields for renewable production of liquid fuel compounds.

Acknowledgements

The authors would like to thank the National Science Foundation, Emerging Frontiers in Research and Innovation #093761 for funding this research. The NMR data was collected by the help of by COBRE award P20 RR024237 from the National Center for Research Resources (NCRR), a component of the National Institutes of Health (NIH) and its contents are solely the responsibility of the authors and do not necessarily represent the official view of NCRR or NIH. Our appreciation goes to Eric Booth for training on thermal desorption, to Dr. W. Berk Knighton for advice on analytical chemistry techniques, to Isabel M. Holtmeyer for proofreading and positive feedback,

and to Heidi Schoen for Figure 3 preparation assistance. Additional thanks to the research groups of Drs. Brent Peyton and Ross Carlson.

CHAPTER 4

OXYGEN AVAILABILITY INFLUENCE ON FUEL-RELATED HYDROCARBON AND LIPID PRODUCTION BY *ASCOCORYNE SARCOIDES*

Abstract

Ascocoryne sarcoides, a cellulolytic fungus which produces fuel-related volatile hydrocarbons, was studied for volatile organics and lipid production at different headspace oxygen concentrations and carbon to nitrogen ratios in the media. The fungus grew to a final biomass density near 0.4 g L^{-1} on a soluble form of cellulose, sodium carboxylmethyl cellulose, except under limited oxygen conditions of 7% O_2 initial headspace concentration. Nitrogen metabolism was impacted by oxygen availability and nitrogen concentration in the form of ammonia. The yield of biomass on nitrogen increased with decreasing nitrogen availability to a maximum of 229 g biomass (moles N)$^{-1}$ and decreased due to oxygen limitation to a minimum of 39 g biomass (moles N)$^{-1}$. A metabolic shift to fermentation was observed at the two lowest starting oxygen concentrations as evidenced by the production of acetate and ethanol.

The total yield of volatile organics (VOC) was less than 1.7 ppm (mg biomass)$^{-1}$. A distinct increase of detected VOC was seen at reduced headspace oxygen availability. The VOC ranged from C_2 to C_{15} in carbon length. C_8 compounds included C_8H_{18}, octane; $C_8H_{18}O$, 2-ethyl-1-hexanol; C_8H_{16}, 1,1-dimethyl-cyclohexane; C_8H_{14}, 1,3-octadiene; and $C_8H_{10}O$, phenylethyl alcohol.

Lipid yields were greatly impacted by initial oxygen concentration, with 10% starting oxygen concentration producing 50% more total lipid than 21% starting oxygen concentration. These results indicate reduced headspace oxygen concentrations increase VOC and lipid production by *A. sarcoides*.

Introduction

Ascocoryne sarcoides is an endophytic fungus capable of producing fuel-related hydrocarbon compounds directly from fermentation of cellulosic substrates (Strobel et al., 2008). This unique ability has been found in few fungi and has the potential to improve cellulosic biofuel production (Mends et al., 2012; Morath et al., 2012; Ul-Hassan et al., 2012; Zhi-Lin et al., 2012). The volatile organic compounds (VOC) produced by *A. sarcoides* include C_5-C_{19} alkanes, C_4-C_{10} alkenes, C_7-C_{11} ketones, and C_3-C_{10} alcohols. Previous laboratory work noted an increase in VOC production at lower oxygen values (unpublished data), which can be a useful trait in industrial scale processes, so this study sought to explore this environmental factor.

Gianoulis et al. (2012) suggested C_8 alcohols and ketones could be produced from the breakdown of linoleic acid ($C_{18}H_{32}O_2$), C18:2 unsaturated fatty acid, a lipid of cell membranes. Linoleic acid is known to be present in *Mucor* spp. and other fungi, along with palmitic (16:0), stearic (18:0) and γ-linoleic acids (18:3) (Somashekar et al., 2001). Culturing conditions are known to influence the production of lipids, e.g. linoleic acid, by oleaginous microorganisms such as *Rhodosporidium toruloides*; nitrogen limitation is especially important (Ratledge and Wynn, 2002). In similar tests, as carbon to nitrogen

ratios (C:N) increased, the lipid yield increased for *Trichosporon fermentans* until C:N of 163 was reached, then yield began decreasing (Zhu et al., 2008). Zhang et al. reported a similar response by *Cryptococcus curvatus* O3 of increasing lipid production with increasing C:N (Zhang et al., 2011).

Lipid production from microorganisms is a high potential feedstock for biodiesel production (Shi et al., 2011). Total biofuel potential of an oleganious organism can be estimated by transesterification of all lipids including intracellular and membrane-bound lipids (Gardner et al., 2013). A possible bioprocess enhancement for fungi like *A. sarcoides* that produce fuel-related VOC would be to harvest the final biomass for lipids, a biodiesel feedstock, after growth for VOC production. It is scientifically and industrially relevant to explore the lipid production potential of *A. sarcoides*.

Special consideration must be given to oxygen availability in industrial biochemical processes due to technical challenges associated with bioreactor operation (Tang et al., 2007). It is not uncommon for the oxygen concentration of a fermentation process to directly influence the metabolic products formed by organisms such as *Saccharomyces cerevisiae* (Varela et al., 2012). It was hypothesized that oxygen availability would impact the type and amount of VOC produced by *A. sarcoides*. It was also theorized that increased lipid production and specifically linoleic acid production should increase C_8 alcohol and ketone production by *A. sarcoides*. To advance the knowledge of *A. sarcoides* VOC and lipid production with these factors, experiments were conducted at three distinct starting oxygen concentrations, 7%, 10% and 21%, and lipid content measured at two distinct carbon to nitrogen ratios, 10 and 100. This chapter

reports the total biofuel potential defined by cellular lipid content at two distinct carbon to nitrogen ratios, shows evidence of enhanced metabolic diversity based on availability of carbon and nitrogen resources, as well as demonstrating VOC production at different oxygen concentrations.

Materials and Methods

Culture Medium and Conditions

Ascocoryne sarcoides (NRRL 50072) was grown in 20 mL sealed test tubes on a minimal cellulose medium consisting of (per liter): sodium carboxyl methylcellulose (10 g), $NaH_2PO_4 \cdot 2H_2O$ (2.75 g), $MgSO_4 \cdot 7H_2O$ (0.86 g), $Ca(NO_3)_2 \cdot 4H_2O$ (0.28 g), yeast extract (0.05 g), and trace salts: KCl (60 mg), KNO_3 (80 mg), $FeCl_3$ (2 mg), $MnCl_2$ (5 mg), $ZnSO_4$ (2.5 mg), H_3BO_3 (1.4 mg), and KI (0.7 mg). 100 millimolar KH_2PO_4 was added as a buffer. The medium was supplemented with ammonium chloride at either 1.76 g L^{-1} or 0.176 g L^{-1} to create two different carbon to nitrogen molar ratios (C:N), 10:1 and 100:1, respectively. The initial medium pH was 4.9. The media were inoculated with a 7-day culture prepared from Microbank^{TM} Bead frozen stocks (-80^{o}C). Three oxygen concentrations were used in the headspace of culture tubes. Tubes were crimp sealed with oxygen impermeable stoppers to prevent any ambient air from entering and altering the headspace conditions. Headspace was purged with N_2 to reach 10% and 7% oxygen concentrations and initial concentrations were confirmed by gas chromatography. Culture tubes were incubated at 21^{o}C at a fixed angle on rotary shakers at 150 rpm. In addition,

each condition was repeated in duplicate as 10 mL volumes in 20 mL solid phase microextraction (SPME) vials.

Biomass was determined in triplicate by cell dry weight (CDW) as described previously (Mallette et al., 2012) and by optical density at 600 nm (OD_{600}). Ammonium was assayed with Hach Method 10031 for High Range Nitrogen (Hach Company, Loveland, CO). Glucose, acetate and ethanol were measured by High Performance Liquid Chromatography on an Agilent 1200 with an Aminex HPX-87H ion exclusion column at 45^{o}C with 0.005 M H_2SO_4 eluent.

At the conclusion of the experiments, samples from the culture tube headspace were measured for oxygen and carbon dioxide concentrations. Concentrations of O_2 were measured with gas chromatography (GC) by 1 mL direct injection of culture tube headspace into a SRI8610C (SRI Instruments, Torrance, CA) with a 6 ft molecular sieve 13x column with helium carrier gas. CO_2 concentrations were measured in the same manner, with a 3 ft Hayesep-D column. CO_2 measurements were confirmed from diluted headspace samples by a LI-840 CO_2/H_2O Gas Analyzer (LI-COR Biosciences, Lincoln, NE). Samples were diluted first by injecting 10 mL of air into the tube headspace, then removing 10 mL after a mixing period of at least 5 minutes. Then diluted again by injecting the 10 mL into a bladder filled with 800 sccm of compressed air monitored by a mass flow controller. All values were corrected for un-inoculated controls. The concentrations were corrected for dilution as follows:

$$C_O = \frac{(C_s - C_b) * \left({}^{V_{Tc}}/_{V_s}\right) * V_t - (C_b * V_b)}{V_O} \qquad \text{eq 4.1}$$

Where C_O is the original concentration of CO_2 in the test tube headspace in ppm, C_s is the concentration reported by the LI-840 for the cultured sample in ppm, C_b is the background concentration of the compressed air used for dilution reported by the LI-840 in ppm, V_{Tc} is the total volume of the bladder corrected for the laboratory atmospheric pressure in mL, V_s is the sample volume in mL which is equivalent to V_b the background air injected into the test tube before the sample was taken, V_t is the volume of the test tube headspace after the addition of 10 mL of air, 31.7 mL, and V_O is the original volume of test tube headspace, 21.7 mL.

Volatile Hydrocarbon Analysis

VOC were measured in the headspace of 20 mL SPME compatible vials (HS-SPME). The vials were stored frozen before measurement by SPME GC-MS. In brief, a SPME fiber (divinylbenzene/Carboxen on polydimethylsiloxane by Supelco, Bellefonte, PA) was exposed to the vial headspace while heating to 30^{o}C for 45 minutes. The fiber was inserted into the injection port of the GC at 240^{o}C. The GC column temperature was held at 40^{o}C for 2 minutes, and then ramped to 230^{o}C at 5^{o}C min^{-1}. The relative amount of identified compounds was estimated by comparison with a 4-bromofluorobenzene (BFB) internal standard calibration curve delivered in methanol over the concentration range of 2 - 75 µg mL^{-1}. The GC was interfaced with a Hewlett Packard 5973 mass spectrometer which was tuned to meet EPA Method 8260 BFB tuning criteria.

Proton transfer reaction-mass spectrometry (PTR-MS) was used to quantify a selected set of volatile compounds produced by *A. sarcoides* by injecting a volume of the

test tube headspace into a pre-filled plastic bladder. The 10 mL volume from the headspace was diluted in the bladder by 800 sccm of compressed air measured by a mass flow controller. The air was allowed to mix for 5 minutes before measurements were taken. The bladder effluent was connected to the PTR-MS before the valve was opened to allow flow. Organic molecules in the gas phase were ionized with H_3O^+, forming protonated molecules (MH^+, where M is the neutral organic molecule) and fragment ions, which were detected by a standard quadrupole mass spectrometer. This process can be used with volatiles in air with or without dilution, since the primary constituents of air (nitrogen, oxygen, argon and carbon dioxide) have a proton affinity less than water and thus are not ionized. Most organic molecules (excepting alkanes) have a proton affinity greater than water and are therefore ionized and detected (Lindinger et al., 1998).

Measurements were made from control and cultured test tubes at the conclusion of the experimental time period or 112 hours after inoculation. Sample lines were constructed from PFA Teflon tubing and stainless steel fittings. Mass spectral scans were acquired from 20 to 220 amu at 0.5 sec/amu.

The absolute concentration of constituents in the sample were quantified directly from the measured ion intensities using the known reaction time and the theoretical reaction rate constant for the proton transfer reaction (Lindinger et al., 1998). Concentrations reported within were derived from the PTR-MS measurements and calculated using equations derived from reaction kinetics, assuming a reaction rate coefficient of 2×10^{-9} ml s^{-1} which is appropriate for the measured compounds (Ezra et al.,

2004; Lindinger et al., 1998). This method provided a means by which the measured ion intensity at any mass can be expressed as an equivalent estimate of concentration.

The total VOC concentration produced by the fungal culture is taken as the difference between the fungal culture and the control measurements. This total reflects only the contribution from those species having proton affinities greater than that of water, which is assumed to represent the majority of the VOCs produced. The concentrations were corrected for dilution similar to equation 1 above.

Lipid Analysis

Biomass harvested by centrifugation was washed to remove media components. Two different analyses were completed on biomass samples: GC-FID for neutral lipids and GC-MS for fatty acid methyl ester (FAME) identification and quantification. Neutral lipid analysis was performed using methods reported by Gardner et al. 2012 with minor modifications. After wet biomass pellet bead beating, 1 mL of chloroform was added to the pellet. The mixture was heated at 100^{o}C with continuous vortexing for 30 minutes. After cooling to at least 30^{o}C, 0.5 mL 15% NaCl was added, then vortexed and centrifuged to phase separate. The bottom layer (chloroform) was removed and added to a GC vial. The samples were analyzed by GC using 1 µL injections onto a 15 m (fused silica) RTX biodiesel column (Restek, Bellefonte PA), where the column temperature ramped from 100°C to 370°C at a rate of 10°C min^{-1} (1 min hold temperature at 100°C) with a 320°C injection temperature. Helium was used as the carrier gas and column flow was ramped at 0.2 mL min^{-2} from 1.3 (0-22 min) to 1.5 (22-24 min) to 1.7 mL min^{-1} (24-

36 min) (Gardner et al., 2013). This GC method allows for quantification of hydrocarbons, free fatty acids (FFA), monoacylglycerol (MAG), diacylglycerol (DAG), and triacylglycerol (TAG) in a single analysis. The total of FFA, MAG, DAG and TAG is defined as the total neutral lipid content.

FAME identification, quantification and fatty acid composition analysis were determined from direct *in situ* transesterification of wet biomass and analyzed with GC-MS on an Agilent 6890N and 5973 Network MS (Agilent, Santa Clara CA) per (Gardner et al., 2013). FAME content in biomass is defined as the total lipid biofuel potential.

Results & Discussion

Growth and Nutrient Use

Growth: A soluble cellulose substrate was used to allow measurement of biomass growth in real time by optical density. The sodium salt of carboxymethyl cellulose has been widely used in place of pure cellulose for endoglucanase enzyme studies of cellulolytic organisms (Lynd et al., 2002; Zhou and Ingram, 2000). Figure 4.1 shows *A. sarcoides* grew rapidly after a lag phase around 24 hours and reached stationary phase within 4 days. At each C:N ratio, the growth curves were very similar for the two highest oxygen concentrations (21% and 10%), but significantly slowed at 7% oxygen (Figure 4.1B). The difference in growth between 10 & 7% indicated that the oxygen threshold for *A. sarcoides* growth was reached by the 7% oxygen headspace and further reductions in

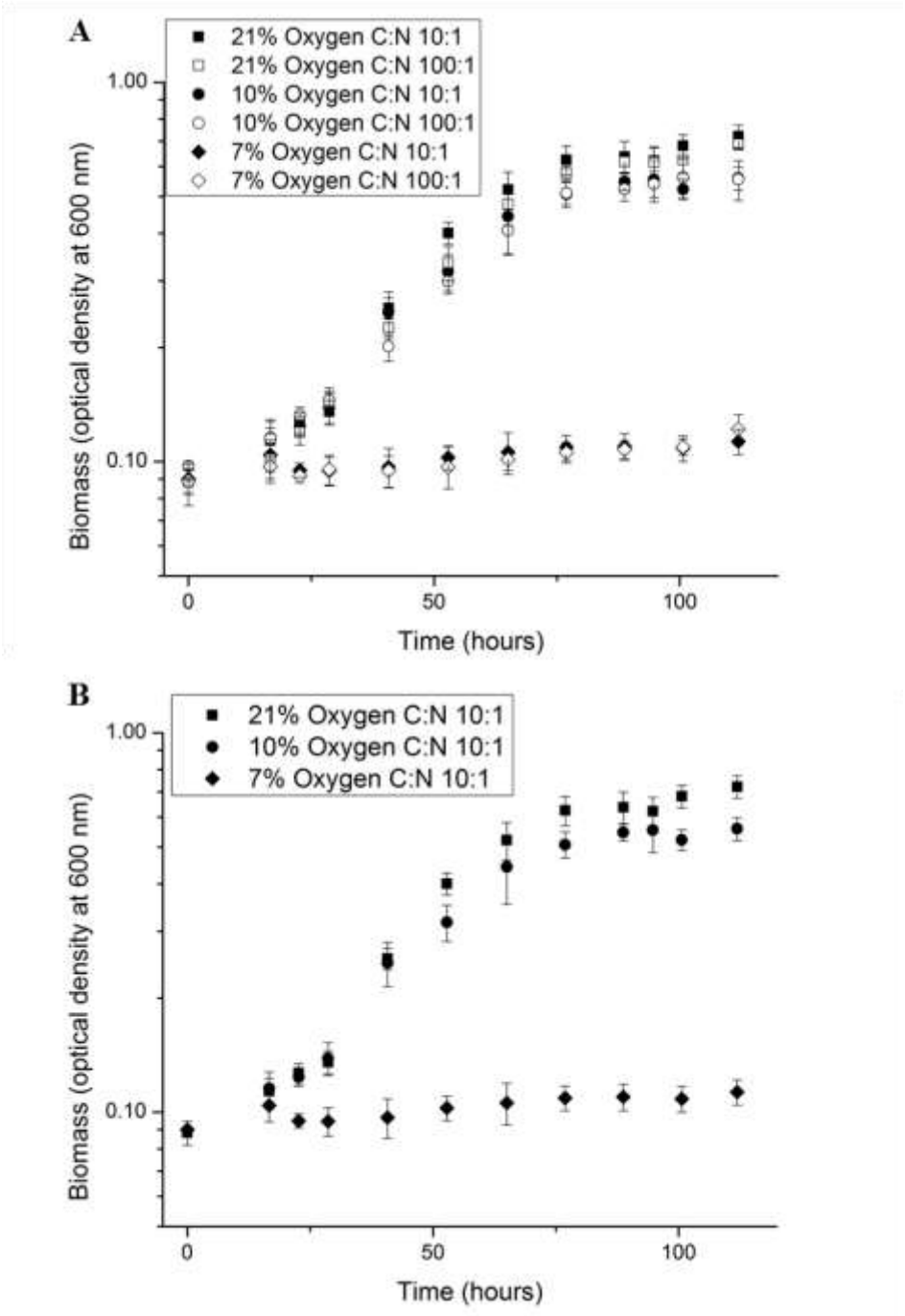

Figure 4.1. A. Growth curves of *A. sarcoides* on CMC at three oxygen concentrations (21, 10 & 7%) and two media formulations for carbon:nitrogen ratios (10:1 and 100:1). B. Growth curves for C:N 10:1 only. Error bars represent standard deviations.

oxygen are not necessary to study metabolic impacts of oxygen on growth. Based on the growth curves, oxygen concentration was the biggest factor, not the C:N ratio (Figure 4.1A). However, the maximum specific growth rates reveal a noticeable trend based on C:N ratio with all rates at the C:N 100 averaging lower than those at C:N 10 (Figure 4.2). The most significant effect was seen at the 10% oxygen concentration. The data indicated inhibition of growth at both C:N 100 at 7% oxygen headspace concentration.

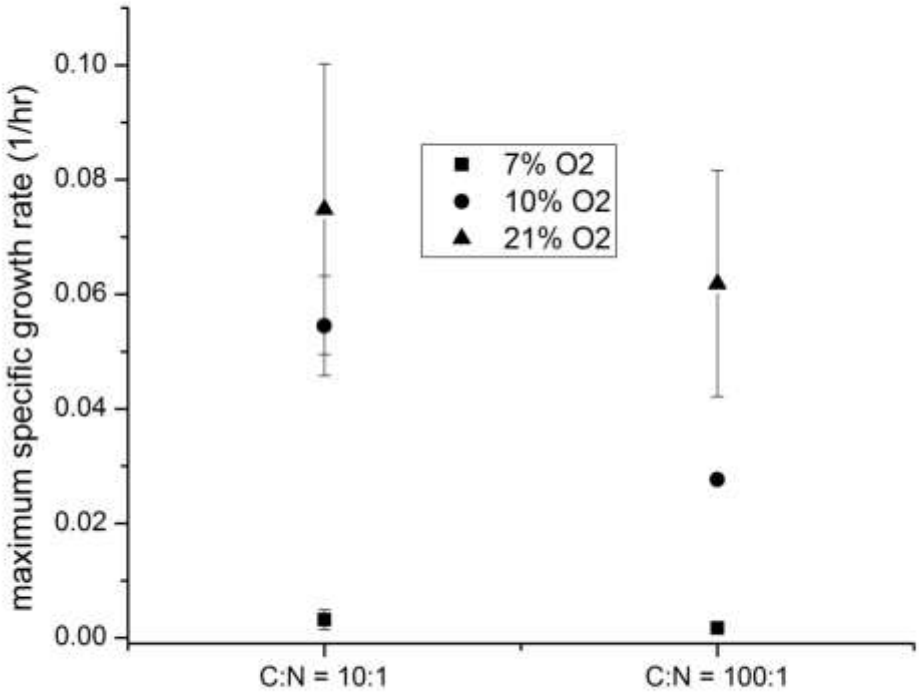

Figure 4.2. Maximum specific growth rates for *A. sarcoides* on CMC at three oxygen levels (21, 10 & 7%) and two media formulations for carbon:nitrogen ratios (10:1 and 100:1). Error bars represent standard deviations.

Substrate Use: A summary of nutrient usage by *A. sarcoides* based on starting oxygen concentration and C:N ratio is listed in Table 4.1. Yields of biomass on millimolar (mM) CMC utilized at 10% starting oxygen concentration were lower, 5.9 and 7.7 mg biomass (mM CMC)$^{-1}$, than at 21% starting oxygen concentration, 8.4 and 9.8 mg biomass (mM CMC)$^{-1}$, respectively. This indicated the use of CMC for growth at the 10% oxygen concentration was less efficient than at 21%. In addition, the yields of biomass on CMC were greater at C:N 100 than at C:N 10.

Nitrogen Use: The final nitrogen concentrations ranged from 0.53 mM N to 23.7 mM N (Table 4.1). The highest consumption of N at both C:N ratios was at 10% starting oxygen concentration (Figure 4.3). The cultures were impacted by the lower N available at C:N 100 given the low final concentrations for N and the higher yield of mg biomass per mM N (Table 4.1). For example, at 10% starting oxygen concentration, the final N concentration at C:N 100 was 0.53 mM and the yield was 113 mg biomass (mM N)$^{-1}$, while at C:N 10, final N was 21.2 mM and the yield was 52 mg biomass (mM N)$^{-1}$. The lower percentages of N consumption at the 7% starting oxygen concentration was not surprising due to the reduced biomass growth (Figure 4.1). Nitrogen use was also impacted by oxygen availability; more nitrogen was consumed by *A. sarcoides* to produce the same amount of biomass at the lower oxygen concentrations (Table 4.1). For example, the yields at 21% starting oxygen concentration are 153 mg biomass (mM N)$^{-1}$ and 229 mg biomass (mM N)$^{-1}$, which are higher than all the yields at 7% and 10% starting oxygen concentrations. This indicated that the nitrogen usage efficiency

Table 4.1. Nutrient usage and yields by *A. sarcoides* with growth on CMC. Respiration Quotient (RQ) is the ratio of CO_2 moles produced to moles of O_2 consumed.

Initial Headspace Oxygen (%)	7		10		21	
Initial Carbon:Nitrogen Ratio	**C:N 10**	**C:N 100**	**C:N 10**	**C:N 100**	**C:N 10**	**C:N 100**
CMC Usage (mM)	0.007±0.007	0.021±0.008	0.045±0.009	0.031±0.011	0.048±0.008	0.044±0.008
Yield (mg biomass/ mM CMC)	9.23	3.3	5.93	7.7	8.36	9.84
Final N (mM)	24.6±0.0	2.1±0.03	21.2±0.6	0.53±0.05	23.7±0.7	0.75±0.04
% N Consumed	6.5	2.2	19.4	80.1	10	71.8
Yield (mg biomass /mM N)	39	120	52	113	153	229
Final O_2 (mM)	221±11.3	223±10.6	191±10.1	219±53.4	542±19.1	548±8.7
Headspace O_2 Consumed (mM)	14.8±11.3	13.1±10.6	124±10.1	95.4±53.4	188±19.1	183±8.7
Yield (mg biomass/ mM O_2)	0.95	0.82	2.04	1.73	2.02	1.82
CO_2 produced (mM)	23.4±2.87	22.9±2.58	129±7.8	101±9.8	162±11.5	167±1.38
Yield (mM CO_2/mg biomass)	1.5	1.44	2.12	1.84	1.74	1.66
RQ	1.6	1.7	1	1.1	0.9	0.9

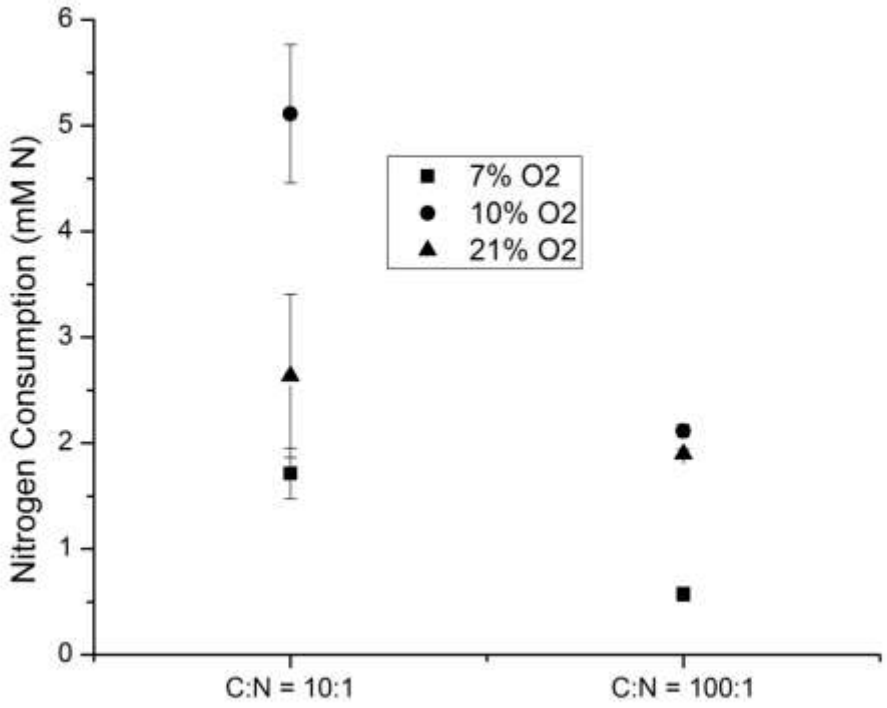

Figure 4.3. Nitrogen consumption by *A. sarcoides* on CMC at three oxygen concentrations (21, 10 & 7%) and two media formulations for carbon to nitrogen (C:N) ratios (10:1 and 100:1). Error bars represent mean difference standard error.

decreased due to oxygen limitation.

Oxygen Use & CO_2 Production: At C:N 100, there was more efficient use of N, but less efficient use of O_2. There was considerable variability in the oxygen concentration measurements, but the averages showed higher oxygen consumption at C:N 10, i.e. 816±83 mM O_2 versus 792±38 mM O_2 at C:N 100 (Table 4.1). Even with the higher consumption, *A. sarcoides* was able to more efficiently utilize oxygen at C:N 10

versus C:N 100 as evidenced by the higher yields of biomass on oxygen. For example, both yields at 10% and 21% starting oxygen concentrations were near 2.0 mg biomass $(mM\ O_2)^{-1}$ for C:N 10, about 10% higher than 1.7-1.8 mg biomass $(mM\ O_2)^{-1}$ for C:N 100. In general, the oxygen consumed by the cultures increased corresponding to the starting oxygen concentration (Figure 4.4A). The CO_2 production followed the same trend as the O_2 consumption with higher usage and yields at C:N 10 (Figure 4.4B and Table 4.1). CO_2 production measurements were only slightly below O_2 consumption measurements, indicating most of the oxygen consumed by *A. sarcoides* is converted to CO_2 through cellular respiration. The respiratory quotient (RQ), the molar ratio of CO_2 production and O_2 consumption, for each starting oxygen concentration are also listed in Table 4.1. The RQ values were consistent within starting oxygen concentrations with the highest values at 7% starting oxygen condition and the lowest at 21% starting oxygen concentration.

Production of Liquid By-products: Acetate and ethanol production by *A. sarcoides* is shown in Figure 4.5. At the 7% starting oxygen concentration, *A. sarcoides* produced significantly more acetate and ethanol at both C:N ratios. Ethanol and acetate were not detected in the 21% starting oxygen concentration cultures. Acetate concentrations at both C:N ratios for 7% starting oxygen concentration were 2.0 mM or greater, and 0.7 mM and 1.4 mM at the 10% starting oxygen concentration, despite much higher biomass at the 10% starting oxygen concentration (Figure 4.1). There was no

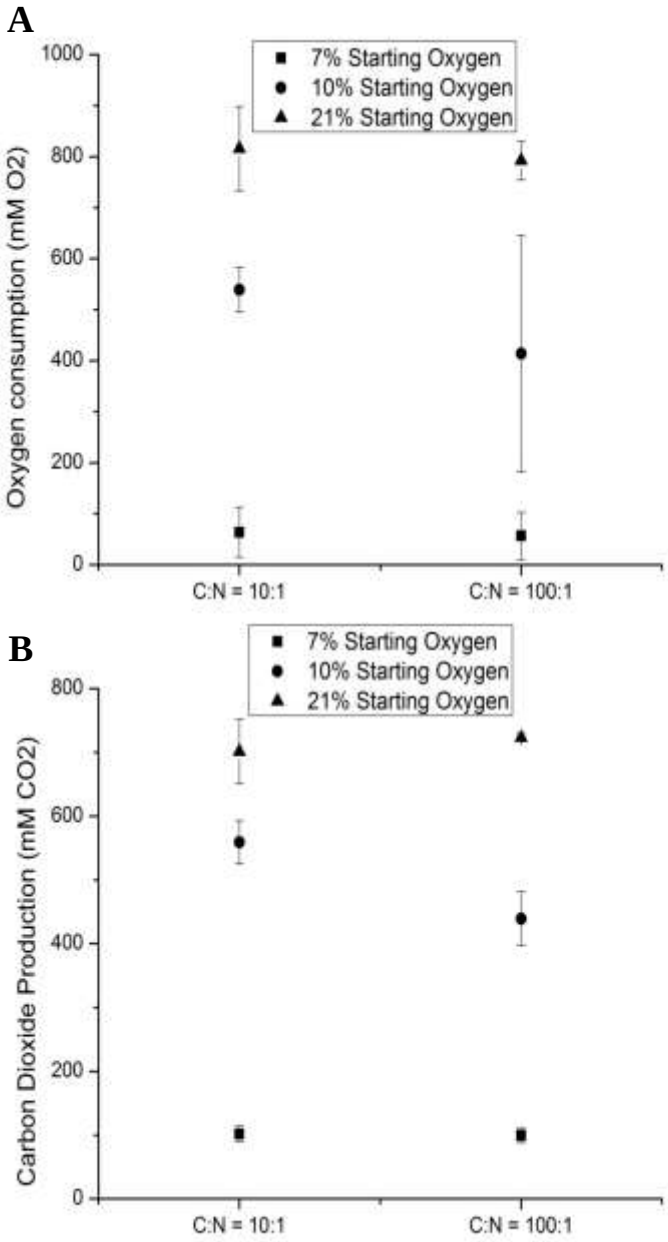

Figure 4.4. Respiration of *A. sarcoides* on CMC at three oxygen concentrations (21, 10 & 7%) and two media formulations for carbon:nitrogen ratios (10:1 and 100:1). A. Oxygen consumption was measured in the headspace and reported as concentration in millimolar (mM). B. Carbon dioxide production. Concentrations were measured by GC and standard deviations reported.

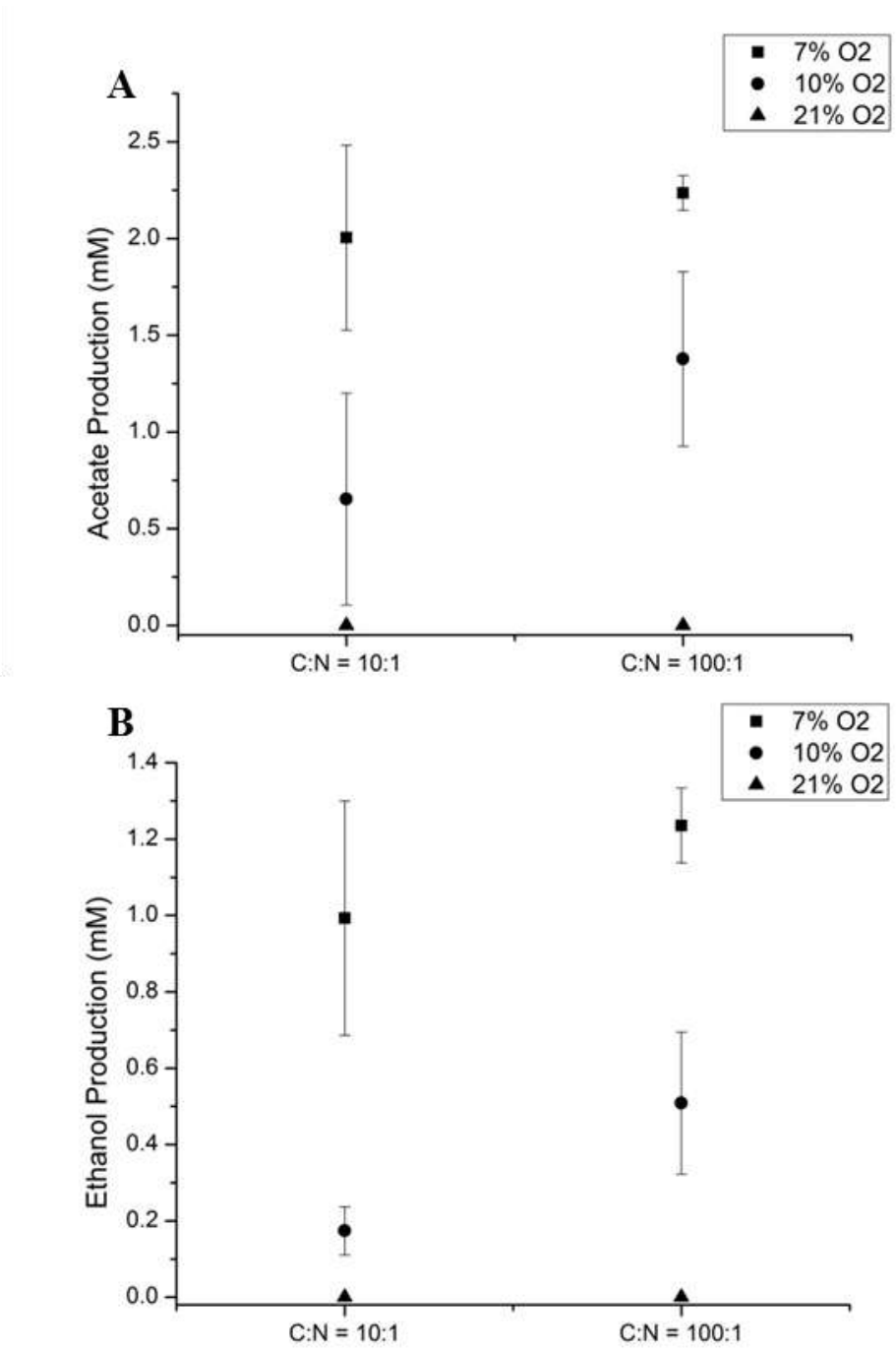

Figure 4.5. Acetate and ethanol concentrations for *A. sarcoides* on CMC at three oxygen concentrations (21, 10 & 7%) and two media formulations for carbon:nitrogen ratios (10:1 and 100:1). Concentrations were measured by HPLC. Error bars represent standard deviations.

glucose detected in any sample, which indicated the fungus was immediately utilizing any released glucose from CMC, keeping the concentration below the detection limit of the HPLC.

This data indicated a metabolic shift to fermentation under reduced oxygen conditions that corresponded to around 220 millimolar O_2 or 7% starting oxygen concentration (Table 4.1). The greatest amount of fermentation byproducts, ethanol and acetate, were seen for the 7% starting oxygen concentration. These byproducts were also detected from the 10% starting O_2 concentration cultures which reached final oxygen concentrations around 200 millimolar O_2, very similar to the 7% cultures. This was not observed at the 21% initial oxygen concentration, most likely because the oxygen available in the system did not require a switch from glycolysis to fermentation.
The metabolic change to fermentation by *A. sarcoides* near 220 millimolar O_2 was also impacted by reduced nitrogen availability with higher concentrations of ethanol and acetate detected at C:N 100 versus C:N 10. Specifically, at C:N 100, the statistically significant decrease in CO_2 production (Figure 4.4B) and increase in ethanol production (Figure 4.5B) at the 10% starting oxygen concentration indicated *A. sarcoides* was breaking apart the TCA cycle to find a shorter pathway to process available carbon to reduce protein processing costs. This was most likely due to the reduced availability of nitrogen for protein synthesis (Table 4.1). It also indicated that fermentative pathways were being used due to the lower availability of oxygen for respiration (Table 4.1). Flamholz et al. have shown varying use of glycolytic pathways by prokaryotes due to oxygen requirements and protein requirements for pathway enzymes (Flamholz et al.,

2013). The results shown here supports their finding that reduced availability of resources such as nitrogen and oxygen will cause metabolic regulation changes.

Volatile Hydrocarbons

At the conclusion of the experiments, there was no statistically significant difference between the diluted culture headspace and the compressed air for VOC measurements recorded by PTR-MS. The total concentration registered in sample was 608 ± 74 ppbv while the un-inoculated control sample was 582 ± 33 ppbv. After correcting for dilution, this corresponds to 3.36 ppm from the culture headspace. For a 1 liter culture under the same conditions, the concentration expected in a relative headspace environment is 671 ppm of total VOC, a yield of less than 0.07 ppm/mL or 1.68 ppm (mg biomass)$^{-1}$. Unfortunately, due to dilutions made in this method, the VOC concentrations were not high enough to be accurately measured, so the reported values must be considered estimates.

Complete quantification of VOC is limited by the HS-SPME technique due to the varied fiber affinity of the compounds in the headspace mixture (Mallette et al., 2012; Stashenko and Martínez, 2007). Therefore, individual compounds were not quantified in Table 4.3. However, an integration of the peak areas of the entire mass spectra shows the total amount of material adsorbed by the fiber without speciation. Details of this analysis are listed in Table 4.2. The amount of VOC material desorbed from the SPME fiber ranged from 123-163% higher than the controls. With the internal standard estimate, this correlated to 20.3 to 113 ng VOC per mg of culture biomass, with an average of 51.3 ng

VOC per mg biomass. The highest values were at the lowest oxygen condition of 7% due to similar levels of VOC and lower biomass concentrations compared to the higher oxygen conditions.

Table 4.2. VOC quantification estimates for *A. sarcoides* growth on CMC at 7, 10 & 21% starting oxygen concentration and C:N = 10 and 100. Standard deviations are reported for VOC area and standard error of the mean difference for VOC mean difference with controls.

Starting Concentration of Oxygen (%)	C:N	VOC area	VOC mean difference with controls (ng/mL)	VOC estimate (ng/mg biomass)
7	10:1	3.31E8±4.3E6	64.2±1.9	95.0
7	100:1	3.74E8±2.1E6	77.6±1.9	112.6
10	10:1	3.58E8±2.3E7	73.5±1.9	27.8
10	100:1	3.71E8±8.1E7	76.5±1.9	32.0
21	10:1	3.91E8±2.9E7	82.1±1.9	20.3
21	100:1	4.0E8±6.3E7	88.3±1.9	20.3

Converting the PTR-MS concentrations to the same conditions as the SPME vials which have less than half the headspace, but twice the culture liquid, the yield for C:N 100 with 10% starting oxygen concentration is 0.061 mg VOC per mg biomass compared to 3.2E-4 mg per mg biomass. So, the yields obtained by HS-SPME GC-MS are substantially lower than measured values from PTR-MS. Due to the dilutions made for

Table 4.3: Volatile compounds detected and identified from *A. sarcoides* cultures grown on CMC at 7, 10 & 21% starting oxygen concentrations and two carbon to nitrogen (C:N) ratios. Analysis completed by HS SPME GC-MS. *Detected from *A. sarcoides* previously (Griffin et al., 2010; Mallette et al., 2012; Strobel et al., 2008).

		7% Oxygen		10% Oxygen		21% Oxygen	
Retention Time (min)	Compound Detected	C:N 10	C:N 100	C:N 10	C:N 100	C:N 10	C:N 100
1.9	Hexane, 3-methyl-	X	X			X	X
2.5	Octane*	X	X	X	X	X	X
3.7	Ethyl Acetate*	X	X	X	X		
4.5	Dimethyl ether	X	X	X	X		
4.8	1,3-Octadiene					X	X
8.4	1-Propanol, 2-methyl-*	X	X				
8.8	1-Butanol, 3-methyl-, acetate*	X	X	X	X		
11.4	1-Butanol, 3-methyl-*	X	X	X	X	X	X
11.9	Furfurylmethylamphetamine			X	X		
13.1	Butanoic acid, 2-methyl-, 3-methylbutyl ester	X	X				
15.4	Cyclopropane, propyl-*	X	X	X	X	X	X
15.8	Acetic acid, pentyl ester*	X	X	X	X		
16.3	2-Nonanone*	X	X	X	X	X	X
18.1	2-Heptanol, acetate	X	X	X	X		
18.5	Acetic acid, heptyl ester*	X	X	X	X	X	X
18.8	Acetic acid*	X	X	X	X	X	X
18.9	1-Hexanol, 2-ethyl-	X	X				
19.4	3-Octen-1-ol, acetate, (Z)-					X	X
19.7	Acetic acid, octyl ester*	X	X				
20.2	Cyclohexane, 1,1-dimethyl-	X	X				
21.1	Acetic acid, nonyl ester*	X	X	X	X	X	X

Table 4.3 Continued

22.8	Butanoic acid, 4-hydroxy-			X	X
23.5	Acetic acid, decyl ester*	X	X	X	X
24.0	4-Hexen-1-ol, acetate, (Z)-			X	X
24.1	3-Decen-2-ol, (E)-			X	X
25.6	2-(1-Cyclopent-1-enyl-1-methylethyl)cyclopentanone			X	X
28.9	Phenylethyl Alcohol*	X	X		

the PTR-MS measurements, the scatter in the data does not allow accurate interpretation and calculation of the yield, so the higher calculated yield is suspect and the method requires larger scale cultivations to avoid extensive dilution. However, the dramatic difference would indicate that the larger scale cultivations would be useful to more accurately determine VOC yields.

Headspace oxygen concentration influenced VOC production (Figure 4.6). Oxygen concentrations below 21% produced greater diversity of HC. The 7% oxygen concentration had similar numbers and levels of VOC to 10% oxygen, despite that the oxygen availability at 7% significantly impaired growth. The compounds identified included alcohols, ketones, aromatics, alkanes, an alkene, an ether, acids and their esters (Figure 4.7, Table 4.3). The greatest number of identified compounds were classified as acid esters for all conditions. The compounds ranged from C_2 to C_{15} in carbon length. C_8 compounds included C_8H_{18}, octane, $C_8H_{18}O$, 2-ethyl-1-hexanol, C_8H_{16}, 1,1-dimethyl-cyclohexane, C_8H_{14}, 1,3-octadiene, and $C_8H_{10}O$, phenylethyl alcohol. A few compounds were only detected at the 21% oxygen concentration; at C:N 10, 3-Octen-1-ol, acetate was present which has also been observed from aerobic cellulose and PDB growth (Mallette et al., 2013), and 1,3-Octadiene, a C_8 alkene, was detected. The 7% oxygen condition had the most identified compounds at 19, while 21% returned the lowest numbers of compounds at 8 and 9 for C:N 100 and C:N 10, respectively. Surprisingly, the lowest oxygen concentration, 7%, had the highest number of alkanes and alcohols despite the significantly lower biomass concentration.

In reference to the possible production of C_8 alcohols and ketones from linoleic acid, one C_8 alcohol was detected, 1-hexanol, 2-ethyl-, but no C8 ketones were found in these analyses (Table 4.3). Equivalent HS-SPME measurements from previous experiments have also detected two additional C_8 alcohols, 1-octanol and 1-octen-3-ol (Griffin et al., 2010; Mallette et al., 2012), as well as three C_8 ketones, 6-methyl-2-heptanone, 3-octanone and 7-octen-2-one (Griffin et al., 2010). However, in the previous studies none of the compounds were detected from *A. sarcoides* growth on a cellulosic carbon source.

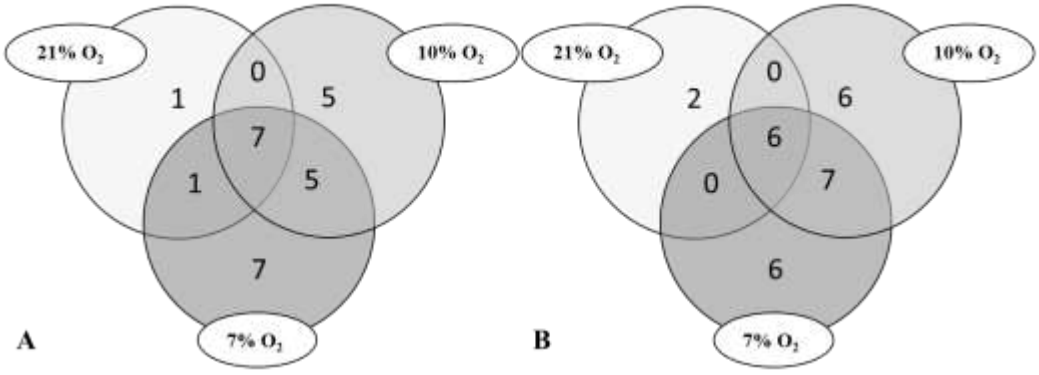

Figure 4.6. VOC distribution among oxygen concentrations for *A. sarcoides* grown on CMC. A. C:N = 10:1 and B. C:N = 100:1. Compounds reported include identified compounds as well as those lacking a match in the mass spectrometry ionization spectra library database.

Another possible reason for the lack of C_8 ketones and alcohols in this study is the levels of VOC in these experiments were below those previously found due to medium and culturing condition variations. A way to improve the recovery of compounds is to continuously collect and concentrate them on an external adsorbent column (Discussed in

Chapter 3), but in this case, it would have required extensive redesign of the experimental conditions and analysis parameters (Booth et al., 2011).

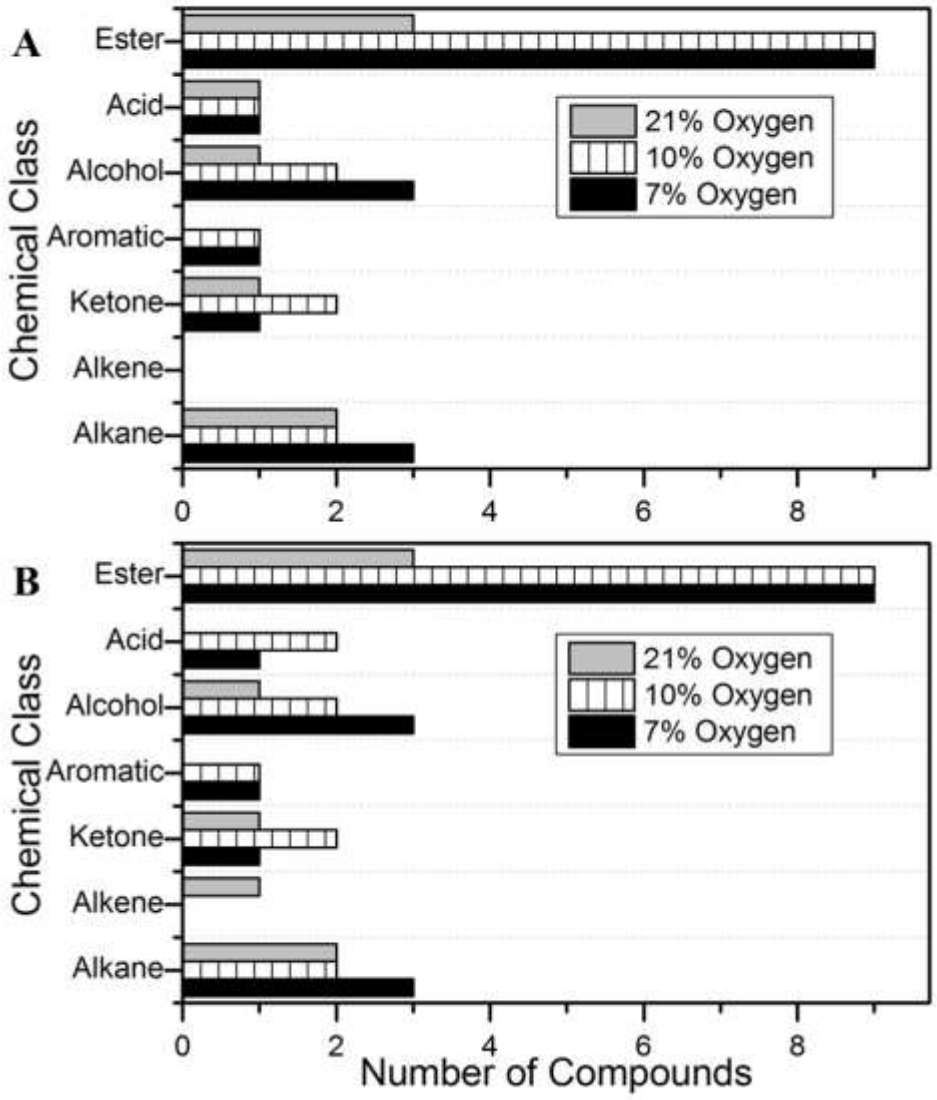

Figure 4.7. Identified VOC classification based on oxygen level and for C:N ratios A. 10:1 and B. 100:1.

Lipid Accumulation

Total and specific lipid accumulation were measured to gain an accurate measure of the residual biofuel potential of *A. sarcoides* in addition to fuel-hydrocarbon production and also to assess changes in linoleic acid production. The 10% oxygen concentration had nearly double the recovered concentration of FAME and total neutral lipids, defined as the total of FFA, MAG, DAG and TAG, than 21% oxygen cultures, regardless of C:N ratio (Figure 4.8). The 7% oxygen concentration did not reach high enough biomass concentrations to be extracted. The neutral lipids ranged from 1.9-2.0% w neutral lipids/w biomass at the 21% oxygen concentration and 3.5-3.9% w/w at the 10% oxygen concentration (Figure 4.8A). Total FAME or lipid biofuel potential ranged from 3.1-3.3% w FAME/w biomass at 21% oxygen and 7.4-7.5% w/w at 10% oxygen (Figure 4.8B). The extractable neutral lipids included C_{12}-C_{18} FFA, MAG, DAG and TAG. The majority of the extractable lipid content was DAG, consistently ranging from 32-42% of the total neutral lipids (Table 4.4). Nile red staining is often used to assess lipid potential, and it can be used to visualize lipid bodies in cells (Gardner et al., 2013). Figure 4.9 shows an example of Nile Red fluorescence of *A. sarcoides*, but microscopy was not used extensively in this study.

No significant difference in lipid production between the C:N ratios was seen for both total extractable lipids and FAME after transesterification even though it was expected based on the final nitrogen concentrations. The final nitrogen concentrations at C:N 100 were 0.75, and 0.53 mM N for the 21% and 10% starting oxygen concentrations, respectively (Table 4.1). These values were significantly lower than at C:N 10 where

final nitrogen concentrations were 26.7 and 23.9 mM N, respectively. In addition, the distribution of nitrogen consumption in this study indicated that the cells at C:N 100 were nitrogen limited at this ratio with both 21% and 10% starting oxygen concentrations consuming over 70% of the available nitrogen; while at C:N 10, 10 and 20% of the N was consumed, respectively (Table 4.1). The results indicated there was an impact of C:N ratio on nitrogen metabolism, but if there exists a threshold for limited nitrogen which inflicts lipid metabolism, it was not reached with these experiments. *Rhodotorula gracilis* showed a significant difference between lipid production at C:N 160 vs. C:N 40, but little difference at C:N 40 vs. C:N 10 (Somashekar and Joseph, 2000). A difference in lipid production by *T. fermentans* was seen between C:N 108 vs. C:N 163 (Zhu et al., 2008). Therefore, a further increase of C:N could result in a lipid composition.

Linoleic acid is a polar membrane lipid component and should be detectable by GC-MS from solvent extracted samples. The polar lipid fraction is the difference between the total FAME and total extractable neutral lipids. C18:1-3 lipids, including the FAME C18:2 of linoleic acid, were by far the highest percentage of FAME detected for all replicates, ranging from 70.8-75.4% of the total FAME (Table 4.4). This study did not find increased VOC production of C_8 alcohols and ketones with increased lipid production. If the mechanism of producing C_8 alcohols and ketones from linoleic acid proposed by Gianoulis et al. (2012) is true, if the total recovery of C18 FAME did not change, then it follows that the production of C_8 alcohols and ketones would also not change. There were not enough detected C_8 VOC compounds in this study to determine if

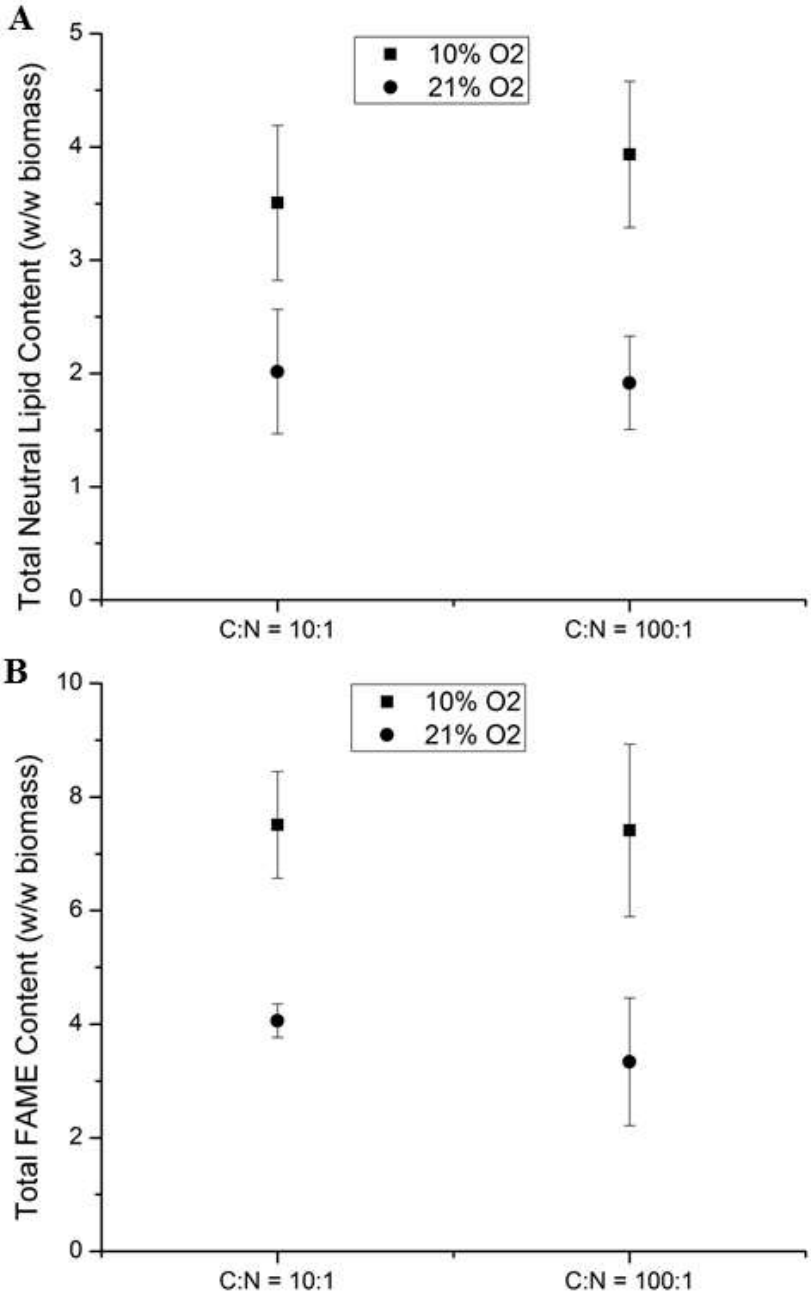

Figure 4.8. Lipid Production by *A. sarcoides*: A. Free Fatty Acid content and B. Fatty Acid Methyl Esters (FAME) weight percentages of extracted biomass at 21 and 10% oxygen and at C:N =10 and C:N = 100 with standard deviations.

Table 4.4. Percent (w/w) extractable neutral lipids, fatty acid methyl esters (FAME)/total biofuel potential and polar lipids as the difference of FAME and the neutral fraction. Reported for *A. sarcoides* cultured on CMC at 10 & 21% starting oxygen concentration and C:N = 10 and 100.

% Oxygen	C:N	FFA (%)	MAG (%)	DAG (%)	TAG (%)	Total Neutral (%)	FAME (%)	Total Polar (%)
10	10:1	0.9±0.4	0.7±0.6	1.3±0.05	0.5±0.5	3.5±0.7	7.5±0.9	4.0
10	100:1	1.2±0.1	0.5±0.3	1.6±0.2	0.7±0.1	3.9±0.7	7.4±1.5	3.5
21	10:1	0.7±0.1	0.3±0.1	0.7±0.2	0.3±0.2	2.0±0.6	4.1±0.3	2.1
21	100:1	0.5±0.3	0.4±0.2	0.7±0.2	0.3±0.1	1.9±0.4	3.3±1.1	1.4

the proposed mechanism is valid. It is possible that the metabolic pathways responsible for linoleic acid breakdown were not active in our experiments.

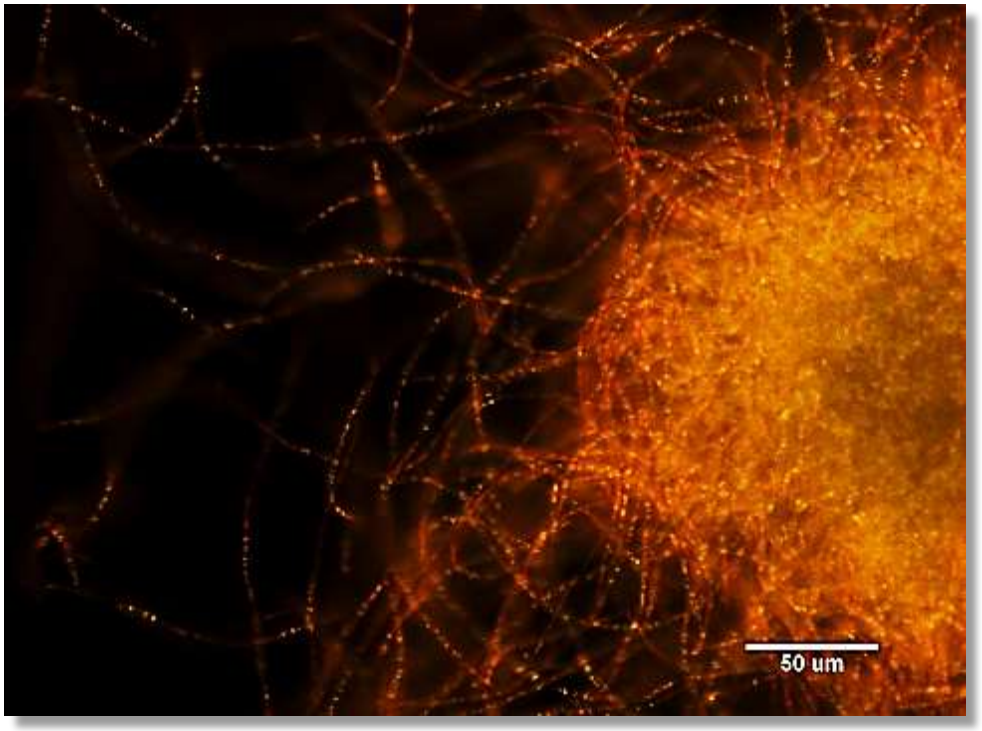

Figure 4.9. A floc of *A. sarcoides* stained with Nile Red which fluoresces yellow/green when bound to lipids. The fluorescence was imaged on a Nikon Eclipse E800 epifluorescence micropcope using a 20x objective and a B2A filter cube (EX 470/40, 500 LP, EM 515).

Conclusion

These results indicate reduced headspace oxygen concentrations boosted VOC and lipid production by *A. sarcoides*. The fungus grew well on CMC with 21 and 10% oxygen at both C:N ratios of 10 and 100. The carbon and nitrogen needed for metabolism and respiration were greatly increased at the lowest oxygen concentration (7%), and the limited oxygen greatly impaired growth. In addition, a fermentative shift was seen at the

7% oxygen concentration to greater acetate and ethanol production yields. The respiratory quotients ranged from 0.9 to 1.7, increasing based on increasing headspace oxygen availability.

The total yield of volatile organics was low, near 1 ppm per mL of culture liquid. The highest VOC yield was 113 ng VOC per mg of biomass with a C:N of 10 and 7% headspace oxygen. In addition, the lowest oxygen concentrations produced the greatest VOC diversity despite low biomass concentrations and more than double the number of compounds were detected compared with the 21% oxygen condition. There were a variety of VOC produced by *A. sarcoides* under the studied conditions including C_4-C_{10} alcohols, C_6-C_8 alkanes, C_4-C_{11} acid esters, and C_2-C_4 acids.

The total biofuel potential measured as FAME was significantly influenced by the oxygen concentration. The highest FAME concentration was at the 10% starting oxygen concentration and there was no significant difference between the two C:N ratios at this concentration. The FAME quantification comprises total polar or membrane bound lipids which include linoleic acid. The contribution from C18:1-3 lipids was over 70% of the total in all conditions, but there was not a significant change in C_8 VOC detected based on lipid variations.

Acknowledgements

The authors would like to thank the National Science Foundation, Emerging Frontiers in Research and Innovation #093761 for funding this research. Our appreciation goes to Dr. Rob Gardner and Egan Lohman for assistance with lipid extraction methods,

Chris Allen and Stephen Markwardt for assistance with total organic carbon measurements and Dr. Albert Parker for help with statistical analysis and modeling of data.

CHAPTER 5

CONCLUSIONS & FUTURE WORK

Project Summary

Before the discovery of *Ascocoryne sarcoides* (Figure 5.1), the possibility that hydrocarbon fuel between C_5 and C_{12} in carbon chain length could be produced by bacteria, fungi or yeasts directly from cellulosic sources was not seriously considered. Prior to the materialization of this project, research on *A. sarcoides* was completed like other mycology research, on solid agar medium. Little engineering research had been completed, especially in relation to the impact of factors related to bioprocess engineering: culturing conditions, growth kinetics, and yields of products. This project fills the gap by describing the conditions necessary to culture *A. sarcoides* in liquid medium, as well as factors influencing the production of volatile fuel-related compounds.

This dissertation is the summary of work completed to evaluate *A. sarcoides* volatile hydrocarbon production and the factors which influence this production. It summarizes experiments conducted to evaluate growth and volatile production by the fungus on different carbon sources and under varying pH, temperature, and oxygen concentrations. It explores the use of established analytical methods for the fungal system, and presents a new way to use the volatile data to better describe the system. The work showed potential fuel production from growth on cellulose and summarized the fuel

potential for many of the compounds detected using enthalpies of combustion and octane ratings.

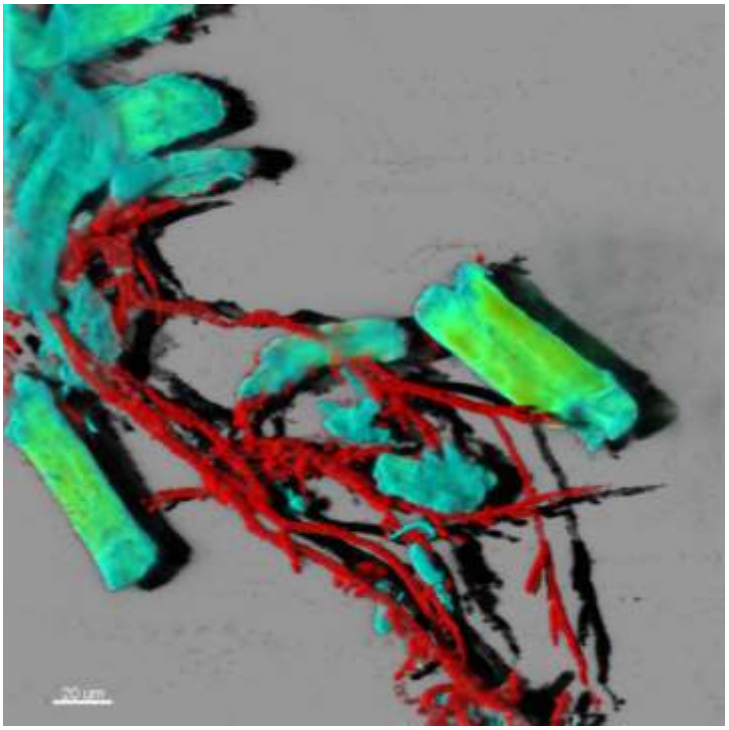

Figure 5.1. *Ascocoryne sarcoides* (red) a filamentous fungus growing on cellulose (blue/green) in liquid culture, imaged with confocal scanning laser microscopy. Hyphae are closely tied to cellulose particles (blue/green), effectively clumping them together. *A. sarcoides* produces gasoline, aviation and diesel fuel-related compounds on cellulose, the most abundant and affordable source for producing biofuels.

Fulfillment of Project Objectives

The specific goals of this project were as follows, and each objective is addressed by the chapters of this dissertation. In most cases, multiple chapters address each objective, so a summary of each goal follows.

i. Achieve *A. sarcoides* Growth
in Liquid Media and Improve to
Industrially Relevant Concentrations.

Appendix A, Preliminary Methods Development with *Ascocoryne sarcoides*, outlines medium development for liquid culture of *A. sarcoides* on glucose. Positive growth was seen in liquid media, but initial biomass densities were quite low - less than 0.5 optical density at 600 nm. Medium formulation was tested, and as a result, nitrogen and phosphorous were altered to improve maximum biomass concentration to nearly 5 g L^{-1} in glucose medium.

ii. Measure the Growth of *A. sarcoides*
and Compare Maximum Specific Growth
Rates Under Different Conditions.

Maximum specific growth rate variation based on medium formulation and headspace oxygen concentrations were found with *A. sarcoides*. The highest average maximum specific growth rate at 0.085 ± 0.035 hr^{-1} was observed from growth on glucose, and the lowest average at 0.014 ± 0.003 hr^{-1} was observed from growth on cellulose. The maximum specific growth rate was influenced by the concentration of nitrogen in the medium, because at lower nitrogen concentrations, the growth rate slowed. The growth rate significantly increased in relation to an increase in the starting oxygen concentration of a sealed culture headspace. The growth rate 0.0032 ± 0.0017 hr^{-1} at a starting headspace oxygen concentration of 7% increased to 0.075 ± 0.025 hr^{-1} with a starting headspace oxygen concentration of 21% from growth on sodium carboxylmethyl cellulose as the carbon source. When the headspace oxygen concentration was held

constant at 21% vs. a starting concentration of 21%, the maximum specific growth rate did not change significantly, $0.037 \pm 0.002\ hr^{-1}$ vs. $0.038 \pm 0.006\ hr^{-1}$, respectively.

iii. Measure Volatile Compound Production by *A. sarcoides* on Both Glucose and Cellulose Carbon Sources. Evaluate the Distribution and Types of Volatiles Produced and How They Relate Constituents of Liquid Petroleum Fuel.

Volatile organic compounds (VOC) production was detected on all carbon sources tested including glucose and cellulose. The distribution of VOC among chemical classes was widespread, but usually included alkanes, alkenes, ketones, alcohols, aldehydes, acids and acid esters. The carbon length of compounds detected and identified in this study ranged from C_2 to C_{19}. The SPME fibers used in this study were designed for C_3 to C_{20} compounds with molecular weights from 40 to 275, while the Carbotrap materials used in the external column were designed for C_4-C_{20} compounds (Hewitt, 1998). The carbon length ranges for individual classes of compounds were as follows: C_2 to C_{12} for acids, C_2 to C_{10} for alcohols, C_2 to C_{11} for aldehydes, C_5 to C_{19} for alkanes, C_6 to C_{15} for aromatics, C_4 to C_{16} for esters, and C_7 to C_{13} for ketones. The majority of the compounds detected were within the range of carbon chain lengths for gasoline fuel, C_5-C_{12}, and aviation fuel, C_8-C_{16} (Yoon and Lee, 2012).

The carbon source had an interesting effect on volatile production type and frequency. Some overlap of volatile production was expected on cellulose and glucose, because cellulose is composed of β(1→4) D-glucose monomers. The majority of compounds produced on glucose were also produced on either cellulose or potato

dextrose broth (PDB). Growth on cellulose and PDB showed more than twice the number of compounds as growth on glucose, with cellulose producing 50 more compounds than glucose. The majority of the compounds were unique, demonstrating the diverse metabolic capability of the organism to produce different compounds on complex substrates. With the exception of alkenes, there was higher production on cellulose vs. glucose in every compound chemical class. Growth on cellulose showed the only detected aldehyde compounds.

Oxygen concentrations below 21% had a marked impact on the type and quantity of volatiles produced by *A. sarcoides* irrespective of biomass growth. At a starting oxygen concentration of 7% in a sealed headspace, higher numbers of alkanes and alcohols were produced than at higher oxygen concentrations. Overall, more than double the number of volatiles were recovered and identified from growth at lower oxygen concentrations despite the 21% oxygen concentration having the greatest accumulation of biomass growth. In addition, *A. sarcoides* produced more oxygenated volatiles versus non-oxygenated volatiles as its growth progressed into late stationary phase.

Many of the VOC detected have fuel potential, such as hexane, 3-methyl- (C_7H_{16}); cyclopropane, propyl- (C_6H_{12}); hexane, 3,3-dimethyl- (C_8H_{18}); 1-octen-3-ol ($C_8H_{16}O$); phenylethyl alcohol ($C_8H_{10}O$); and d-limonene ($C_{10}H_{16}$) (Table 5.1). Octane ratings, cetane numbers and enthalpies of combustion (ΔH_{comb}) were used to evaluate fuel applicability. In general, ΔH_{comb} are more available that either octane or cetane numbers, and though the energy content of a compound is only one aspect of its fuel properties, most fuels are a complex mixture of many compounds. Therefore, a low octane or cetane

number would not preclude the compound from being a valuable component of a fuel. From compounds selected based on availability of values in the literature, there was a mixture of energy content ranging from 3074 to 10,545 kJ mol^{-1} and octane ratings ranging from -40 to 109 (Table 5.1).

Some of the lipids extracted from *A. sarcoides* have diesel fuel potential (Table 5.1). The long chain (C_{14}+) acids in Table 5.1 had the highest ΔH_{comb} by class, though these properties would change after transesterification for biodiesel production. For gasoline fuel, the isoparaffins had the highest ΔH_{comb} by class with undecane, 3-methyl- at 7528 kJ mol^{-1} and nonane, 4,5-dimethyl- at 6916 kJ mol^{-1}, but also the lowest octane ratings. The aromatics and alcohols generally have the highest octane ratings and the cetane ratings increase with increasing acid chain length and decreasing saturation. It is clear from Table 5.1 that *A. sarcoides* has the potential to produce valuable compounds for use in fuels.

iv. Quantify the Volatile Production of *A. sarcoides*.

The established analytical methods (HS-SPME GC-MS) used for quantification of volatile hydrocarbon production by *A. sarcoides* were evaluated and determined to be sensitive to gas composition changes (Chapter 2). In general, the accuracy of quantitative values depends upon the method used to obtain them. For example, when quantifying volatiles from liquid cultures, the quantities in both the liquid and the headspace must be considered in order to determine the total. Only quantifying the volatiles in the headspace of a culture ignores what may still be present in the liquid, while quantifying volatiles in

Table 5.1. Volatile compounds detected from *A. sarcoides* with fuel potential. Octane ratings are an average of motor octane number and research octane number.

Compound Identification	Formula	Octane Rating	ΔH_{comb} (kJ/mol)	CAS No.
Butanal, 3-methyl-	$C_5H_{10}O$		2908	590-86-3
Butane, 2-methyl- (isopentane)	C_5H_{12}	91	3240	78-78-4
1-Butanol, 3-methyl-	$C_5H_{12}O$		3074	123-51-3
Cyclopropane, propyl-	C_6H_{12}	92	3765	2415-72-7
Benzaldehyde	C_7H_6O		3401	100-52-7
Benzyl Alcohol	C_7H_8O	100^+	3570	100-51-6
Heptanal	$C_7H_{14}O$		4139	111-71-7
2-Hexanone, 4-methyl-	$C_7H_{14}O$		4105	105-42-0
Hexane, 3-methyl-	C_7H_{16}	75	4466	589-34-4
Benzene, 1,3-dimethyl-	C_8H_{10}	109	4338	108-38-3
p-Xylene	C_8H_{10}	109	4339	106-42-3
Phenylethyl Alcohol	$C_8H_{10}O$	100^+	4185	60-12-8
1,4-Hexadiene, 3-ethyl-	C_8H_{14}	84	N/A	2080-89-9
1-Heptene, 6-methyl-	C_8H_{16}	84	4959	5026-76-6
1-Octen-3-ol (data for 1-octanol)	$C_8H_{16}O$	100^+	4750	3391-86-4
3-Octanone (data for 2-octanone)	$C_8H_{16}O$		4717	106-68-3
Hexane, 3,3-dimethyl-	C_8H_{18}	72	5072	563-16-6
Nonanal	$C_9H_{14}O$		5363	124-19-16
2-Nonanone	$C_9H_{18}O$		5334	821-55-6
Benzene, 2-ethenyl-1,4-dimethyl-	$C_{10}H_{12}$	104	5434	2039-89-6
Benzene, 1-methyl-2-(1-methylethyl)-	$C_{10}H_{14}$	104	5562	527-84-4
Benzene, 2-ethyl-1,4-dimethyl-	$C_{10}H_{14}$	104	5555	1758-88-9
Benzene, 1,2,4,5-tetramethyl-	$C_{10}H_{14}$	104	5520	95-93-2
d-Limonene	$C_{10}H_{16}$	104	5824	138-86-3

Table 5.1 Continued

2-Undecanone	$C_{11}H_{22}$		6559	112-12-9
Nonane, 4,5-dimethyl-	$C_{11}H_{24}$	55	6916	17302-23-7
Undecane, 3-methyl-	$C_{12}H_{26}$	5	7528	1002-43-3
Dodecane	$C_{12}H_{26}$	-40	7530	112-40-3
Esters for Biodiesel	**Formula**	**Cetane Number~**	**ΔH_{comb} (kJ/mol)**	**CAS No.**
1-Butanol, 3-methyl-, acetate	$C_7H_{14}O_2$		3898	123-92-2
Acetic acid, hexyl ester	$C_8H_{16}O_2$		4515	142-92-7
Formic acid, heptyl ester	$C_8H_{16}O_2$		4552	112-23-2
Acetic acid, phenylmethyl ester	$C_9H_{10}O_2$		4397	140-11-4
Acetic acid, heptyl ester	$C_9H_{18}O_2$		5129	112-06-1
Acetic acid, octyl ester	$C_{10}H_{20}O_2$		5742	112-14-1
Acetic acid, nonyl ester	$C_{11}H_{22}O_2$		6353	143-13-5
Tetradecanoic acid, methyl ester*	$C_{14}H_{28}O_2$	66.2	9431~	544-63-8
Pentadecanoic acid, methyl ester*	$C_{15}H_{30}O_2$		8723	1002-84-2
Hexadecanoic acid, methyl ester*	$C_{16}H_{32}O_2$	74.5	9414~	57-10-3
Octadecadienoic acid, methyl ester* (Sum of C18:1-3 FAMEs)	$C_{18}H_{32}O_2$	39.7#	11676#~	60-33-3
Octadecanoic acid, methyl ester*	$C_{18}H_{36}O_2$	86.9	11832~	57-11-4

*Detected after transesterification of extracted lipids to methyl esters

~ (Nag, 2008)

#Average of 18:1,18:2 and 18:3 methyl esters

the liquid can result in yield per culture volume or culture biomass without considering the amount of volatiles that transferred to the culture headspace.

PTR-MS results showed the VOC production measured in the culture headspace was dominated by ethanol and acetaldehyde, both C_2 compounds, while the concentration of the remainder of headspace volatiles, C_4 –C_{18}, consistently reached 2,000 ppbv. Liquid-liquid extractions of cell-free culture liquid quantified diesel range organics (C_9-C_{36}) and gasoline range organics (C_5-C_{12}) at maximums of 45 mg of diesel range organics per gram biomass from growth on cellulose and 1.1 mg of gasoline range organics per gram biomass from growth on glucose, while desorption of the headspace volatiles on an external collection column showed 30.1 mg total volatiles from cellulose culture and 23.9 mg from glucose culture recovered from the purged headspace. Normalized to biomass in the culture, the cellulose culture had a total of 60.2 mg desorbed VOC per gram biomass, and the glucose culture had a total of 14.2 mg desorbed VOC per gram biomass recovered from the culture headspace. To estimate the total production potential, the yield of liquid extracted compounds were added with the collected headspace compounds for a total of 105.3 mg VOC per gram biomass from growth on cellulose and 23.9 mg VOC per gram biomass from growth on glucose.

The SPME fiber quantifies volatiles in the headspace as well as a portion of the volatiles in the liquid as long as the total adsorptive capacity of the fiber is not reached. This is due to the removal of volatiles from the headspace, reducing their total partial pressure in the headspace and shifting the liquid-vapor equilibrium toward the vapor phase, liberating more volatiles from the liquid. Using the total SPME fiber capacity as

an indicator of production potential, the maximum volatiles recorded from carboxylmethyl cellulose growth was 0.113 mg VOC per g of culture biomass, and the minimum measured was 0.0203 mg VOC per g of culture biomass. Both quantities were 182% and 250% higher, respectively, than the background from the medium alone. These values are indicators, not absolute values of production potential, because the values are obtained using one internal standard as a reference for quantification of all compounds. It was shown in Chapter 2 that the efficiency of SPME recovery for compounds with different chemical properties will vary. For example, the internal standard bromofluorobenzene, an aromatic, will not likely be an accurate quantitative measure of alcohols. The recovery and identification of alcohols does however have merit, and many alcohols have been identified by this study and the work of others on *A. sarcoides*.

The yield data (i.e. 0.0113 mg VOC per g culture biomass) from SPME methods were much smaller than from the extraction and external collection methods. This was not surprising mostly due to the amount of time the SPME fiber is exposed the vial headspace. Therefore, SPME yields indicate potential at a discrete timepoint, while total extraction of the liquid and continuous collection by the external column accounts for volatiles produced throughout the growth period.

Compared with what is achieved by other fermentative organisms, commonly yeasts such as *Saccharomyces cerevisiae*, the yields of ethanol from *A. sarcoides* are drastically lower (Table 5.2). On 100 g of glucose, *S. cerevisiae* can produce 50 g of ethanol, only slightly lower than the theoretical yield of 51.4 g of ethanol (Badger, 2002). Comparatively, *A. sarcoides* would produce 0.2 g of ethanol from 100 g of glucose. It

Table 5.2 Yields of ethanol and isobutanol from yeasts and bacteria compared to *A. sarcoides*. Sources are: 1. (Badger, 2002), 2. (Hahn-Hägerdal et al., 2006), 3. This dissertation, 4. (Dererie et al., 2011), 5.(Smith and Liao, 2011).

Organism	Substrate	Ethanol Yield (g/g initial sugar)	Isobutanol Yield (g/g initial sugar)	Reference
Saccharomyces cerevisiae	Glucose	0.5		1
Escherichia coli KO11	Bagasse hemicellulose	0.49		2
S. cerevisiae 424A	Corn fiber	0.36		2
S. cerevisiae TMB3006	Spruce	0.37		2
A. sarcoides	Glucose	0.002		3
S. cerevisiae J672	Oat straw	0.15		4
Escherichia coli JCL16	Glucose		0.24	5
E. coli JCL260	Glucose		0.30	5
A. sarcoides	Glucose		0.002*	3
A. sarcoides	Cellulose		0.001**	3

*Assumes volatiles have properties similar to isobutanol and Henry's Law constant of 3-methyl-1-butanol.
**Includes gasoline and diesel range organics from the liquid and weight of volatiles excluding ethanol and other C_2 compounds.

should be noted that the yields presented in Table 5.2 were improved from wild-type yields by genetic modifications which has not been attempted with *A. sarcoides*. From cellulosic substrates, the ethanol yields from *S. cerevisiae* are on the order of 0.4 g per g of substrate sugar (Hahn-Hägerdal et al., 2006). Estimations for *A. sarcoides* on cellulosic

substrates are not accurate, because the analytical methods used for those studies gave overall values without specific compound values such as ethanol.

A. sarcoides is of primary interest for its fuel-like compound production, not its ethanol production. Since this is a relatively unstudied aspect of fungi, direct comparisons are difficult. However, some values for isobutanol production by the bacterial strains of *Escherichia coli* show that yields from *A. sarcoides* need to be dramatically improved (Table 5.2). Assuming on average that the produced volatiles excluding ethanol and acetaldehyde were combined of fuel value similar to isobutanol, the yield is 0.002 g per g of glucose consumed from *A. sarcoides*, much smaller than those for *E. coli* at 0.30 g per g of glucose consumed (Smith and Liao, 2011). Again, *E. coli* strains producing isobutanol are optimized through gene manipulations and mutant isolations, and this type of work has not been performed with *A. sarcoides*. The isobutanol yield of 0.001 g per g cellulose for *A. sarcoides* uses the total cellulose added to the culture. It is visibly apparent that the entire amount of substrate is consumed, so this yield would be higher with quantitative data on cellulose substrate usage. Even with this consideration, the fuel-relevant compound yields from *A. sarcoides* must be improved in order to compete with more developed biofuel technologies.

v. Evaluate the Impact of Oxygen Availability
on the Production of Volatiles by *A. sarcoides.*

Limited oxygen conditions, below 21% starting concentration, produced greater numbers of VOC and specifically greater numbers of alcohols, alkanes, ketones and esters. The 7% and 10% starting oxygen concentrations had the same numbers of VOC

detected, 19 total, despite inhibited growth at 7%, while growth at the 21% starting oxygen concentration had 9 distinct VOCs detected. The compounds at reduced oxygen concentrations ranged from C_2 to C_{15} in carbon length, and from C_2 to C_{11} at the 21% starting oxygen concentration. The quantity of VOC material recovered was 0.104±0.012 mg (g biomass)$^{-1}$, 0.030±0.003 mg (g biomass)$^{-1}$ and 0.020±0.0001 mg (g biomass)$^{-1}$ for 7%, 10% and 21% starting oxygen concentration, respectively. These values included the yields from the two different medium nitrogen concentrations. The significantly lower biomass concentration, 0.07 mg mL^{-1} versus 0.25 mg mL^{-1} and 0.42 mg mL^{-1} at the 10 % and 21% starting oxygen concentrations, makes the yield of VOCs from the 7% oxygen concentration cultures significantly higher than the others.

Initial screening by NMR of batch cultures for VOC production also confirmed that the non-oxygenated hydrocarbons measured were impacted by the oxygen available to the culture. With increasing oxygen availability, the total non-oxygenated hydrocarbons decreased per mg of biomass. These results illustrate that oxygen concentration is a processing parameter that can be used for by-product control.

In addition, oxygen concentrations below 21% had an impact on factors other than VOC production. At reduced oxygen concentrations, the yield of biomass on nitrogen (mg biomass/mmol ammonia) by *A. sarcoides* was much lower than at the 21% concentration. The amount of carbon necessary for metabolism and respiration at the lowest oxygen condition of 7% was greatly increased compared to 10% and 21%. The results from this objective were shared with the modeling group to contribute to possible pathway construction.

vi. Explore the Lipid Biofuel Potential of *A. sarcoides* Following Growth for Volatile Fuel Production.

Although some fungal strains have reported total lipid production or biofuel potential near 55% (w/w biomass) (Somashekar and Joseph, 2000), the greatest total biofuel potential calculated in this work was 7.5% (w/w). Reduced headspace oxygen concentrations increased lipid production by *A. sarcoides*. The 10% starting oxygen concentration cultures yielded around 50% higher lipids than the cultures grown with 21% starting oxygen headspace concentration. The lipids recovered and identified included C_{12}-C_{20} free fatty acids (FFA), C_{12}-C_{18} mono-glycerides (MAG), C_{12}-C_{18} di-glycerides (DAG), and C_{11}-C_{18} tri-glycerides (TAG). After direct *in situ* transesterification of wet biomass, the fatty acid methyl ester (FAME) content included $C_{14:0}$-$C_{24:0}$ FAMEs. The majority of the extractable lipid content was DAG, consistently ranging from 32-42% of the total neutral lipids, while the majority of the FAME detected for all replicates was C18:1-3 lipids ranging from 70.8-75.4% of the total FAME. This fraction included the FAME of C18:2, linoleic acid, which has been implicated in the metabolic pathways to final production of C8 alcohols and ketones. There was also a significant change in VOC detected based on lipid variations; the 10% starting oxygen concentration also yielded greater diversity of VOC recovered and identified, including greater numbers of alkanes and ketones.

The final lipid potential of *A. sarcoides* following growth for VOC production was not remarkable at 7.5% or less in all conditions studied, but the numbers provide quantitative data for future work which may include economic feasibility calculations.

Future Work

The wide spread use of a limited supply of petroleum will not change dramatically in the foreseeable future, particularly for transportation needs. Therefore, development of economical and sustainable alternatives to liquid petroleum fuel is an ongoing need. It is reasonable to assume that in the future some biofuels will result from biologically based technology such as genetic engineering. Studying organisms such as *A. sarcoides* which are able to convert sustainable cellulosic feedstocks into hydrocarbon fuels could be a piece of the solution to finding liquid replacement fuels. However, much higher yields are necessary for commercial production of these fuels. Therefore, it is necessary to discover the production mechanisms to enable metabolic engineering improvements or find another organism with higher production potential.

Suggested future work includes further exploring the mechanisms behind HC production and to assess the impact of cellulosic pre-processing on HC yields. In addition, screening of new fungal strains should be completed in order to enhance this work. Knowledge of the HC production mechanisms could assist genetic engineering efforts, and the discovery of a fungal strain with high yields could improve the likelihood of commercial production.

The goal of carbon metabolism investigation is to elucidate the mechanisms of HC production, so the carbon flux from substrate to the valuable volatile compounds can be improved. One strategy to test the metabolic functionality of extracellular enzymes is to combine fungal culture supernatant or protein fractions with intermediate compounds

and measure the conversion of the compounds. A similar method has shown that the hydroperoxide lyase of the 10-hydroperoxide isomer of linoleic acid was responsible for the production of 1-octen-3-ol by *Psalliota bispora*, also produced by *A. sarcoides* (Mallette et al., 2012; Wurzenberger and Grosch, 1984). Since linoleic acid has been suggested by Gianoulis et al. (2012) as the precursor for C_8 compounds from *A. sarcoides*, including alkanes and ketones, this study could be repeated to test this hypothesis. This study could be repeated for other products identified.

Another possibility for discovering the fungal metabolic pathways that produce valuable compounds is to use ^{13}C labeled substrates (Blank et al., 2005). The substrates are expensive, so the data value of this method would need to be weighed against economic resources. As an example, a fungus could be grown on an unlabeled substrate to build up biomass then switch to a ^{13}C labeled substrate such as glucose, or add in ^{13}C labeled precursor such as linoleic acid. The conversion of the ^{13}C labeled compound can be traced to intermediates and product formation. There are several methods available to measure the identity of intermediates and products (Niittylae et al., 2009). For example, the MSU Chemistry department has an HPLC-MS which could be used to measure intermediates such as amnio acids. A GC-MS is a valuable method for ^{13}C work in general and could be combined with the microextraction procedures discussed earlier to measure product identities and ^{13}C content (Nanchen et al., 2007). Real-time NMR is a valuable technique for distinguishing if a compound contains ^{13}C labeled carbon and could be used to directly measure reaction kinetics of metabolic processes, and specifically the conversion of linoleic acid to hydrocarbons (Davey et al., 2012).

The VOC data from glucose and cellulose substrates indicate that mild pre-processing of cellulosic feedstocks may improve the total production of VOC by *A. sarcoides due* to the high yield values on microcrystalline cellulose. Complete hydrolysis of feedstocks would reduce them to the simple sugars including glucose, and the data indicate that this is not ideal. However, some breakdown of the crystalline structure could improve the efficiency of *A. sarcoides* utilization of the feedstock and enhance overall production. Therefore, the fungus could be grown on cellulosic feedstocks treated and untreated including microcrystalline cellulose. Other easily obtainable feedstocks are preferable for their industrial applicability, and those obtained in the past include Montana switchgrass, corn stover, sawdust particles from local pine beetle killed conifers, and sugar beet pulp from Eastern Montana farmers. Physical and chemical treatment methods should be considered based upon the substrate used. Physical treatment is straight-forward and can reduce the crystallinity of the substrate; while dilute acid chemical pre-treatment has been shown to enhance the reactivity of cellulose to enzymes ((Keshwani and Cheng, 2009; Lynd et al., 2002; Weil et al., 1994). Limiting the time period of dilute acid pre-treatment could enhance cellulolytic degradation by the fungus, and preserve the diversity of produced VOC.

A series of experiments quantifying the volatiles of interest on these cellulosic feedstocks should be completed using very moist (100% relative humidity) and reduced oxygen (below 15%) gas (Polizzi et al., 2012). The reduced oxygen can be achieved by mixing the outlet from a pure air generator with flow from a nitrogen tank using flow meters and mixture ratios confirmed by measuring the diluted oxygen concentration by

gas chromatography (GC). A very specific ratio can be achieved using mass flow controllers, but the oxygen measurements should be sufficient in the absence of mass flow controllers. The culture vessels can be sealed from air exchange to preserve the accumulation of volatiles.

In terms of locating high yield strains, Dr. Gary Strobel and his lab are constantly discovering new strains of fungus with bioactive potential (Mends et al., 2012; Tomsheck et al., 2010). Whenever a new strain is obtained, care must be taken to preserve the metabolic integrity by ensuring repeated transfers are not made. Another way to identify strains with volatile potential is to use related species of isolates confirmed to have volatile production capabilities (Ahamed and Ahring, 2011; Griffin et al., 2010).

To screen the new strains for high yield, small scale volatile quantification can be quickly and easily completed using sealed liquid cultivation of the strain. Sealed liquid growth avoids two complicating factors of fungal growth with volatile production. Continuous collection of volatiles is not necessary due to the sealed headspace, and liquid cultivation prevents growth and production variations based on humidity levels.

Ahamed and Ahring (2011) showed that the production of volatiles from *Gliocladium roseum* spp. was dramatically improved up to 91-fold by co-culture with *Escherichia coli* strain Nissle 1917 (DSM 6601), though the quantitative numbers reported are not exact due to the use of HS-SPME for extraction before quantification with GC-MS. Therefore, it is suggested that at the beginning stages of the work, the isolates are grown alone and in liquid co-culture with *E. coli*.

The two most important parameters to measure during the screening process are biomass density and hydrocarbon production potential. Biomass can be measured on a cellulose substrate with a modified protein assay (Chapter 4) or with dry weight measurements of total solids and residual cellulose, or optical density with a soluble substrate in the absence of production of extracellular pigments (Ahamed and Vermette, 2009). The hydrocarbon production potential can be quantified by nuclear magnetic resonance (NMR). An important aspect of this study would be to grow the cultures in a sealed environment to prevent the loss of volatiles during the growth period and to minimally process the liquid before quantitative measurement. The volatile production can be normalized to the amount of biomass to calculate a yield of volatiles per biomass weight.

It will be necessary to obtain access to an NMR instrument to make this project successful. If the NMR instrument is unobtainable, an alternate option is the use of a sensitive CO_2 instrument like the LI-840 CO_2/H_2O Gas Analyzer (LI-COR Biosciences, Lincoln, NE) used in Chapter 4 in combination with a platinum catalyst. This method can accurately measure hydrocarbon compounds converted by the platinum catalyst to CO_2 and H_2O. The CO_2 measured by the LI-840 would be the sum of the background CO_2 in the sample and the CO_2 from the converted hydrocarbons. The background CO_2 can be measured and subtracted to get a total amount of carbon in the form of hydrocarbons. Figure 5.2 shows the layout of the design. The flow of the gas sample is accurately controlled by a mass flow controller. A pump moves the gas sample through Teflon tubing to a three-way valve where it travels either directly to the CO_2 monitor or through

a heated platinum catalyst before reaching the CO_2 monitor. Prior calibration of the CO_2 instrument has shown accuracy in the ±3 ppm and linearity from 0 – 400 ppm. This method is less technically preferable to the NMR method despite its affordability, because it gives a total value for carbon in products without any structural information and accuracy can be compromised by dilution, while the NMR results give information on non-oxygenated HC, aromatics and oxygenated compounds. The best analytical solution is probably a combination of both techniques based upon which information is most needed.

A strain showing high potential can then be further characterized to identify the specific compounds produced using the methods discussed in this dissertation, such as liquid-liquid extraction, PTR-MS and HS SPME GC-MS. In addition, solvent microextraction (SME) methods not mentioned in the body of this dissertation could prove useful. Dynamic hollow fiber liquid phase microextraction (HF LPME) is useful for measuring hydrophobic compounds which have a higher solubility in an organic solvent compared with water (Saraji and Khaje, 2012). The method fills the pores of a hollow fiber membrane with the extracting organic solvent. The porosity of the fiber causes a considerable portion of the solvent to be a thin film, increasing mass transfer

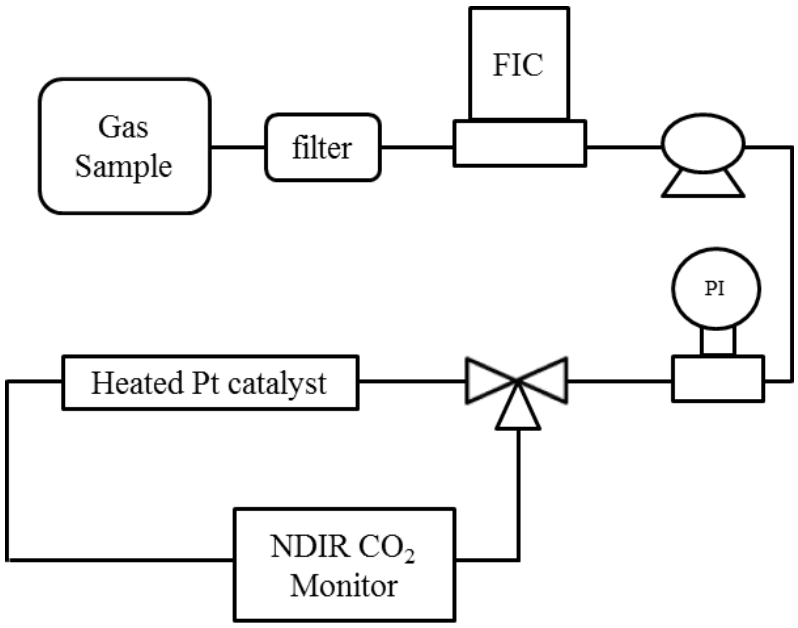

Figure 5.2. Schematic of experimental set-up for quantitative determination of volatiles from fungal cultures using a mass flow controller (FIC), pressure gauge (PI), heated platinum catalyst and a nondispersive infared (NDIR) CO_2 monitor.

efficiency of compounds into the solvent. This method can achieve very pure extracts from complex matrices, such as liquid media, and has shown accurate measurements down to 0.25 ng mL^{-1}. For very volatile compounds, single-drop microextraction (SDME) could be a powerful technique when used in the headspace (HS) of sealed vials. This technique uses a solvent drop in the headspace to collect analytes before analysis by GC-MS and/or matrix-assisted laser desorption ionization mass spectrometry (MALDI-MS). The accurate measurement of compounds has been achieved down to 0.01 µg mL^{-1} for Z-ligustilide in rabbit plasma using GC-MS (Saraji and Khaje, 2012). The choice of extracting solvent will depend upon the solubility of the compound of interest as well as miscibility in the aqueous phase (Kocúrová et al., 2012; Saraji and Khaje, 2012).

Compounds from cultures grown in sealed vials can be measured by the aforementioned methods. In addition, if the compounds of interest are not alkanes or alkenes, PTR-MS can be used to monitor the headspace of a culture for accurate quantification of the compound ion signal.

In conclusion, further characterization of *A. sarcoides* along with metabolic pathways and modeling should be undertaken and as available, new fungal strains screened for HC production. The results are important for advancing the fundamental understanding of metabolic hydrocarbon production and could lead to genetic engineering efforts with more easily culturable yeasts where process engineering is well established, e.g. alcohol brewery production. These future studies could be completed with several strains of cellulolytic fungi to advance the fundamental knowledge of fungal physiology and lead to information that can be applied to future industrial processing.

REFERENCES

Ahamed A, Ahring BK. 2011. Production of hydrocarbon compounds by endophytic fungi *Gliocladium* species grown on cellulose. *Bioresour. Technol.* **102**:9718–9722.

Ahamed A, Vermette P. 2009. Effect of culture medium composition on *Trichoderma reesei*'s morphology and cellulase production. *Bioresour. Technol.* **100**:5979–5987.

Altekar M, Homon CA, Kashem MA, Mason SW, Nelson RM, Patnaude LA, Yingling J, Taylor PB. 2007. Assay optimization: a statistical design of experiments approach. *Clin. Lab. Med.* **27**:139–154.

Aprea E, Biasioli F, Carlin S, Endrizzi I, Gasperi F. 2009. Investigation of Volatile Compounds in Two Raspberry Cultivars by Two Headspace Techniques: Solid-Phase Microextraction/Gas Chromatography−Mass Spectrometry (SPME/GC−MS) and Proton-Transfer Reaction−Mass Spectrometry (PTR−MS). *J. Agric. Food Chem.* **57**:4011–4018.

Aprea E, Biasioli F, Carlin S, Versini G, Märk TD, Gasperi F. 2007. Rapid white truffle headspace analysis by proton transfer reaction mass spectrometry and comparison with solid-phase microextraction coupled with gas chromatography/mass spectrometry. *Rapid Commun. Mass Spectrom.* **21**:2564–2572.

Arthur CL, Pawliszyn J. 1990. Solid phase microextraction with thermal desorption using fused silica optical fibers. *Anal. Chem.* **62**:2145–2148.

Atlas RM. 2004. Handbook of Microbiological Media Third Edition. Boca Raton, Florida: CRC Press 2060 p.

Aulakh JS, Malik AK, Kaur V, Schmitt-Kopplin P. 2005. A Review on Solid Phase Micro Extraction—High Performance Liquid Chromatography (SPME-HPLC) Analysis of Pesticides. *Crit. Rev. Anal. Chem.* **35**:71–85.

Bäck J, Aaltonen H, Hellén H, Kajos MK, Patokoski J, Taipale R, Pumpanen J, Heinonsalo J. 2010. Variable emissions of microbial volatile organic compounds (MVOCs) from root-associated fungi isolated from Scots pine. *Atmos. Environ.* **44**:3651–3659.

Badger PC. 2002. Ethanol From Cellulose: A General Review. In: Janick, J, Whipkey, A, editors. *Trends New Crops New Uses*. Alexandria, VA: ASHS Press, pp. 17–21. http://www.hort.purdue.edu/newcrop/ncnu02/v5-017.html.

Bajtarevic A, Ager C, Pienz M, Klieber M, Schwarz K, Ligor M, Ligor T, Filipiak W, Denz H, Fiegl M, Hilbe W, Weiss W, Lukas P, Jamnig H, Hackl M, Haidenberger

A, Buszewski B, Miekisch W, Schubert J, Amann A. 2009. Noninvasive detection of lung cancer by analysis of exhaled breath. *BMC Cancer* **9**:348.

Banerjee D, Strobel G, Booth E, Geary B, Sears J, Spakowicz D, Busse S. 2010. An endophytic *Myrothecium inundatum* producing volatile organic compounds. *Mycosphere* **1**:229–240.

Bates D, Maechler M, Bolker B. 2013. lme4: Linear mixed-effects models using S4 classes. R package version 0.999999-2. http://CRAN.R-project.org/package=lme4.

Blakey S, Rye L, Wilson CW. 2011. Aviation gas turbine alternative fuels: A review. *Proc. Combust. Inst.* **33**:2863–2885.

Blank L, Kuepfer L, Sauer U. 2005. Large-scale C-13-flux analysis reveals mechanistic principles of metabolic network robustness to null mutations in yeast. *Genome Biol.* **6**.

Booth E, Strobel G, Knighton B, Sears J, Geary B, Avci R. 2011. A rapid column technique for trapping and collecting of volatile fungal hydrocarbons and hydrocarbon derivatives. *Biotechnol. Lett.* **33**:1963–1972.

Bouvier-Brown NC, Holzinger R, Palitzsch K, Goldstein AH. 2007. Quantifying sesquiterpene and oxygenated terpene emissions from live vegetation using solid-phase microextraction fibers. *J. Chromatogr. A* **1161**:113–120.

Brás I, Ratola N, Alves A. 2011. Uncertainty in the quantification of pentachlorophenol in wood processing wastewaters by SPME-GC-MS. *J. Anal. Chem.* **66**:756–762.

Buhr K, van Ruth S, Delahunty C. 2002. Analysis of volatile flavour compounds by Proton Transfer Reaction-Mass Spectrometry: fragmentation patterns and discrimination between isobaric and isomeric compounds. *Int. J. Mass Spectrom.* **221**:1–7.

Bunge M, Araghipour N, Mikoviny T, Dunkl J, Schnitzhofer R, Hansel A, Schinner F, Wisthaler A, Margesin R, Mark TD. 2008. On-Line Monitoring of Microbial Volatile Metabolites by Proton Transfer Reaction-Mass Spectrometry. *Appl Env. Microbiol* **74**:2179–2186.

Carlson RP, Taffs RL. 2010. Molecular-level tradeoffs and metabolic adaptation to simultaneous stressors. *Curr. Opin. Biotechnol.* **21**:670–676.

Carroll A, Somerville C. 2009. Cellulosic Biofuels. *Annu. Rev. Plant Biol.* **60**:165–182.

Ciapetta FG, Wallace DN. 1972. Catalytic Naphtha Reforming. *Catal. Rev.* **5**:67–158.

Cochrane VW. 1963. Physiology of Fungi. New York: Wiley 524 p.

Dagbagli S, Goksungur Y. 2008. Optimization of beta-galactosidase production using *Kluyveromyces lactis* NRRL Y-8279 by response surface methodology. *Electron. J. Biotechnol.* **11**.

Dale BE, Ong RG. 2012. Energy, wealth, and human development: why and how biomass pretreatment research must improve. *Biotechnol. Prog.* **28**:893–898.

Davey PT, Hiscox WC, Lucker BF, O'Fallon JV, Chen S, Helms GL. 2012. Rapid triacylglyceride detection and quantification in live micro-algal cultures via liquid state 1H NMR. *Algal Res.* **1**:166–175.

Dererie DY, Trobro S, Momeni MH, Hansson H, Blomqvist J, Passoth V, Schnürer A, Sandgren M, Ståhlberg J. 2011. Improved bio-energy yields via sequential ethanol fermentation and biogas digestion of steam exploded oat straw. *Bioresour. Technol.* **102**:4449–4455.

Dien BS, Cotta MA, Jeffries TW. 2003. Bacteria engineered for fuel ethanol production: current status. *Appl. Microbiol. Biotechnol.* **63**:258–266.

Doran P. 2012. Bioprocess Engineering Principles, 2nd Edition. Waltham, MA: Academic Press 928 p.

Ezra D, Jasper J, Rogers T, Knighton B, Grimsrud E, Strobel G. 2004. Proton transfer reaction-mass spectrometry as a technique to measure volatile emissions of *Muscodor albus*. *Plant Sci.* **166**:1471–1477.

Flamholz A, Noor E, Bar-Even A, Liebermeister W, Milo R. 2013. Glycolytic strategy as a tradeoff between energy yield and protein cost. *Proc. Natl. Acad. Sci.* **110**:10039–10044.

Gardner RD, Lohman E, Gerlach R, Cooksey KE, Peyton BM. 2013. Comparison of CO2 and bicarbonate as inorganic carbon sources for triacylglycerol and starch accumulation in *Chlamydomonas reinhardtii*. *Biotechnol. Bioeng.* **110**:87–96.

Ghosh P, Hickey KJ, Jaffe SB. 2005. Development of a Detailed Gasoline Composition-Based Octane Model. *Ind. Eng. Chem. Res.* **45**:337–345.

Ghosh P, Jaffe SB. 2005. Detailed Composition-Based Model for Predicting the Cetane Number of Diesel Fuels. *Ind. Eng. Chem. Res.* **45**:346–351.

Gianoulis TA, Griffin MA, Spakowicz DJ, Dunican BF, Alpha CJ, Sboner A, Sismour AM, Kodira C, Egholm M, Church GM, Gerstein MB, Strobel SA. 2012.

Genomic Analysis of the Hydrocarbon-Producing, Cellulolytic, Endophytic Fungus *Ascocoryne sarcoides*. *PLoS Genet.* **8**.

Griffin DH. 1994. Fungal physiology. New York: Wiley-Liss.

Griffin MA, Spakowicz DJ, Gianoulis TA, Strobel SA. 2010. Volatile organic compound production by organisms in the genus *Ascocoryne* and a re-evaluation of myco-diesel production by NRRL 50072. *Microbiology* **156**:3814–3829.

Hahn-Hägerdal B, Galbe M, Gorwa-Grauslund MF, Lidén G, Zacchi G. 2006. Bio-ethanol – the fuel of tomorrow from the residues of today. *Trends Biotechnol.* **24**:549–556.

Hewitt CN ed. 1998. Reactive Hydrocarbons in the Atmosphere. San Diego, CA: Academic Press 336 p.

Insam H, Seewald MSA. 2010. Volatile organic compounds (VOCs) in soils. *Biol. Fertil. Soils* **46**:199–213.

International Energy Agency. 2012. 2012 Key World Energy Statistics. Paris, France: International Energy Agency. http://www.iea.org/publications/freepublications/publication/kwes.pdf.

Jo JH, Lee DS, Park D, Choe W-S, Park JM. 2008. Optimization of key process variables for enhanced hydrogen production by *Enterobacter aerogenes* using statistical methods. *Bioresour. Technol.* **99**:2061–2066.

Kai M, Crespo E, Cristescu SM, Harren FJM, Francke W, Piechulla B. 2010. *Serratia odorifera*: analysis of volatile emission and biological impact of volatile compounds on *Arabidopsis thaliana*. *Appl. Microbiol. Biotechnol.* **88**:965–976.

Karl T, Yeretzian C, Jordan A, Lindinger W. 2003. Dynamic measurements of partition coefficients using proton-transfer-reaction mass spectrometry (PTRâ€“MS). *Int. J. Mass Spectrom.* **223-224**:383–395.

Keller NP, Turner G, Bennett JW. 2005. Fungal secondary metabolism - from biochemistry to genomics. *Nat Rev Micro* **3**:937–947.

Keshwani DR, Cheng JJ. 2009. Switchgrass for bioethanol and other value-added applications: A review. *Bioresour. Technol.* **100**:1515–1523.

King J, Mochalski P, Kupferthaler A, Unterkofler K, Koc H, Filipiak W, Teschl S, Hinterhuber H, Amann A. 2010. Dynamic profiles of volatile organic compounds in exhaled breath as determined by a coupled PTR-MS/GC-MS study. *Physiol. Meas.* **31**:1169–1184.

Kocúrová L, Balogh IS, Šandrejová J, Andruch V. 2012. Recent advances in dispersive liquid–liquid microextraction using organic solvents lighter than water. A review. *Microchem. J.* **102**:11–17.

Ladygina N, Dedyukhina EG, Vainshtein MB. 2006. A review on microbial synthesis of hydrocarbons. *Process Biochem.* **41**:1001–1014.

Langenfeld JJ, Hawthorne SB, Miller DJ. 1996. Quantitative Analysis of Fuel-Related Hydrocarbons in Surface Water and Wastewater Samples by Solid-Phase Microextraction. *Anal. Chem.* **68**:144–155.

Lee SK, Chou H, Ham TS, Lee TS, Keasling JD. 2008. Metabolic engineering of microorganisms for biofuels production: from bugs to synthetic biology to fuels. *Curr. Opin. Biotechnol.* **19**:556–563.

Lindinger W, Hansel A, Jordan A. 1998. On-line monitoring of volatile organic compounds at pptv levels by means of proton-transfer-reaction mass spectrometry (PTR-MS) medical applications, food control and environmental research. *Int. J. Mass Spectrom. Ion Process.* **173**:191–241.

Linstrom PJ, Mallard WG. 2011. NIST Chemistry WebBook, NIST Standard Reference Database Number 69. In: Gaithersburg, MD 20899: National Institute of Standards and Technology. http://webbook.nist.gov/chemistry/.

Lynd LR, Weimer PJ, van Zyl WH, Pretorius IS. 2002. Microbial Cellulose Utilization: Fundamentals and Biotechnology. *Microbiol Mol Biol Rev* **66**:506–577.

Maleknia S, Bell T, Adams M. 2007. PTR-MS analysis of reference and plant-emitted volatile organic compounds. *Int. J. Mass Spectrom.* **262**:203–210.

Mallette ND, Knighton WB, Strobel GA, Carlson RP, Peyton BM. 2012. Resolution of volatile fuel compound profiles from *Ascocoryne sarcoides*: a comparison by proton transfer reaction-mass spectrometry and solid phase microextraction gas chromatography-mass spectrometry. *AMB Express* **2**:23.

Mallouchos A, Komaitis M, Koutinas A, Kanellaki M. 2002. Investigation of Volatiles Evolution during the Alcoholic Fermentation of Grape Must Using Free and Immobilized Cells with the Help of Solid Phase Microextraction (SPME) Headspace Sampling. *J. Agric. Food Chem.* **50**:3840–3848.

Matysik S, Herbarth O, Mueller A. 2009. Determination of microbial volatile organic compounds (MVOCs) by passive sampling onto charcoal sorbents. *Chemosphere* **76**:114–119.

Mends MT, Yu E, Strobel GA, Riyaz-Ul-Hassan S, Booth E, Geary B, Sears J, Taatjes CA, Hadi MZ. 2012. An Endophytic *Nodulisporium* Sp. Producing Volatile Organic Compounds Having Bioactivity and Fuel Potential. *J. Pet. Environ. Biotechnol.* **03**.

Morath SU, Hung R, Bennett JW. 2012. Fungal volatile organic compounds: A review with emphasis on their biotechnological potential. *Fungal Biol. Rev.* **26**:73–83.

Myers RH. 1995. Response surface methodology: process and product optimization using designed experiments. New York: Wiley. (Wiley series in probability and statistics. Applied probability and statistics).

Nag A. 2008. Biofuels Refining and Performance. New York, NY: McGraw-Hill.

Nanchen A, Fuhrer T, Sauer U. 2007. Determination of Metabolic Flux Ratios From 13C-Experiments and Gas Chromatography-Mass Spectrometry Data. In: Weckwerth, W, editor. *Metabolomics*. Totowa, NJ: Humana Press, Vol. 358, pp. 177–197.

Niittylae T, Chaudhuri B, Sauer U, Frommer WB. 2009. Comparison of Quantitative Metabolite Imaging Tools and Carbon-13 Techniques for Fluxomics. In: Belostotsky, DA, editor. *Plant Syst. Biol.*, Vol. 553, pp. 355–372.

Parkerton TF, Stone MA, Letinski DJ. 2000. Assessing the aquatic toxicity of complex hydrocarbon mixtures using solid phase microextraction. *Toxicol. Lett.* **112-113**:273–282.

Pawliszyn J. 1997. Solid Phase Microextraction: Theory and Practice. Wiley-VCH 247 p.

Pawliszyn J, Smith RM eds. 1999. Applications of solid phase microextraction. The Royal Society of Chemistry 655 p.

Perlack RD, Wright LL, Turhollow AF, Graham RL, Stokes BJ, Erbach DC. 2005. Biomass as feedstock for a biomass and bioproducts industry: the technical feasibility of a 1 billion ton annual feedstock supply. Oak Ridge, TN: Oak Ridge Natl. Lab./US DOE/USDA.

Polizzi V, Adams A, De Saeger S, Van Peteghem C, Moretti A, De Kimpe N. 2012. Influence of various growth parameters on fungal growth and volatile metabolite production by indoor molds. *Sci. Total Environ.* **414**:277–286.

R Core Team. 2013. R: A language and environment for statistical computing. Vienna, Austria: R Foundation for Statistical Computing. http://www.R-project.org/.

Ragauskas AJ, Williams CK, Davison BH, Britovsek G, Cairney J, Eckert CA, Frederick WJ, Hallett JP, Leak DJ, Liotta CL, Mielenz JR, Murphy R, Templer R, Tschaplinski T. 2006. The Path Forward for Biofuels and Biomaterials. *Science* **311**:484 –489.

Ramirez KS, Lauber CL, Fierer N. 2009. Microbial consumption and production of volatile organic compounds at the soil-litter interface. *Biogeochemistry* **99**:97–107.

Ratledge C, Wynn J. 2002. The biochemistry and molecular biology of lipid accumulation in oleaginous microorganisms. *Adv. Appl. Microbiol.* **51**:1–51.

Regalbuto JR. 2009. Cellulosic Biofuels—Got Gasoline? *Science* **325**:822–824.

Robinson AL, Boss PK, Heymann H, Solomon PS, Trengove RD. 2011. Development of a sensitive non-targeted method for characterizing the wine volatile profile using headspace solid-phase microextraction comprehensive two-dimensional gas chromatography time-of-flight mass spectrometry. *J. Chromatogr. A* **1218**:504–517.

Rude MA, Schirmer A. 2009. New microbial fuels: a biotech perspective. *Curr. Opin. Microbiol.* **12**:274–281.

Ruth V, M S, Lonneke D, Eugenio A, Sachiko O. 2005. Comparison of Volatile Flavour Profiles of Kidney Beans and Soybeans by GC-MS and PTR-MS. *Food Sci Technol Res* **11**:63–70.

Saraji M, Khaje N. 2012. Recent advances in liquid microextraction techniques coupled with MS for determination of small-molecule drugs in biological samples. *Bioanalysis* **4**:725–739.

Shi S, Valle-Rodriguez JO, Siewers V, Nielsen J. 2011. Prospects for microbial biodiesel production. *Biotechnol. J.* **6**:277–285.

Silva SL, Silva AMS, Ribeiro JC, Martins FG, Da Silva FA, Silva CM. 2011. Chromatographic and spectroscopic analysis of heavy crude oil mixtures with emphasis in nuclear magnetic resonance spectroscopy: A review. *Anal. Chim. Acta* **707**:18–37.

Smith KM, Liao JC. 2011. An evolutionary strategy for isobutanol production strain development in *Escherichia coli*. *Metab. Eng.* **13**:674–681.

Solomons TWG, Fryhle CB. 2002. Organic Chemistry [Book]. New York, New York: John Wiley & Sons, Inc.

Somashekar D, Joseph R. 2000. Inverse relationship between carotenoid and lipid formation in *Rhodotorula gracilis* according to the C/N ratio of the growth medium. *World J. Microbiol. Biotechnol.* **16**:491–493.

Somashekar D, Venkateshwaran G, Srividya C, Krishnanand, Sambaiah K, Lokesh BR. 2001. Efficacy of extraction methods for lipid and fatty acid composition from fungal cultures. *World J. Microbiol. Biotechnol.* **17**:317–320.

Speight JG. 2002. Handbook of Petroleum Product Analysis - Knovel. Hoboken, NJ: John Wiley & Sons, Inc. 454 p.

Stashenko EE, Martínez JR. 2007. Sampling volatile compounds from natural products with headspace/solid-phase micro-extraction. *J. Biochem. Biophys. Methods* **70**:235–242.

Steeghs M. 2004. Proton-Transfer-Reaction Mass Spectrometry as a New Tool for Real Time Analysis of Root-Secreted Volatile Organic Compounds in Arabidopsis. *PLANT Physiol.* **135**:47–58.

Stewart JC, Parry JB. 1981. Factors Influencing the Production of Cellulase by *Aspergillus fumigatus* (Fresenius). *J. Gen. Microbiol.* **125**:33–39.

Stinson M, Ezra D, Hess WM, Sears J, Strobel G. 2003. An endophytic *Gliocladium* sp. of *Eucryphia cordifolia* producing selective volatile antimicrobial compounds. *Plant Sci.* **165**:913–922.

Strobel GA, Knighton B, Kluck K, Ren Y, Livinghouse T, Griffin M, Spakowicz D, Sears J. 2008. The production of myco-diesel hydrocarbons and their derivatives by the endophytic fungus *Gliocladium roseum* (NRRL 50072). *Microbiology* **154**:3319–3328.

Strobel GA, Knighton B, Kluck K, Ren Y, Livinghouse T, Griffin M, Spakowicz D, Sears J. 2010. The production of myco-diesel hydrocarbons and their derivatives by the endophytic fungus *Gliocladium roseum* (NRRL 50072). *Microbiology* **156**:3830 –3833.

Suryanarayanan TS, Thirunavukkarasu N, Govindarajulu MB, Sasse F, Jansen R, Murali TS. 2009. Fungal endophytes and bioprospecting. *Fungal Biol. Rev.* **23**:9–19.

Tang Y-J, Zhu L-W, Li H-M, Li D-S. 2007. Submerged Culture of Mushrooms in Bioreactors -- Challenges, Current State-of-the-Art, and Future Prospects. *Food Technol. Biotechnol.* **45**:221–229.

Tomsheck AR, Strobel GA, Booth E, Geary B, Spakowicz D, Knighton B, Floerchinger C, Sears J, Liarzi O, Ezra D. 2010. *Hypoxylon* sp., an Endophyte of *Persea indica*,

Producing 1,8-Cineole and Other Bioactive Volatiles with Fuel Potential. *Microb. Ecol.* **60**:903–914.

Treybal R. 1959. Liquid Extraction. *Ind. Eng. Chem.* **51**:378–388.

U.S. Energy Information Administration. 2013. Monthly Energy Review. U.S. Energy Information Administration. http://www.eia.gov/totalenergy/data/monthly/.

Ul-Hassan SR, Strobel GA, Booth E, Knighton B, Floerchinger C, Sears J. 2012. Modulation of volatile organic compound formation in the Mycodiesel-producing endophyte *Hypoxylon* sp. CI-4. *Microbiology* **158**:465–473.

Varela C, Torrea D, Schmidt SA, Ancin-Azpilicueta C, Henschke PA. 2012. Effect of oxygen and lipid supplementation on the volatile composition of chemically defined medium and Chardonnay wine fermented with *Saccharomyces cerevisiae*. *Food Chem.* **135**:2863–2871.

Wald M. 2007. Is ethanol for the long haul? *Sci. Am.* **296**:16–16.

Weil J, Westgate P, Kohlmann K, Ladisch M. 1994. Cellulose Pretreatments of Lignocellulosic Substrates. *Enzyme Microb. Technol.* **16**:1002–1004.

Weldegergis BT, Crouch AM, Górecki T, de Villiers A. 2011. Solid phase extraction in combination with comprehensive two-dimensional gas chromatography coupled to time-of-flight mass spectrometry for the detailed investigation of volatiles in South African red wines. *Anal. Chim. Acta* **701**:98–111.

Wercinski SAS. 1999. Solid phase microextraction - a practical guide. CRC Press 257 p.

Wurzenberger M, Grosch W. 1984. The formation of 1-octen-3-ol from the 10-hydroperoxide isomer of linoleic acid by a hydroperoxide lyase in mushrooms (Psalliota bispora). *Biochim. Biophys. Acta BBA - Lipids Lipid Metab.* **794**:25–30.

Xu Q, Singh A, Himmel ME. 2009. Perspectives and new directions for the production of bioethanol using consolidated bioprocessing of lignocellulose. *Curr. Opin. Biotechnol.* **20**:364–371.

Yacobucci BD, Schnepf R. 2007. Selected Issues Related to an Expansion of the Renewable Fuel Standard (RFS). Open CRS. http://opencrs.com/document/RL34265/2007-12-03/.

Yaws CL. 1998. Yaws' Handbook of Thermodynamic and Physical Properties of Chemical Compounds. McGraw-Hill n/a p. http://www.knovel.com/web/portal/browse/display?_EXT_KNOVEL_DISPLAY_bookid=49.

Yaws CL. 2003. Yaws' Handbook of Thermodynamic and Physical Properties of Chemical Compounds - Knovel. http://www.knovel.com/web/portal/basic_search/display?_EXT_KNOVEL_DISPLAY_bookid=667.

Yoon SH, Lee CS. 2012. Effect of undiluted bioethanol on combustion and emissions reduction in a SI engine at various charge air conditions. *Fuel* **97**:887–890.

Zeng EY, Noblet JA. 2002. Theoretical Considerations on the Use of Solid-Phase Microextraction with Complex Environmental Samples. *Environ. Sci. Technol.* **36**:3385–3392.

Zhang J, Fang X, Zhu X-L, Li Y, Xu H-P, Zhao B-F, Chen L, Zhang X-D. 2011. Microbial lipid production by the oleaginous yeast *Cryptococcus curvatus* O3 grown in fed-batch culture. *Biomass Bioenergy* **35**:1906–1911.

Zhi-Lin Y, Yi-Cun C, Bai-Ge X, Chu-Long Z. 2012. Current perspectives on the volatile-producing fungal endophytes. *Crit. Rev. Biotechnol.* **32**:363–373.

Zhou S, Ingram LO. 2000. Synergistic Hydrolysis of Carboxymethyl Cellulose and Acid-Swollen Cellulose by Two Endoglucanases (CelZ and CelY) from *Erwinia chrysanthemi*. *J. Bacteriol.* **182**:5676–5682.

Zhu LY, Zong MH, Wu H. 2008. Efficient lipid production with *Trichosporon fermentans* and its use for biodiesel preparation. *Bioresour. Technol.* **99**:7881–7885.

APPENDICES

APPENDIX A

PRELIMINARY METHODS DEVELOPMENT WITH *ASCOCORYNE SARCOIDES*

Introduction

The first tasks associated with researching the unique *Ascocoryne sarcoides* were to demonstrate growth in liquid culture on a variety of carbon and nitrogen sources. Once that was successfully achieved, the preliminary tasks of the project aimed to i) improve growth performance by increasing growth rate and final biomass titer, as well as ii) improve the characterization of *A. sarcoides* growth behavior. In the process, much was learned about the physiology of *A. sarcoides*. The merit of these studies was the foundation they provided for later work on *A. sarcoides* volatile organic compounds (VOC) production and metabolic modeling.

The media studies were needed to improve the growth performance of *A. sarcoides* in liquid culture as this was the first time the fungus had been grown in submerged liquid culture. The fungus had visible growth, but the results were weak ($OD_{600} > 0.1$). Once higher biomass density was seen, growth in batch culture systems was monitored over an extended period to characterize the physiology and growth behavior of *A. sarcoides*.

Response surface design and analysis can assist in efficient optimization of fungal systems (Dagbagli and Goksungur, 2008). Response surface design is a method that uses mathematical modeling to determine the minimum number of experiments necessary for an optimization study. The desired optimized variable is deemed the response while each variable impacting the response is a predictor. Generally, for a second-order design, experiments focus at the extrema of the predictors and a fewer number are completed in

the median range. This is often known as a cubic or face center cube design (Figure A.1) (Altekar et al., 2007). For example, the extrema for the variable pH as seen in Figure A.2, are pH=5.0 and 7.0. The result of response surface analysis is a three-dimensional surface or graphical representation of the relationship of the response variable with the predictors. In the response space, the highest point corresponds to the optimal combination of all predictors (Myers, 1995). An example is shown in Figure A.2 for hydrogen production by the bacterium *Clostridium tyrobutyricum* (Jo et al., 2008). The method of response surface design was used to choose the variables on many of the experiments discussed in this section.

Overall, this appendix contains many separate studies with methods distinct from each other. Therefore, this Appendix is formatted with the study methods preceding the results and conclusions before the next study is presented.

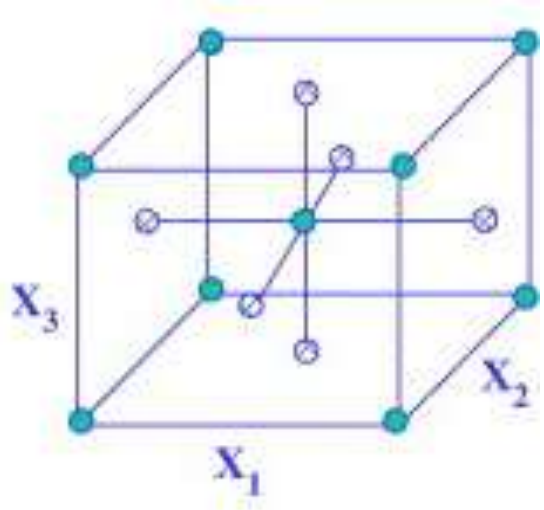

Figure A.1. A representation of face center cubic design, where X_1, X_2, and X_3 are predictors for the interested response variable. (Altekar et al. 2007)

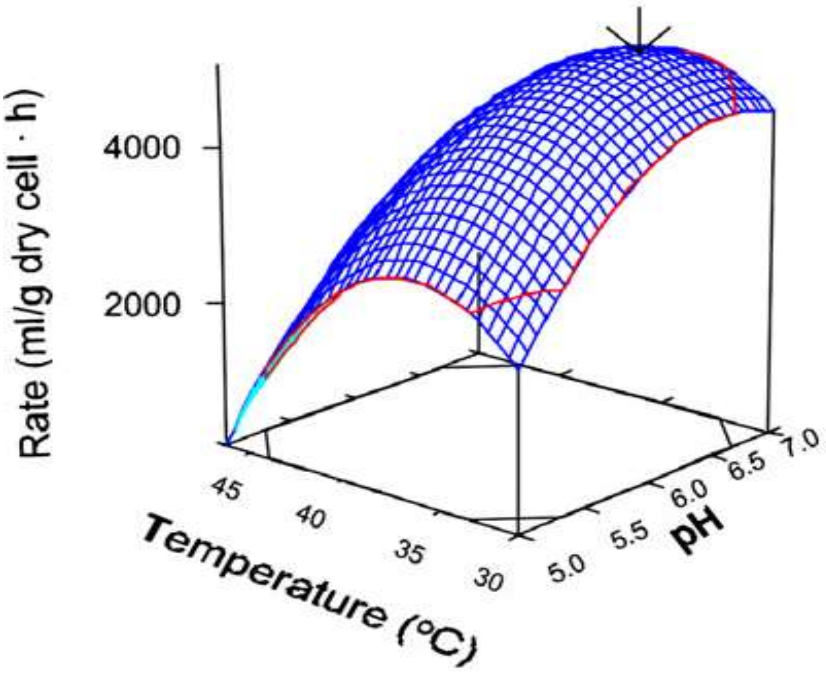

Figure A.2. An example of a response surface resulting from experimental design experimentation. In this case, the response is H_2 gas (Jo et. al., 2008).

Study Methods and Results

Carbon Source Screening

The aim of this study was determine which carbon sources could be utilized by *A. sarcoides* for submerged growth in liquid media.

Methods. *A. sarcoides* was cultured on solid media agar plates and liquid media. Plate media consisted of per liter: 18 g of agar (Difco), 20 g of carbon source and 0.5 g of yeast extract. The carbon sources used were cellobiose, cellulose, glucose, maltose, sucrose, xylose. Agar was boiled with dissolved in water by boiling before adding yeast extract and autoclaving. Before pouring plates, a sterile concentrated sugar stock solution

was added. Oatmeal agar was prepared by boiling 20 g L^{-1} of rolled oats for 5 minutes and filtering through cheesecloth before boiling with 18 g of agar. To finish the oatmeal agar, 1 mL of trace salts was added before autoclaving. Final trace salt concentrations per liter were: $NaH_2PO_4 \cdot 2H_2O$ (1 mg), $MgSO_4 \cdot 7H_2O$ (360 mg), $Ca(NO_3)_2 \cdot 4H_2O$ (280 mg), KCl (60 mg), KNO_3 (80 mg), $FeCl_3$ (2 mg), $MnCl_2$ (5 mg), $ZnSO_4$ (2.5 mg), H_3BO_3 (1.4 mg), and KI (0.7 mg). Plates were inoculated with a Microbank™ bead from frozen stocks (-80°C) and incubated at 21°C and visually monitored for growth. Growth was rated based on presence (+) or absence (-) on the agar plate surface independent of the inoculum plug.

Liquid cultures were grown in the medium listed above without agar and inoculated with a Microbank™ bead from frozen stocks (-80°C). Cultures were grown at 21°C on a rotary shaker at 150 rpm. Growth was grouped in low (+) and high (++) groups based on fungal flocculent density in the medium. Optical density measurements at 600 nm were taken for cultures with translucent media and are listed in Appendix B.

Results. Positive growth of *A. sarcoides* on all solid and liquid media tested was seen (Table A.1 and Figure A.3). The highest growth density was observed on glucose and cellobiose in liquid media. Therefore, these carbon substrates were chosen for the next step of nitrogen source screening.

Table A.1 Growth results of *A. sarcoides* on agar plates and liquid shake flasks. All observations are listed 5 days after inoculation with the exception of cellulose (non-soluble substrate prevents visual growth determination until biofilm formation on flask surface).

Medium (20 g/L carbon source with 0.5g/L YE)	Solid Growth (Agar Plate)	Liquid Growth (Shake Flask)
Oatmeal	+	+
Cellobiose	+	++
Cellulose	+	+
Glucose	+	++
Maltose	+	+
Sucrose	+	+
Xylose	+	+

Figure A.3. A. Hyphael mat of *A. sarcoides* on potato dextrose agar. The filamentous nature of the fungus is readily apparent. B. Flasks of liquid medium containing *A. sarcoides*. The liquid would be translucent in the absence of the fungus.

Nitrogen Source Screening

The aim of this study was determine the best defined nitrogen source that would support *A. sarcoides* growth in liquid culture.

Methods. Liquid cultures of *A. sarcoides* were grown on 60 mL of liquid media consisting of 20 g L^{-1} carbohydrate source, glucose or cellobiose, and a nitrogen

compound, 0.5 g L^{-1} casamino acids, 0.5 g L^{-1} glycine, 0.053g L^{-1} potassium nitrate (KNO_3), 0.5 g L^{-1} ammonium tartrate ($(NH_4)_2C_4H_4O_6$), 0.053 g L^{-1} ammonium chloride (NH_4Cl), 2 g L^{-1} ammonium sulfate ($(NH_4)_2SO_4$), or yeast extract. The nitrogen compounds and concentrations were chosen from a review of the Handbook of Microbiological Media (Atlas, 2004). 250 mL shake flasks were inoculated with 1 mL of culture from a 7 day old culture grown from a Microbank™ bead a Microbank™ bead frozen stock (-80°C) on 20 g L^{-1} glucose and 0.5 g L^{-1} yeast extract at room temperature and 150 rpm rotary shaking. Inoculated 250 mL shake flasks covered with gas permeable cloths were incubated at 21°C on rotary shakers at 150 rpm for 12 days. Growth was analyzed through daily samples of optical density at 600 nm or visual observation. Once removed from the oven, filters were allowed to equilibrate at room temperature in a desiccator and then weighed. Growth was rated on a scale of 1 to 4 based on visual observation or optical density at 600 nm(available values listed in Appendix B).

Results. The most complex and rich nitrogen sources, casamino acids and yeast extract, resulted in the highest concentration of biomass (Table A.2). Among the defined nitrogen sources, ammonium chloride, NH_4Cl, was superior as it resulted in the highest biomass density. So, it was chosen for future media formulations to allow the results of this work to be more applicable to metabolic modeling and the ability to calculate more nutrient specific kinetics, if required. Due to the higher growth on complex sources, a trace salt mixture containing many micronutrients was added to the medium to enhance

growth and account for any nutrient deficiencies in a defined way. The salts are given in the next methods section (Medium Development).

Table A.2 Growth results of *A. sarcoides* in liquid media with two different carbon sources: glucose and cellobiose (both at 20 g/L) and listed nitrogen sources. Cultures were grown in aerobic shake flasks at room temperature and 150 rpm rotary shaking.

Nitrogen Source	Glucose Carbon Source	Cellobiose Carbon Source
Casamino acids	+++	+++
Glycine	+	+
Potassium nitrate	+	+
Ammonium tartrate	+	+
Ammonium chloride	++	++
Ammonium sulfate	–	–
Yeast extract	++++	++++

Medium Development

It was desirable to replace yeast extract with more defined sources of nutrients. However, with ammonium chloride as the nitrogen source, the growth was significantly lower than on yeast extract alone. Therefore, this study was completed to assess if the fungus experienced any nutrient limitations in the defined medium by the depletion of phosphorous or sulfur. This study was also designed to assess the tolerance of *A. sarcoides* to salinity in the form of sodium chloride.

Methods. Liquid cultures were grown in baffled Erlenmeyer flasks (250mL) with 60 mL of the medium composed of 20 g L^{-1} glucose, 5 g L^{-1} NH_4Cl, 0.05 g L^{-1} yeast extract and trace salts. The salts included per liter: $NaH_2PO_4 \cdot 2H_2O$ (1 mg), $MgSO_4 \cdot 7H_2O$ (360 mg), $Ca(NO_3)_2 \cdot 4H_2O$ (280 mg), KCl (60 mg), KNO_3 (80 mg), $FeCl_3$ (2 mg), $MnCl_2$ (5 mg), $ZnSO_4$ (2.5 mg), H_3BO_3 (1.4 mg), and KI (0.7 mg). The base medium recipe was

supplemented with (per liter) 2.5 g Na_2HPO_4 and/or 0.5 g $MgSO_4*7H_2O$, or 24.7 g NaCl. Phosphorous and sulfur sources and concentrations were chosen from a review of the Handbook of Microbiological Media (Atlas, 2004). NaCl was used to test the tolerance of the fungus to salinity.

The 250 mL shake flasks were inoculated with 1 mL of culture from a 7 day old culture grown from a Microbank^{TM} bead frozen stock (-80^{o}C) on 20 g L^{-1} glucose and 0.5 g L^{-1} yeast extract. Cultures were sealed with sterile gas permeable cloths and grown for 14 days at 21^{o}C on a rotary shaker (150 rpm). Growth was analyzed on days 8 and 14 by cell dry weight, where samples were filtered onto glass fiber filters (Whatman GF/F), rinsed with deionized water and dried overnight in an oven at 99^{o}C. Once removed from the oven, filters were allowed to equilibrate at room temperature in a desiccator for a minimum of one hour before being weighed on a milligram-specific balance, MT5 by Mettler Toledo (Columbus, OH).

Results.Table A.3 shows the media combinations used in this study. Biomass accumulation was increased from 0.5 g L^{-1} with Medium A to 4.6 g L^{-1} with Mediums B and D (Figure A.4). The 9 fold increase suggested Medium A was limited for phosphorus. Sulfur levels appeared adequate for medium composition A, as additional $MgSO_4$ did not further increase the final biomass concentrations. As a result, Medium A was modified with 2.5 g L^{-1} Na_2HPO_4 for future experimentation. Reaching a fungal biomass density level near 5 g L^{-1} was valuable for future experimentation with *A. sarcoides.* The cultures showed tolerance to salinity at 24.7 g L^{-1} concentration.

Table A.3 Media A-F nutrient combinations for medium development biomass study. Medium A is the control medium with B-F being a variation of A. Trace Salt mixture composition is listed in the Methods section.

A	20 g/L Glucose 5 g/L NH_4Cl 0.05 g/L Yeast Extract Trace Salts
B	A with 2.5 g/L Na_2HPO_4
C	A with 0.5 g/L $MgSO_4*7H_2O$
D	A with 2.5 g/L Na_2HPO_4 & 0.5 g/L $MgSO_4*7H_2O$
F	A with 24.7 g/L NaCl

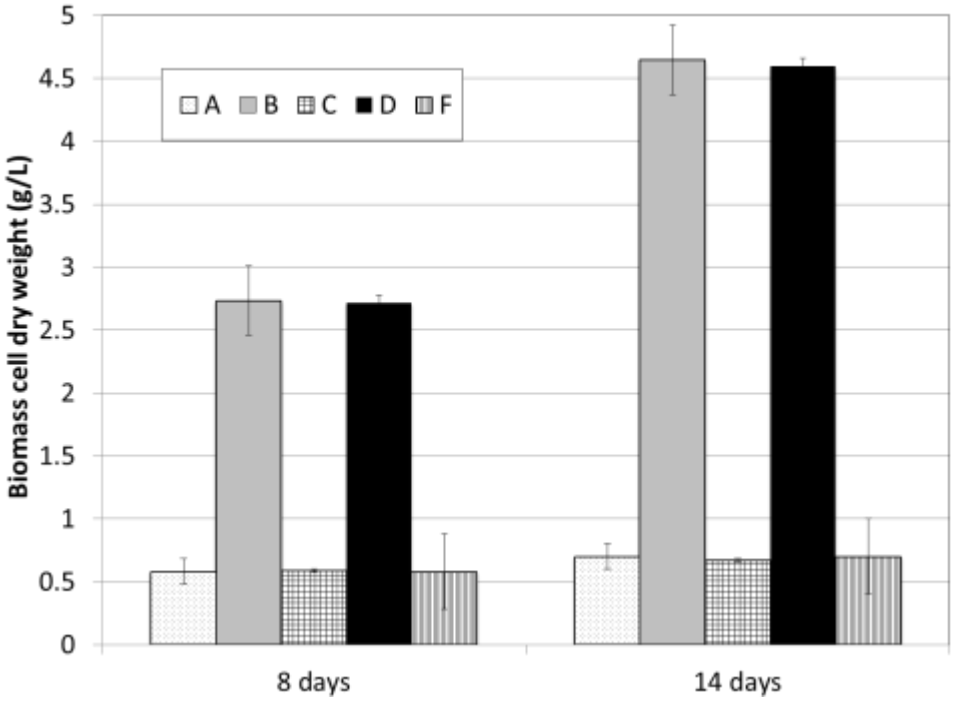

Figure A.4. *A. sarcoides* biomass concentrations for shake flask cultures grown on five different medium compositions. Two samples were taken from each culture. The first was taken after 8 days of cultivation and the second sample was taken after 14 days of cultivation. Medium E results are not shown due to oxygen infiltration. Medium composition (A-F) can be found in Table 1. Media was not pH buffered.

As a result of these studies, the final medium recipe became 20 g L^{-1} carbon source, 5 g L^{-1} NH_4Cl, 2.75 g L^{-1} $NaH_2PO_4{\cdot}2H_2O$, 0.86 g L^{-1} $MgSO_4{\cdot}7H_2O$, 0.05 g L^{-1}

yeast extract and trace salts per liter: 280 mg $Ca(NO_3)_2 \cdot 4H_2O$, 60 mg KCl, 80 mg KNO_3, 2 mg $FeCl_3$, 5 mg $MnCl_2$, 2.5 mg $ZnSO_4$, 1.4 mg H_3BO_3, and 0.7 mg KI and is hereafter referred to as 1x AS medium.

Optimal Medium pH Identification

Preliminary data indicated acidic pH range tolerance by *A. sarcoides*. This study was completed to determine what pH range was tolerated by *A. sarcoides* and which starting pH resulted in the highest accumulated biomass.

Methods. Medium A was adjusted to pH 4 and 7 and the media was buffered with 50 mM potassium hydrogen phthalate (pKa 5.4) and 50 mM potassium phosphate (mixtures of K_2HPO_4 and KH_2PO_4), respectively. Further studies used Medium A buffered at four different pH values: pH 3, 4, 5 using 0.1 M potassium hydrogen phthalate buffer and pH 6 with 0.1 M potassium phosphate buffer. Cultures were incubated at 23^{o}C with rotary shaking at 150 rpm. Triplicate flasks were used for each pH value. Samples (1 mL each) were removed every 2-3 days to assay for pH. On day 11, the remaining culture was harvested for final biomass concentration as measured by cell dry weight as described previously.

Non-buffered 250 mL flasks contained 60 mL of 20 g L^{-1} glucose, either 0.5 g L^{-1} ammonium tartrate ($(NH_4)_2C_4H_4O_6$) or 0.2 g L^{-1} ammonium chloride (NH_4Cl), with and without 0.05 g L^{-1} yeast extract to make four separate nitrogen source combinations. Culture flasks were inoculated with 1 mL of culture from a 7 day old culture grown from a Microbank^{TM} bead frozen stock (-80^{o}C) on 20 g L^{-1} glucose and 0.5 g L^{-1} yeast extract.

Cultures were sealed with sterile gas permeable cloths and grown for 10 days at 21^{o}C on a rotary shaker (150 rpm). Samples (1 mL each) were removed daily to assay for pH.

Results. Biomass growth curves were recorded at different initial culture pH values. A representative example of experimental results shows the biomass density as a function of time and highly dependent upon the initial pH (Figure A.5). Essentially no growth was observed at pH 7, and pH 4 had no inhibitory effects on growth rate or biomass accumulation of *A. sarcoides*.

Studying distinct starting pH levels, the highest final cell densities (3 g cell dry weight per liter (cdw/L)) were achieved using a starting medium pH of 4 (Figure A.6). However, it is important to note that the buffer concentration of 0.1 M was not sufficient to maintain a constant pH throughout the 11 day experiment with all media reaching a final pH between 3 and 4 (Figure A.7). There was a slight increase in pH by all cultures by day 2 before the pH started dropping. The pH declined as growth progressed (with the exception of pH 3) was most likely due to the metabolism of glucose to acids such as acetic acid. In some cases, pH may indicate the amount of metabolic activity of *A. sarcoides*. When grown on glucose with four different nitrogen source combinations, the amount of growth on ammonium chloride was approximately double that of the growth on ammonium tartrate (Table A.2). This result is reflected by the pH trends of each combination with the NH_4 cultures experiencing a quick decline in pH to a final around

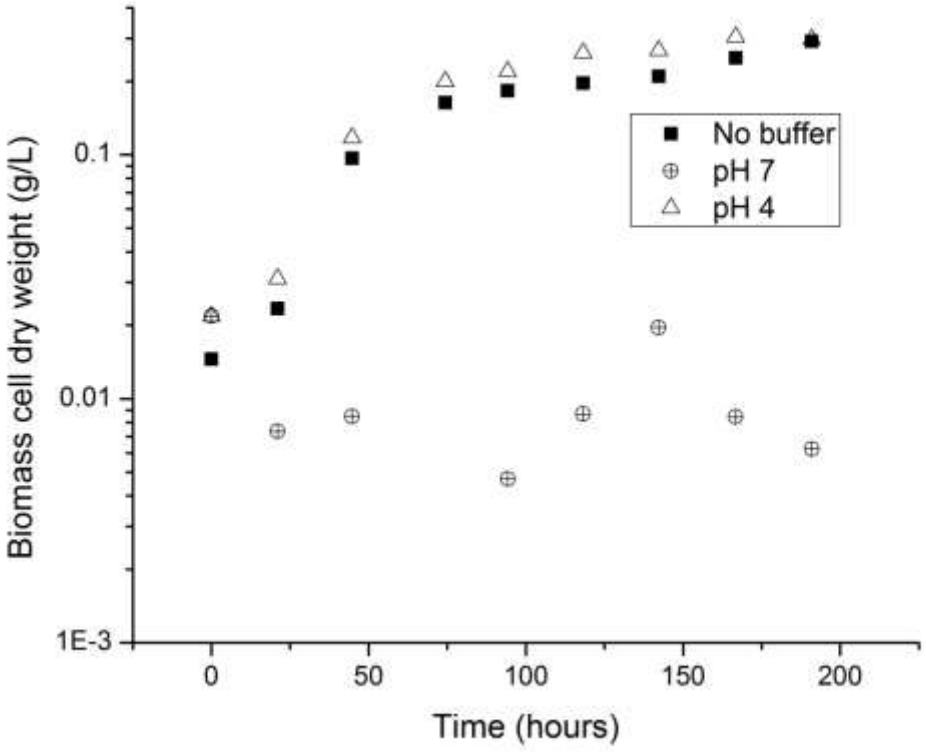

Figure A.5. *A. sarcoides* biomass concentration as a function of time for shake flask cultures grown on minimal medium A. Buffered cultures utilized 50 millimolar (mM) potassium phosphate buffer for pH 7 and 50 mM Potassium hydrogen phthalate buffer for pH 4.

3.5, while the ammonium tartrate cultures have a slow decline to around pH 5.5 (Figure A.8). In addition, Figure A.8 shows that the yeast extract improved the growth of the cultures, as their pH trends lower than those without added yeast extract.

It was clear from the biomass results that a starting pH of 7 has inhibitory effects on the final biomass accumulation of *A. sarcoides*, while a smaller effect was seen at pH

3 (Figures A.5 & A.6). Therefore, any future work was limited to a pH range from 3.5 to 6.5.

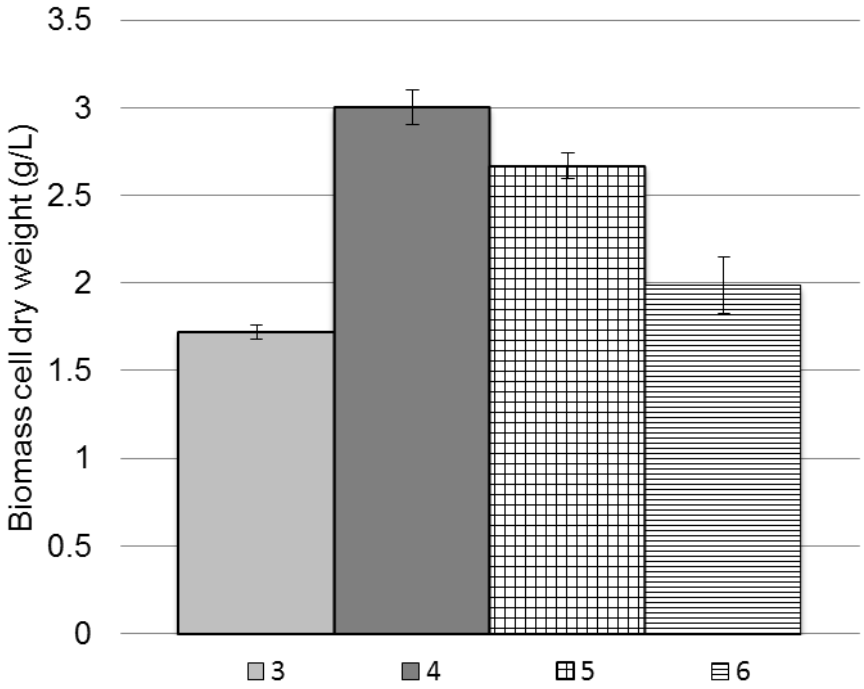

Figure A.6. Final *A. sarcoides* biomass densities for shake flask cultures grown at the listed pH on the horizontal axis. Cultures were grown for 11 days at room temperature on Medium A buffered at three different pH values (3, 4, 5) with 0.1 M potassium hydrogen phthalate buffer and pH 6 with 0.1 M potassium phosphate buffer.

Light Availability

Dr. Gary Strobel had observed the growth and VOC production of some fungal strains being impacted by the amount of light available in their growth environment. To determine whether *A. sarcoides* growth was impacted by the availability of light, it was grown in complete darkness and with a 14-10 light-dark cycle (in hours).

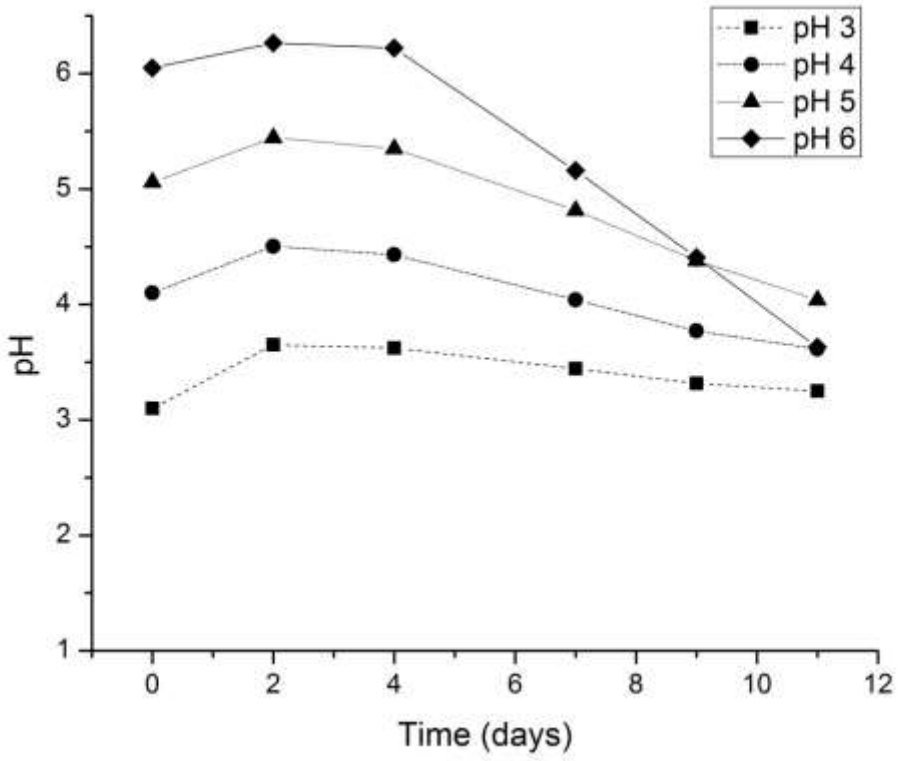

Figure A.7. pH trends of *A. sarcoides* cultures grown on buffered medium A in shake flasks. Medium A was buffered at three different pH values (3, 4, 5) using 0.1 M potassium hydrogen phthalate buffer and at pH 6 with 0.1 M potassium phosphate buffer. The data are the average of three replicates and include standard deviation error bars, but variation is too minor to be seen.

Methods. *A. sarcoides* was cultured in baffled Erlenmeyer flasks (250mL) with 60 mL of the medium composed of 20 g L^{-1} Glucose 1x AS medium. The flasks were inoculated with 2.7 mL of culture from a 7 day old culture grown from a Microbank™ bead frozen stock (-80°C) on 20 g L^{-1} glucose and 0.5 g L^{-1} yeast extract. Cultures were sealed with gas permeable cloths and grown for 14 days at 23°C on a rotary shaker (150 rpm). Growth was analyzed on days 6 and 8 by cell dry weight, where samples were

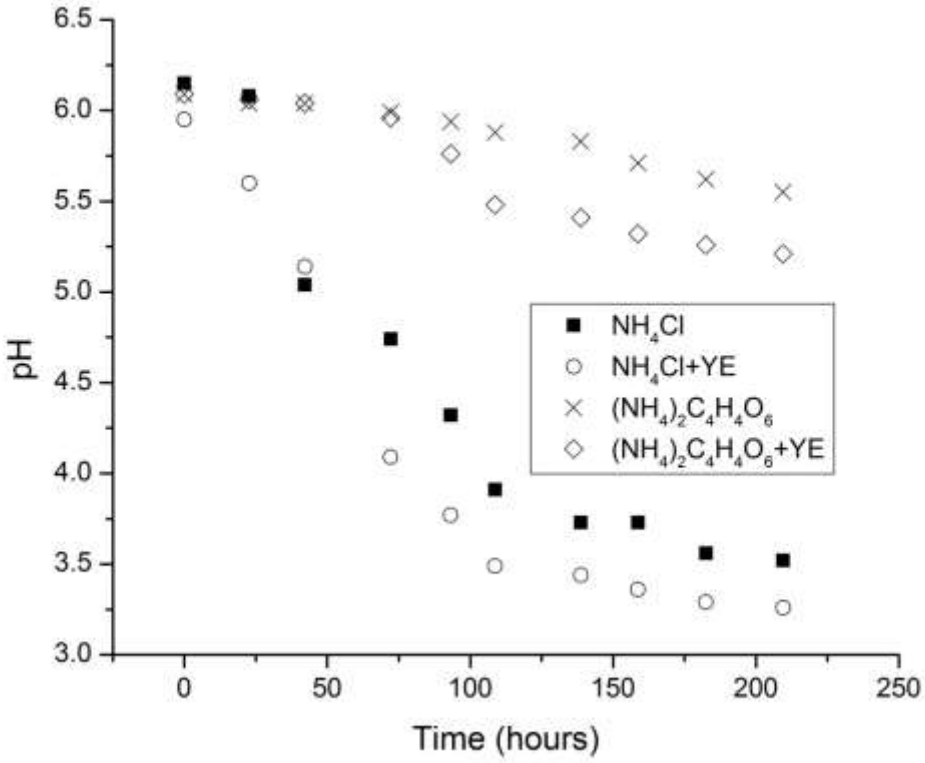

Figure A.8. pH trends of *A. sarcoides* cultures grown on glucose and combinations of nitrogen sources, YE is yeast extract. Cultures were grown in shake flasks with rotary shaking at room temperature.

filtered onto glass fiber filters (Whatman GF/F), rinsed with deionized water and dried overnight in an oven at 80^{o}C. Once removed from the oven, filters were allowed to equilibrate at room temperature in a desiccator for a minimum of one hour before being weighed on a milligram-specific balance. The flasks grown in the "dark" were thoroughly covered with foil and placed on the same shaker as the "light" flasks. The shaker was located under a light bank on a timed light cycle, illuminated for 14 hours and dark for 10 hours daily.

Results. There was no statistically significant difference in *A. sarcoides* growth under the varying light conditions (Figure A.9). Biomass as measured by cell dry weight was near 1.4 g L^{-1} and 2.0 g L^{-1} on days 6 and 8, respectively, regardless of light conditions. For light sensitive fungi observed in Dr. Strobel's lab, light had an impact on growth and on VOC production. Therefore, it was assumed for *A. sarcoides* that no difference in growth most likely meant insignificant difference in VOC production. In future experiments, the amount of light available to the fungus was not carefully controlled. However, all cultures are grown away from natural light and only had light when the laboratory lights were illuminated.

Optimization of Biomass

To assess the impact of multiple environmental factors on *A. sarcoides* growth and VOC production, response surface experimental design was used. This design method reduced the overall number of experiments necessary and allowed for future statistical analysis. In this section, the results of biomass optimization using this method are shown.

Methods. The variables pH, temperature and nutrient level were tested for *A. sarcoides*, and modeling used cubic centered design to determine iterations and variable parameters of experiments (Table A.4). Preliminary work helped shape the range limits of the variables. Culture starting pH ranged from 3.5 to 6.5, so for the cubic design,

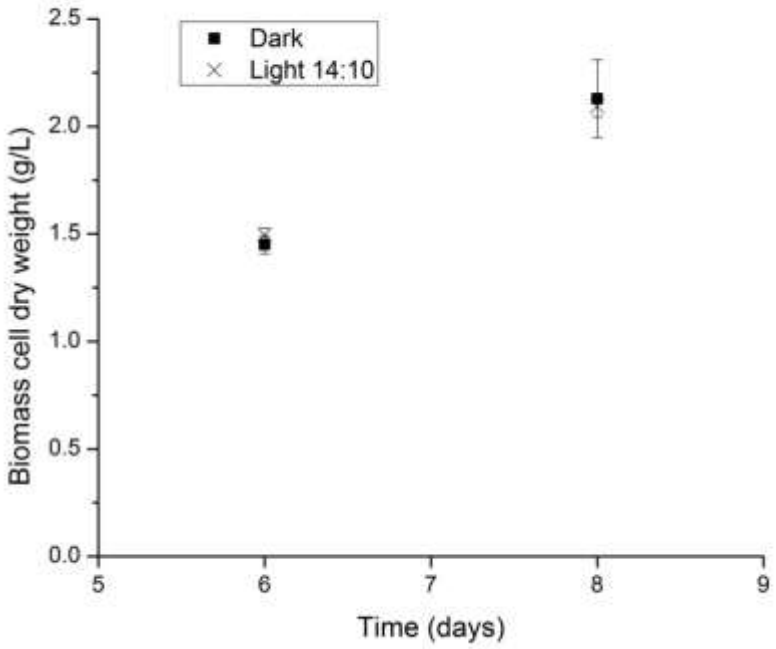

Figure A.9. Total biomass accumulation (cell dry weight) of *A. sarcoides* grown on glucose with 150 rpm rotary shaking at 23°C. Dark flasks were not exposed to visible light. Light flasks were grown with a 14-10 light-dark cycle (hours).

experiments were run at 3.5, 5, and 6.5. Temperature ranged from 13°C to 28°C, so with the cubic design of experiments, the main temperatures tested were 13°C, 20°C and 28°C, although some experiments were conducted at room temperature in the range of 21 °C to 23°C. Nutrient level was varied from the original medium recipe to two or three times the concentration of medium constituents with the exception of calcium and magnesium, because at higher concentration levels they precipitated from solution. Cultures were grown with 60 mL of glucose 1x AS medium with 100mM KH_2PO_4 buffer with rotary shaking at 150 rpm. Starting pH adjusted with 1M HCl or 2 M NaOH as required.

Table A.4. Experimental design matrix used for small-scale batch cultures to explore effects of the variables on VOC production by *A. sarcoides* growth on glucose and cellulose. A. Experimental variables, B. Combination of variables.

A.

Value	Medium Nutrient Level	pH	Temperature (^{o}C)	Headspace Condition
-1	1x	3.5	13	Anoxic
0	2x	5	20	Sealed Batch
1	3x	6.5	28	Aerobic

B.

Medium Nutrient Level	Temperature (^{o}C)	pH	Headspace Condition
-1	1	1	-1
0	0	0	-1
1	-1	-1	-1
-1	-1	-1	-1
0	0	0	-1
1	1	1	-1
1	-1	1	-1
-1	-1	1	-1
-1	1	-1	-1
1	1	-1	-1
-1	1	1	0
0	0	0	0
1	-1	-1	0
-1	-1	-1	0
1	1	1	0
1	-1	1	0
-1	-1	1	0
-1	1	-1	0
1	1	-1	0
-1	1	1	1
0	0	0	1
1	-1	-1	1
-1	-1	-1	1
0	0	0	1
0	0	0	1
1	1	1	1
1	-1	1	1
-1	-1	1	1
-1	1	-1	1
1	1	-1	1

After 14 days of growth, a known volume of well-mixed culture liquid was collected and filtered to determine cell dry weight (as above).

Three headspace conditions were used: aerobic, sealed batch and anoxic. Aerobic flasks were sealed with gas permeable cloth; sealed batch cultures were stopper and crimp sealed 120 mL culture bottles, effectively sealing the headspace. Anoxic cultures were prepared by bubbling the inoculated medium with nitrogen for 15 minutes before sealing and crimping the bottle. After the first iteration of aerobic experiments which determined a temperature below 20^{o}C to be the optimal temperature for biomass density, the range 13 to 20^{o}C was divided again, and some experiments run at 16.5^{o}C to obtain more data to determine the optimum temperature more accurately. The same is true of pH and nutrient level, so experiments were conducted at pH 5.6 and a nutrient level of 2.3 times original medium recipe.

Results. The experiments completed showed a unique maximum biomass response under the varying conditions. The results from aerobic cultures are shown by Figure A.10A, indicating the maximum biomass was achieved near a pH of 5.5 and a temperature near 20^{o}C. There was a slow increase in biomass for increasing nutrient level up to 3-fold medium recipe concentration. Within the tolerant pH range of *A. sarcoides*, pH did not have a very significant effect on final biomass density as seen in Figure A.10A, with only a slight slope increase for biomass due to pH, and the maximum is reached before pH 6 (Figure A.10A). Sealed batch results showed increasing biomass with decreasing temperature and increasing nutrients (Figure A.10B). In addition, a pH

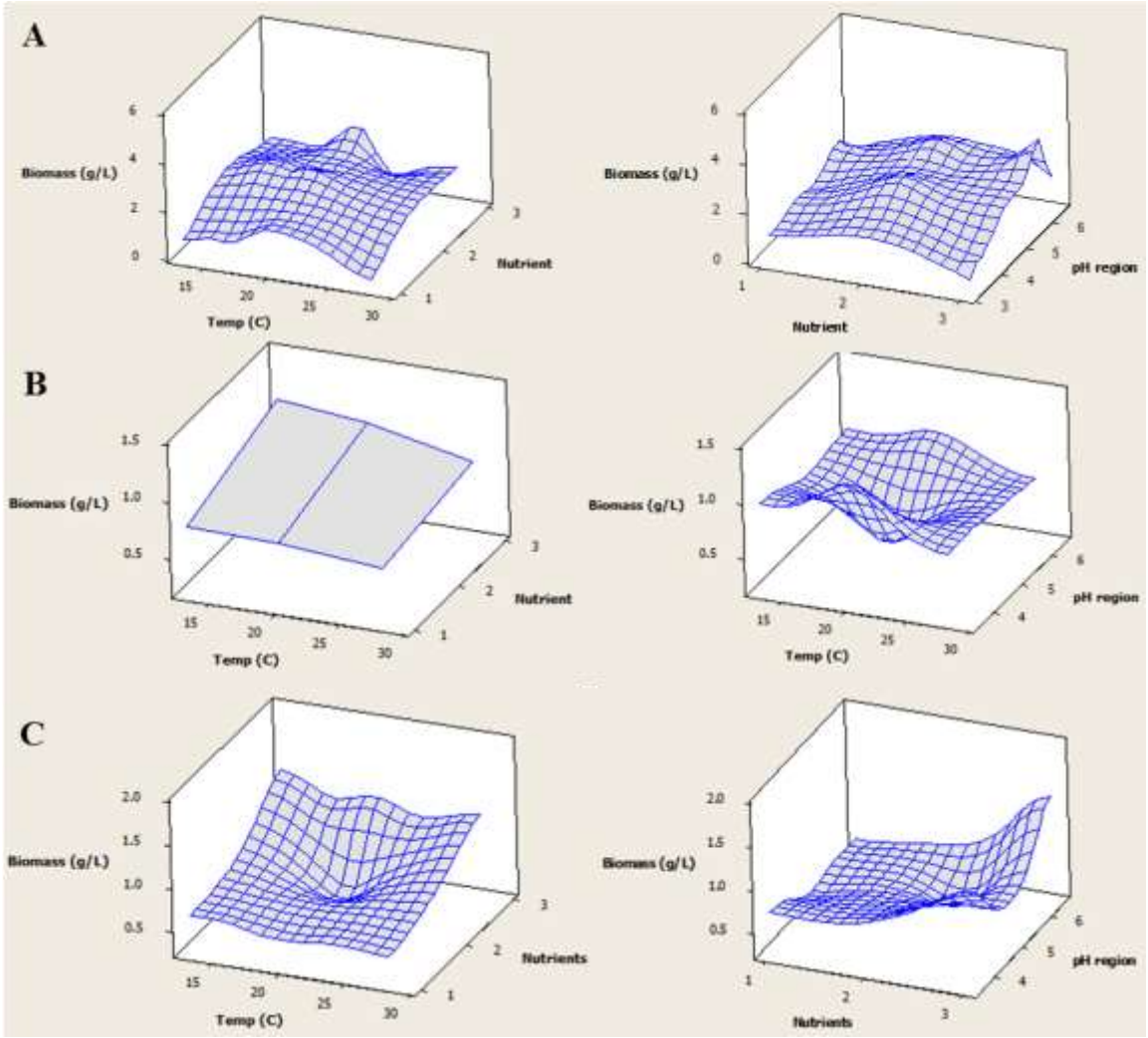

Figure A.10 Response surfaces modeled from experimental data of maximum biomass after 14 days of growth with the following headspace conditions: A. Aerobic, B. Sealed Batch, and C. Anoxic.

above 5 appeared favorable for biomass growth, but there was not a significant interaction between temperature and pH. Results from anoxic bottles showed increasing biomass with increasing nutrient level, and a slight impact from temperature with a slight increase at lower temps (Figure A.10C). The impact of pH under anoxic conditions was unclear.

Growth Rates

In order for fungal products from *A. sarcoides* to be measured more accurately, it was necessary to improve the growth of the fungus to higher concentrations and to determine the impact of environmental conditions upon them. The growth rate of the organism is also an important factor, because a faster growth rate reduces the amount of time necessary to reach the culture's maximum biomass density. The equations necessary to calculate growth rates are listed below (Equations A.2 and A.3). In addition to the exponential phase, where the equations apply, there are also lag, a declining growth rate, a stationary and death phases associated with fungi (Griffin 1994).

Batch culture growth rates are proportional to the amount of dry weight of fungus produced over time:

$$dX/dt = \mu * X, \qquad \text{eqn. A.1}$$

Where: X is the dry weight of the fungus, μ is the specific growth rate, and t is time. Using integration, dry weight data can be used to directly calculate the specific growth rate:

$$\ln X = \mu * t + b, \qquad \text{eqn. A.2}$$

Where: b is the natural log of the starting concentration of the batch culture due to the addition of the inoculum.

Methods. Cultures were grown with 60 mL of glucose 1x AS medium with 100mM KH_2PO_4 buffer. Starting pH adjusted with 1M HCl or 2 M NaOH as required. The carbon sources used were glucose, sodium salt of carboxylmethyl cellulose, and

microcrystalline cellulose powder. A variety of environmental conditions were tested for *A. sarcoides* growth on glucose carbon substrate: Three headspace conditions were used, aerobic, sealed batch and anoxic. Aerobic flasks were sealed with gas permeable cloth; sealed batch cultures were stopper and crimp sealed 120 mL culture bottles, effectively sealing air in the headspace. Anoxic cultures were prepared by bubbling the inoculated medium with nitrogen for 15 minutes before sealing and crimping the bottle. Cultures were grown at varying temperatures ranging from 13 to 28^{o}C and varying pH values from 3.5 to 6.5 on a rotary shaker at 150 rpm. Design of experiments used cubic centered design to determine iterations and variable parameters of experiments (Table A.4).

During the growth cycle, a known volume of well-mixed culture liquid was collected and filtered to determine cell dry weight (as above). Aerobic shake flask measurements were corrected for evaporation based on control flask evaporation rates per equation A.1 above.

To measure growth on cellulose, an insoluble substrate, a modified Bradford protein assay (Bio-Rad, Hercules, CA) was used. Optical density at 600 nm (OD_{600}) was also employed for growth measurements of carboxylmethyl cellulose.

Results. The lag, exponential, declining and stationary phases of growth were visually apparent when dry weight of *A. sarcoides* was graphically represented (Figure A.11). Note that there was not a lag phase for these experiments, most likely due to

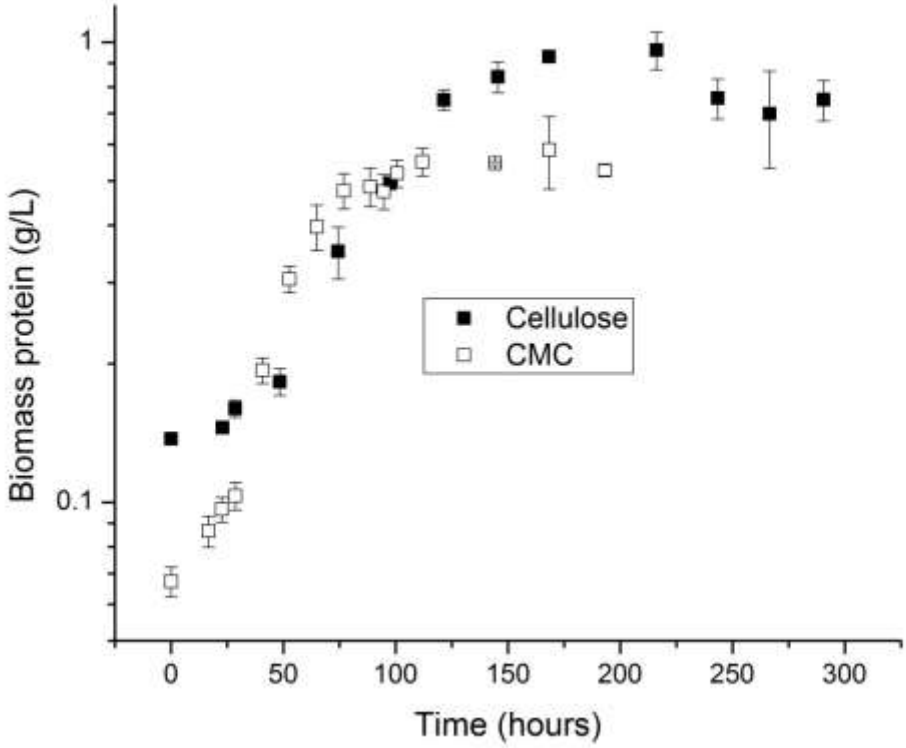

Figure A.11. Growth curves for *A. sarcoides* on cellulose and carboxymethyl cellulose (CMC). Cultures were grown with 21% oxygen sealed headspace.

media improvements discussed in the previous section. In general, *A. sarcoides* has an extended stationary phase several times longer than exponential phase before entry into death phase.

The maximum specific growth rates of *A. sarcoides* were compared with glucose, cellulose and carboxylmethyl cellulose as carbon sources. There was some variation among the values, but the averages are clearly distinct and show statistically faster growth on glucose (0.085 ± 0.035 hr^{-1}), followed by CMC (0.039 ± 0.003 hr^{-1}), then

cellulose (0.014 ± 0.003 hr^{-1}) (Table A.5). These results are what would be expected considering the availability of the carbohydrate sugars in each of the carbon sources, with glucose being the most easily available to *A. sarcoides* for carbohydrate metabolism.

Table A.5. Maximum specific growth rates (hr^{-1}) of *A. sarcoides* on three different carbon sources. Measurements were taken at 20°C, pH 5 and under sealed batch conditions by optical density and modified Bradford protein assay.

Glucose	**CMC**	**Cellulose**
0.1251	0.0392	0.0129
0.0598	0.0388	0.0131
0.0686	0.0385	0.0126
	0.0346	0.0173
	0.0398	0.0161
	0.0439	0.0161
		0.0098

Growth rate results ranged from 0.022 ± 0.017 hr^{-1} to 0.075 ± 0.022 hr^{-1} based on variations in temperature and headspace condition (Figure A.12). There was a clear difference among oxygen conditions at 20°C, but not at 13°C or 28°C. Starting pH of the culture did not show a significant impact on the maximum specific growth rates at any temperature. The growth rates achieved after improving the medium recipe (Medium Development Section) were 0.062 hr^{-1} improved from 0.033 hr^{-1}. So, pH control had no significant improvement over the original medium formulation without buffer capacity.

From these results, it was learned that cell dry weights were insufficient to give accurate growth rates. This was due not only to the accuracy of weights obtained, but the

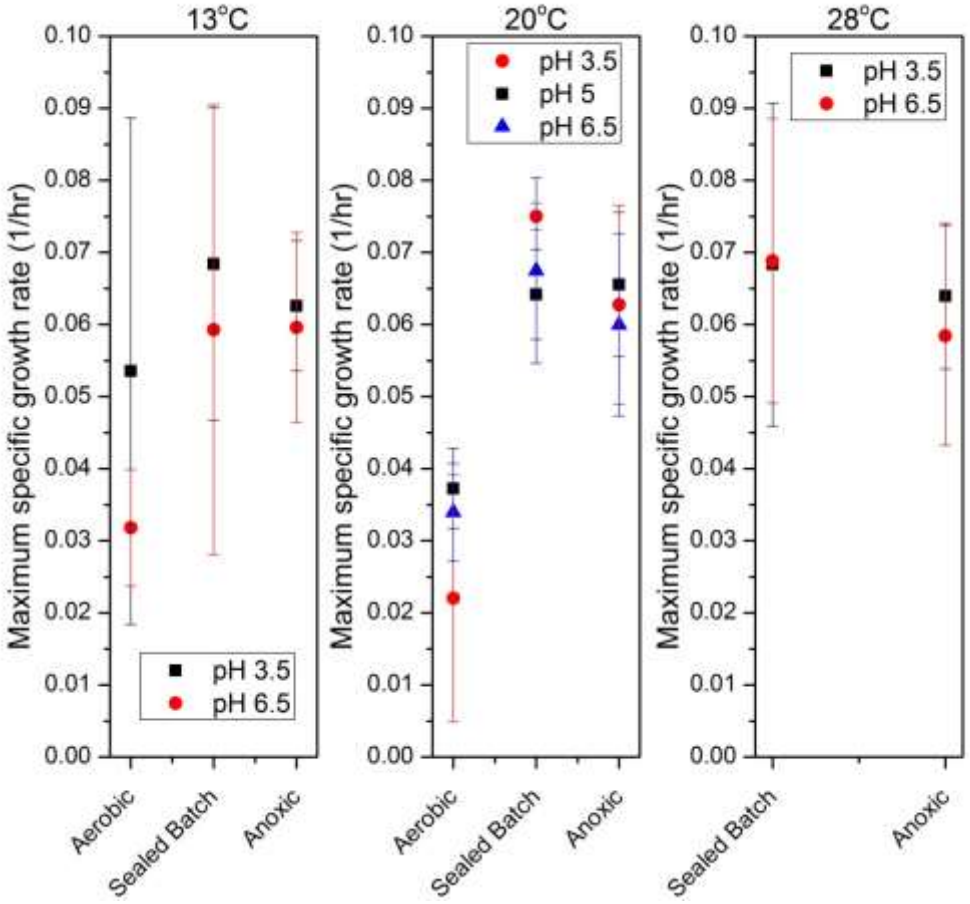

Figure A.12. Specific growth rates for *A. sarcoides* with glucose as the carbon source as measured by cell dry weight. Three different temperature (top axis) and oxygen (bottom axis) conditions are reported. Errors bars represent standard deviations.

physical limits of the total number of samples that can be removed from a single culture especially early in the exponential phase when total biomass accumulation was low. Therefore, a protein assay was developed to measure growth for cellulose and optical density measurements at 600 nm were further explored and decided to be valuable for real-time growth measurements. The accuracy of the measurements was improved as

indicated by the error bars in FigureA.11. The values in Table A.5 were taken with these methods.

Respiration Monitoring

To gain more knowledge on the metabolism of *A. sarcoides*, the fungus was cultured in a batch reactor system equipped with an off-gas analyzer. The goals of the experiments were to monitor the respiration of the fungus in liquid batch culture and gain some bioprocess information important in commercial fermentations such as oxygen uptake, carbon dioxide evolution, and the respiratory quotient (Doran, 2012). These values taken together with the oxygen uptake rate indicate the efficiency of aerobic respiration as well as energy requirements of the fungus (Cochrane, 1963)

Methods: *A. sarcoides* was cultured in Biostat B Twin Plus 5L jacketed reactors (Sartorius Stedim Biotech, Germany) (Figure A.13). pH and dissolved oxygen were monitored by internal Hamilton Easyferm Plus & Oxyferm FDA probes, respectively. 2.7 L of 1x AS medium was inoculated with 300 mL of a 7 day old culture grown from a Microbank^{TM} bead frozen stock (-80^{o}C) on 20 g L^{-1} glucose and 0.5 g L^{-1} yeast extract for a final volume of 3 L. Stir rate (250 or 300 rpm) and temperature (23^{o}C) were controlled to maintain a constant value. When applicable, control of pH was maintained with 0.5 M NaOH and 1.0 M HCl. The reactor effluent gas was routed to a GMUX 8 multiplexer then to an EGAS-L analyzer unit (both by Sartorius Stedim Biotech). Background concentrations of CO_2 and O_2 were determined from the inlet air stream. The analyzer

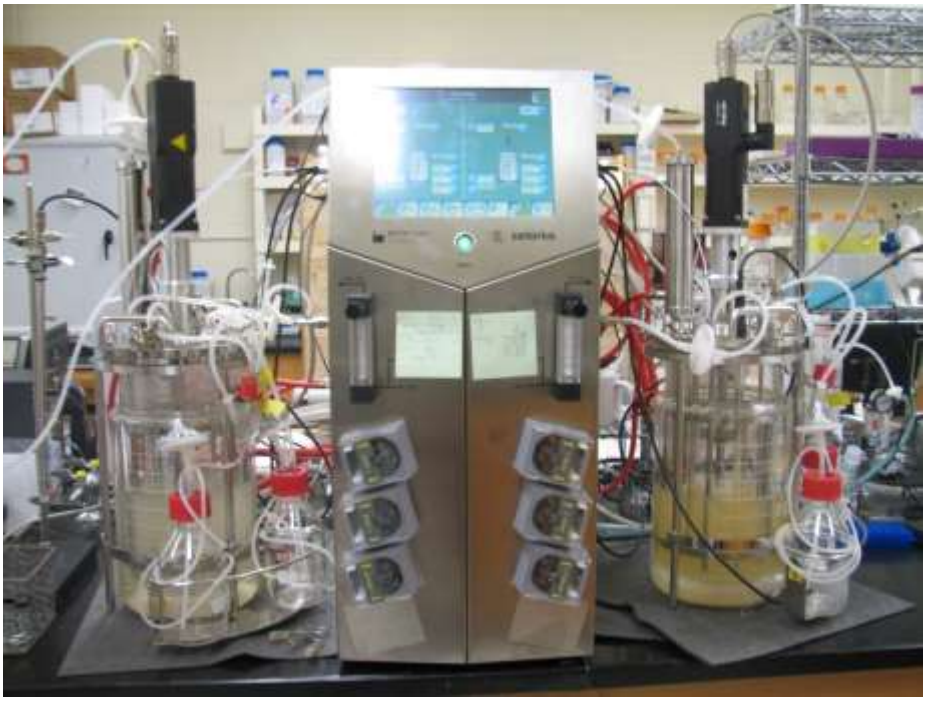

Figure A.13. Biostat B Twin Plus 5L jacketed reactors by Sartorius Stedim Biotech as seen under operation with temperature and stir rate control. Both reactors are filled with cultures of *A. sarcoides*.

output data (CO_2 and O_2 mole percent) were recorded by the MCFS Win 2.1 software. Daily samples of approximately 12 mL were removed from each culture vessel, and filtered onto glass fiber filters (Whatman GF/F) then dried overnight in a drying oven at 80^{o}C. Once removed from the oven, the filters were allowed to come to room temperature in a desiccator and weighed on a milligram specific scale. Additional liquid culture samples were collected daily, centrifuged to remove cells and frozen for substrate utilization assays.

The consumption of oxygen and the production of carbon dioxide were calculated as follows.

$$O_2 consumed(t) = y_{O_2 in}(t) - y_{O_2 out}(t) \qquad \text{eqn. A.3}$$

Where: y_{O2in} = the concentration of oxygen entering the reactor, %,

y_{O2out} = the concentration of oxygen leaving the reactor, %,

$$CO_2\ produced\ (t) = y_{CO_2 out}(t) - y_{CO_2 in}(t) \qquad \text{eqn. A.4}$$

Where: y_{CO2out} = the concentration of carbon dioxide leaving the reactor, %,

y_{CO2in} = the concentration of carbon dioxide entering the reactor, %,

Mass transfer performance of fermenters can be analyzed by comparing the specific oxygen uptake rate, q_{O2} (eqn. A.6). It is a measure of the oxygen required by *A. sarcoides* for growth and product synthesis. It is calculated by dividing the volumetric rate of cell oxygen uptake, N_{O2} (eqn. A.7), by the cell concentration (Doran, 2012).

$$q_{O_2}(t) = \frac{N_{O_2}}{C_{biomass}(t)} \qquad \text{eqn. A.5}$$

Where: q_{O2} = rate of O_2 consumption per gram biomass, %/(g*hr),

N_{O2} = rate of cell oxygen uptake, $\%O_2$/(L*hr)

$C_{biomass}$ = the concentration of biomass in g L^{-1}.

With: $$N_{O_2}(t) = \frac{F * (y_{O_2 in}(t) - y_{O_2 out}(t))}{V} \qquad \text{eqn. A.6}$$

Where: F = flow rate of air through the reactor volume, L/hour,

y_{O2in} = the concentration of oxygen entering the reactor, converted from % in air to gram moles with the ideal gas constant, L*atm/(g moles*K).

y_{O2out} = the concentration of oxygen leaving the reactor, g moles,

V = the volume of liquid culture in the reactor in L.

Due to the large amount of scatter in the oxygen data, average rates of the difference between inlet and outlet measured concentrations were used to calculate N_{O2} for a specific growth period.

Results: Aerobic respiration is clearly seen by *A. sarcoides* in liquid culture. Consumption of O_2 and production of CO_2 (eqn A.3 & A.4) follow a similar trend as shown by Figures A.14 and A.15. The higher values of O_2 consumption, maximum near 0.13 compared with CO_2 production, maximum near 0.095, are expected.

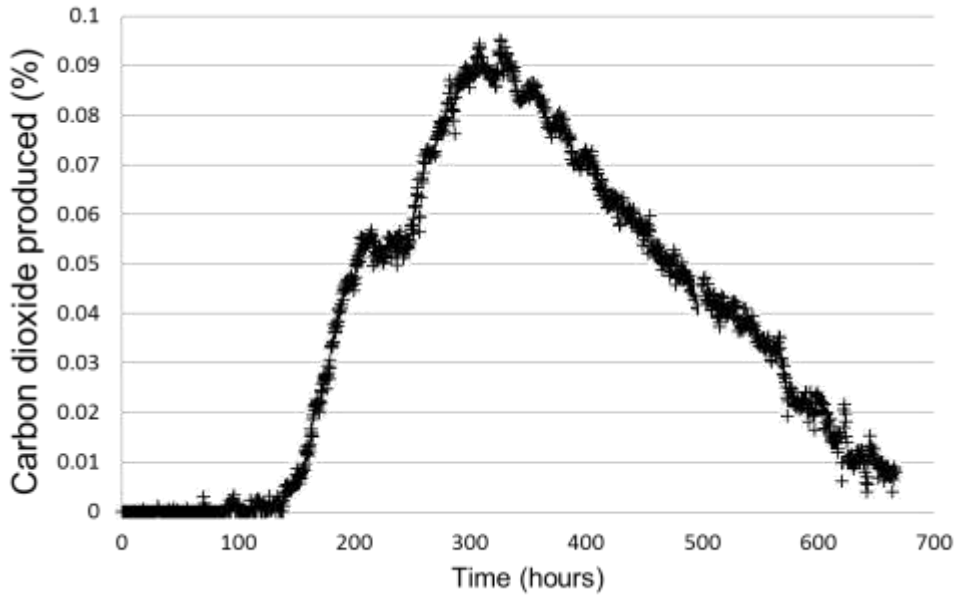

Figure A.14. Carbon dioxide profiles for *A. sarcoides* culture over 28 days in a non-pH controlled Biostat 5 Liter fermentor. Measurements are taken continuously and recorded at 30 minute intervals.

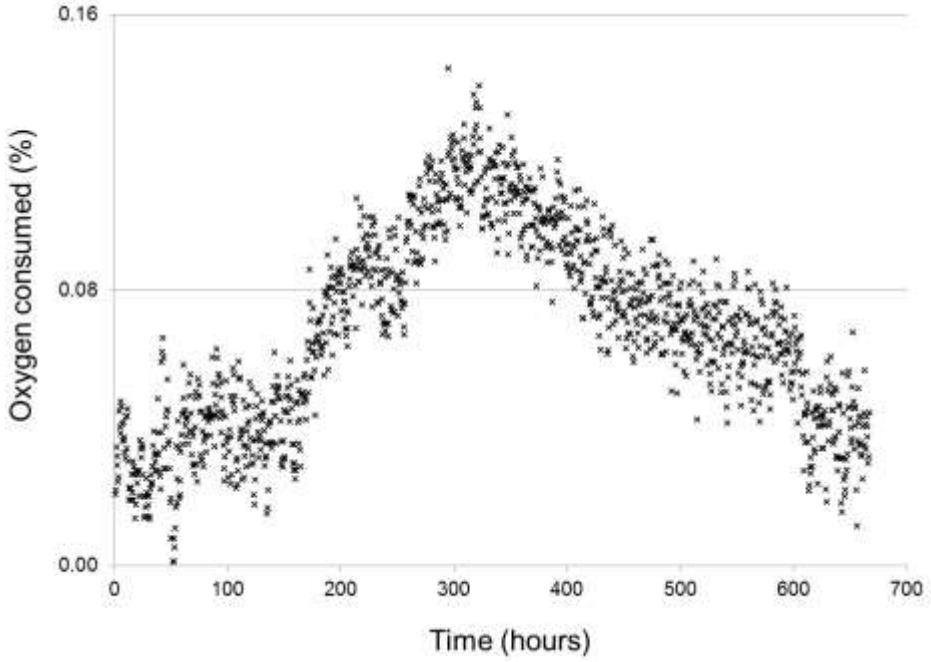

Figure A.15. Oxygen profile for *A. sarcoides* culture over 28 days in a non-pH controlled Biostat 5 Liter fermentor.

To calculate average oxygen consumption rates for comparison between experiments, time periods were chosen which corresponded to specific phases of growth. For the following example, exponential phase and decline phase are used (decline is the transition phase between exponential and stationary phase). The oxygen consumption rates were not constant in exponential phase indicating the reactor was not at steady state.

The entry into decline and stationary phase can be seen by the change in q_{O2} to a near constant value (Figure A.16). In general, the oxygen consumption rates steadily decrease until stationary phase. The specific oxygen consumption rate was higher in exponential phase for all listed cases, which indicated a higher need for oxygen during rapid growth (Table A.6). The highest exponential phase rates were seen in the

uncontrolled pH reactors. For all the reactor runs, pH control lead to a lower oxygen consumption rate versus no pH control, which indicated the organism may experience oxidative stress at the lower pH values.

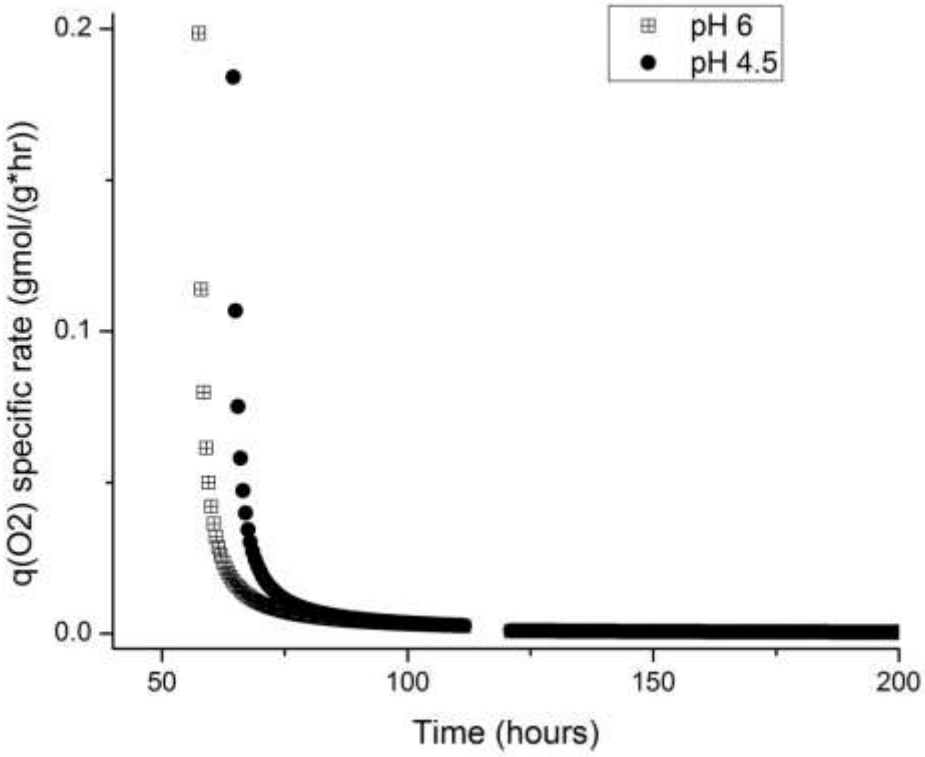

Figure A.16. Specific oxygen consumption rates for *A. sarcoides* grown on glucose at 23^{o}C in Biostat reactors at 2 different pH values.

The respiratory quotient (RQ) is a bioprocess parameter which compares oxygen consumption to carbon dioxide production and reflects the biological state of the culture (eqn. A.7) (Doran, 2012). Oxygen consumption is not necessarily proportional to CO_2 produced, especially when complex metabolic processes could be making biomass or

other products, such as oxygenated HCs. To measure the degree CO_2 produced versus the amount of O_2 consumed, the respiratory quotient can be calculated for each time point (eqn A.8). As the respiratory quotient increases, the amount of CO_2 produced increases compared to the amount of O_2 consumed. For reactors with same starting pH and temperature, but varying stirring rate (Rep 1 was stirred at 300 rpm, while Rep 2 used 250 rpm), the RQ was always higher in the pH controlled reactor (Table A.7). This indicated that less oxygen was needed for respiration at higher pH. As the pH is known to decrease as growth progresses, without pH control, the fungus would have been experiencing a more acidic environment, leading to increased osmotic stress (Figure A.17).

$$RQ = \frac{moles CO_2 produced}{moles O_2 consumed} \qquad \text{eqn. A.7}$$

Table A.6. Specific oxygen consumption rates in gram moles of O_2 per g biomass, per hour (q (O_2)) for 3 Liter *A. sarcoides* cultures grown in Biostat controlled fermenters at 23^{o}C with continuous mixing. The rates are normalized to biomass growth and are listed by growth phase: exponential or decline (median values for exponential phase). Units of q (O_2) are gram moles of O_2 per gram biomass per hour.

pH	pH control	q (O_2) Exponential	q (O_2) Decline
4.5	Y	1.28E-3 ± 9.09E-5	6.88E-4 ± 2.81E-5
5.5	N	2.73E-4 ± 8.28E-5	1.09E-4 ± 2.37E-4
5.5	N	7.58E-4 ± 6.70E-5	2.74E-4 ± 1.82E-5
5.5	Y	1.32E-4 ± 9.82E-5	3.11E-4 ± 5.94E-5
5.5	Y	5.57E-4 ± 6.76E-5	1.53E-4 ± 1.07E-5
6	Y	1.41E-3 ± 9.57E-5	4.19E-4 ± 2.66E-5

Table A.7. Respiratory Quotient (RQ) values for Biostat reactors with 3 liters of *A. sarcoides* culture at 23°C and starting pH of 5.5. Half of the reactors were controlled at pH 5.5 for the duration of the experiment. The RQ values listed are at 48 hours after the entry into stationary phase.

rpm	pH control	RQ
300 rpm	N	0.345
300 rpm	Y	0.594
250 rpm	N	0.594
250 rpm	Y	0.612

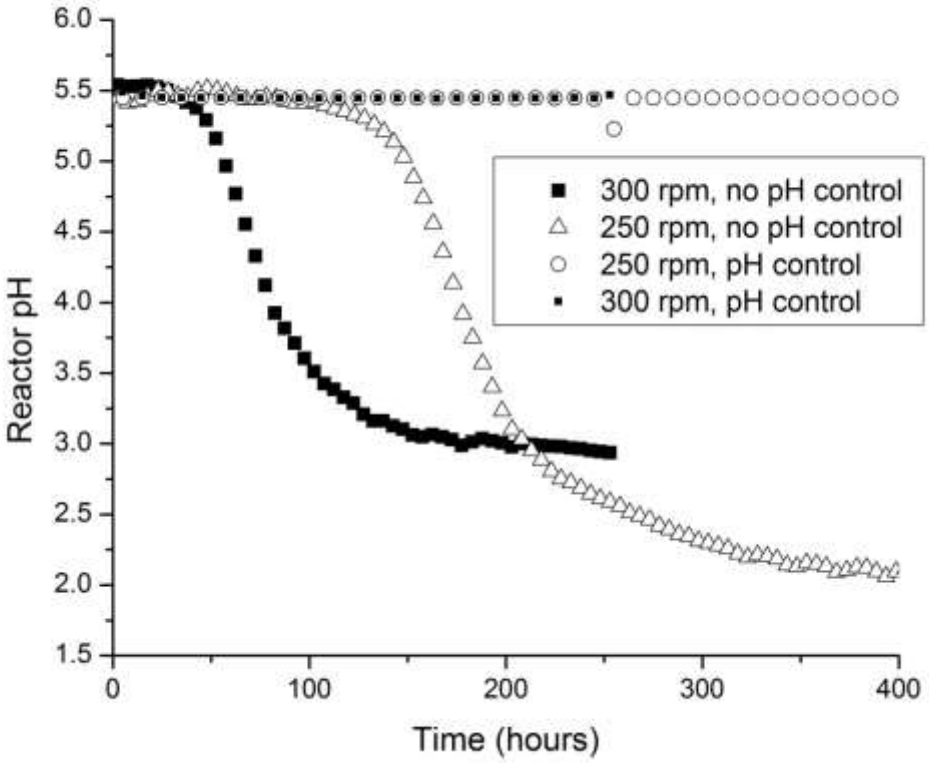

Figure A.17. pH trends for reactor runs represented in Table 7.

Carbon Balance

The respiration analysis allowed an important piece of the carbon balance to be captured, and was used to determine how much carbon consumed was going to biomass, CO_2, and VOC products. Initial work on a carbon balance with glucose suggested a complete balance was a very complex undertaking (eqn. A.88).

$$a(C_6H_{12}O_6) + b(NH_3) + c(O_2) = d(CH_{2.0}O_{0.65}N_{0.16}P_{0.025}) + e(CO_2) + f(H_2O) + g(CH_iO_j) \quad \text{eqn. A.8}$$

With the help of VOC monitoring by proton transfer reaction-mass spectrometry (PTR-MS), a step closer to the carbon balance was achieved. However, the PTR-MS is unable to monitor any compounds with a proton affinity less than water, therefore excluding non-oxygenated alkanes. Based on information in Chapter 2 which showed oxygenated volatiles excluding ethanol and acetaldehyde were much lower in concentration than the ethanol signal, it is reasonable to assume that the total amount of carbon in non-oxygenated alkanes did not exceed that of carbon in ethanol as measured by PTR-MS. This assumption takes into account that the total number of carbon atoms in the alkanes would be on the order of 5 to 15 unlike ethanol which has 2 carbon atoms per compound. A disadvantage to using the PTR-MS is that it does not measure the quantity of compounds produced by the fungus that remain in the liquid phase. Figure A.19 shows the experimental set-up for the PTR-MS with the reactor system.

Methods. *A. sarcoides* was grown in a Biostat B Twin Plus 5-liter jacketed reactor (Sartorius Stedim Biotech) on 2.7 L of 1x AS medium was inoculated with 300 mL of a 7 day old culture grown from a Microbank^{TM} bead frozen stock (-80^{o}C) on 20 g L^{-1} glucose

and 0.5 g L^{-1} yeast extract for a final volume of 3 L. The cultures were grown for a minimum of 110 hours into stationary phase. Stirring rate (250 rpm) and temperature (23^{o}C) were controlled to maintain a constant value. The pH was controlled at 4.5 and 5.5 with with 0.5 M NaOH and 1.0 M HCl when applicable.

The reactor effluent gas was routed to a GMUX 8 multiplexer then to an EGAS-L analyzer unit (both by Sartorius Stedim Biotech). Background concentrations of CO_2 and O_2 were determined from the inlet air stream. The analyzer output data (CO_2 and O_2 mole percent) were recorded by the MCFS Win 2.1 software. A portion of the reactor effluent gas was diverted to the PTR-MS to quantify volatiles from the cultured and un-inoculated controls (Figure A.18).

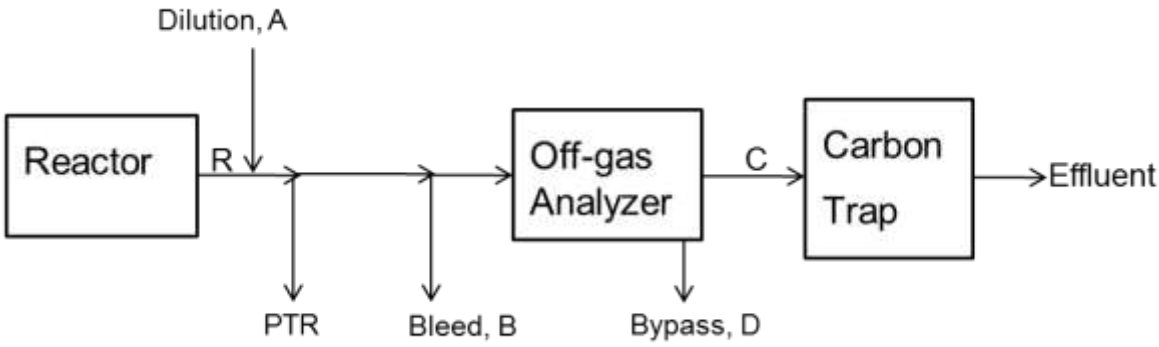

Figure A.18. Schematic of Biostat reactor set-up with PTR-MS and off-gas analyzer used for carbon balance.

The PTR-MS instrument ionized organic molecules in the gas phase through their reaction with H_3O^+, forming protonated molecules (MH^+, where M is the neutral organic molecule) and fragment ions, which were detected by a standard quadrupole mass spectrometer. At times, it was necessary to dilute the reactor gas effluent to lower the

volatile concentrations to within the linear range of the PTR-MS. Therefore, the resulting data for each ion signal were corrected for dilution by equations A.10-A.12.

$$x_{oA}A + x_{oR}R = x_{oPTR}PTR + x_{oB}B + x_{oC}C + x_{oD}D \qquad \text{eqn. A.10}$$

Where: x_o is the concentration of the measured ion in ppbv for each corresponding flow, A is volume of dilution flow in mL/min, and each flow in Figure A.19 is correspondingly labeled by capital letters.

With $x_{oA} = 0$ and $x_{oPTR} = x_{oB} = x_{oC} = x_{oD}$, equation A.10 becomes:

$$R = \frac{x_{oPTR}}{x_{oR}}\left(PTR + B + C + D\right) \qquad \text{eqn. A.11}$$

Rearranging equation A.10, the original concentration of an ion leaving the reactor is:

$$x_{oR} = \frac{x_{oPTR}}{R}\left(PTR + B + C + D\right) \qquad \text{eqn. A.12}$$

Because x_{oA} was not equal to zero for either CO_2 or O_2, the dilution correction equations were slightly different for the CO_2 and O_2 concentrations as follows.

$$x_{oR}R = x_{oPTR}\left(PTR + B + C + D\right) - Ax_{oA} \qquad \text{eqn. A.13}$$

$$x_{oR} = \frac{x_{oPTR}}{R}\left(PTR + B + C + D\right) - x_{oA}\frac{A}{R} \qquad \text{eqn. A.14}$$

Carbon balances (eqn A.9) were completed based on the growth phase of the fungus at the end of exponential phase and at 100 hours into stationary phase. All measured values obtained during the experimentation were converted to molar values. PTR-MS ion signals are recorded in ppbv which is equivalent to 1 nanomole of the ion in

1 mole of air. Using the ideal gas law (eqn A.15) to calculate the total moles of air, the total number of moles for the PTR-MS reactor runs were 0.0521 moles min^{-1}.

$$PV = nRT \qquad \text{eqn. A.15}$$

Where P = 0.8444 atm, T = 296 K, R = .08206 L atm/gmol K, V = 1.5 L

For each individual ion, the number of carbon moles is specific to the number of carbon molecules in the compound (eqn A.16).

Ion signals in ppbv were converted to carbon moles as follows:

$$\text{ion}_i = \text{ppbv} * 10^{-9} * n \frac{\text{Cmoles}}{\text{ion mole}} \qquad \text{eqn. A.16}$$

Where ion_i = the number of carbon moles of ion i,

ppbv = the signal measured by the PTR-MS for ion i,

n = total moles of air (above) in moles min^{-1}.

Cmoles/ion mole = the number of carbon atoms in a molecule of ion i.

To calculate the total moles for the entire signal (eqn A.17), a conservative estimate was made with Cmoles/ion mole equal to 2. This is because the majority of the PTR-MS ion signal was dominated by acetaldehyde and ethanol, both of which have 2 carbons. The result underestimated the total carbon moles, because the remainder of volatiles had carbon lengths ranging from C_2 to C_{15}. The conservative number was chosen to prevent overestimation of volatiles which could not be scientifically defended.

$$\sum_{i=1}^{n} \text{ion} = \sum_{i=1}^{n} \left[\text{ion}_i \left(t_i - t_{i-1}\right)\right]_n \qquad \text{eqn. A.17}$$

Where n = the total number of ions detected and t = time in minutes.

The ideal gas law (equation A.15) was also used to convert CO_2 and O_2 percent concentration in air to mole with P = 1 atm, T = 296 K, R = 82.06 mL atm/gmol K, V_{CO2} $=\Delta CO_2$*flow, with ΔCO_2 = (%CO_2out- %CO_2in), V_{O2} $=\Delta O_2$*flow, with ΔO_2 = (%O_2in-%O_2out), and flow = 1500 mL/min. It then follows that the total number of CO_2 moles produced and the total number of O_2 moles consumed are:

$$\sum n = \sum \frac{PV}{RT} \Delta t \qquad \text{eqn. A.18}$$

With Δt = 30 minutes for off-gas analyzer reporting frequency.

Biomass concentrations were converted to moles with eqn A.19 below.

$$bm(Cmoles) = \frac{bm}{MW} V_{reactor} \qquad \text{eqn. A.19}$$

Where bm = biomass in grams per liter,

MW = molecular weight of biomass at 27.399 g/mole based on

$CH_{2.0}O_{0.65}N_{0.16}P_{0.025}$ from elemental analysis of biomass grown on glucose,

Vreactor = volume of the reactor in liters.

There is one carbon atom per biomass molecule, so the number of biomass moles is equivalent to the number of biomass carbon moles. Glucose concentrations were converted from gram moles to carbon moles using 6 carbon moles per gram mole of glucose.

Results. As a total percentage of carbon, the VOC measured by PTR-MS were less than 1% of the total consumed carbon in the form of glucose (Table A.8). This small percentage makes sense considering the theory behind endophytic symbiosis with the

host plant would not encourage high levels of production. In most experiments, VOC were not measured by PTR-MS, so the unknown category included potential VOC and liquid-bound products. Two time points were calculated separately as shown in Table A.8, the first is the end of exponential phase and the second listed is 100 hours into stationary phase.

Overall, there is a large amount of missing carbon (unknown) which could be attributed to incorrect biomass or CO_2 measurements or liquid bound products such as acetic acid and ethanol which were not measured in these cases. Of the known measurable carbon metabolism byproducts, biomass ranged from 9% up to 35% of input carbon, with CO_2 ranging from 7% to 42% of the total input carbon. In general, the total carbon accounted for by CO_2 increased at the stationary phase time point, leaving less carbon for the unknown or potential products category and indicating possibly greater percentage of VOC production near the end of exponential phase.

Table A.8. Percentages of carbon accounted for by known products: CO_2, biomass and VOC. Values are listed as end of exponential phase (Exp) followed by within 100 hours of stationary phase (Stat). VOC are measured in the effluent gas stream not including non-oxygenated hydrocarbons. The unknown category is the remainder of the balance.

	Source of Carbon (%)							
	CO_2		**Biomass**		**VOC**		**Unknown**	
pH condition	**Exp**	**Stat**	**Exp**	**Stat**	**Exp**	**Stat**	**Exp**	**Stat**
4.5 control	16.7	42.0	27.4	35.0	0.13	0.41	55.8	22.6
5.5 control	16.4	17.3	19.9	14.1			63.7	68.6
5.5 control	11.5	6.6	8.9	8.9			79.6	84.5
5.5 starting	8.6	18.7	14.6	15.2			76.9	66.1
5.5 starting	11.9	26.8	15.1	26.6			73.0	63.9

The pH 4.5 condition had the lowest percentage of unknown carbon in both the exponential and stationary phase, and it is the one condition where volatiles were measured with the PTR-MS. Due to the higher percentage of unknown carbon at the 5.5 pH condition, it is possible *A. sarcoides* could have produced a higher percentage of VOC. However, this was not completed considering the expense associated with the PTR-MS and the likely low yield improvements.

The monitoring with PTR-MS allowed for a continuous carbon balance to be completed over the growth cycle of *A. sarcoides*. Figure A.19 shows data for the total carbon moles consumed or produced at given time, and the inset shows the carbon moles of biomass on a log scale for comparison with growth phase. The unaccounted for carbon is represented by the difference between the dotted line representing the total carbon input and the line noting the total carbon known including carbon input in the form of glucose and carbon output. This difference could be from liquid-bound products or from alkanes and alkenes not measured by the PTR-MS. Measuring 90% of the total carbon in an experimental system is a reasonable result, so the unmeasured potential of VOC production by *A. sarcoides* can be considered to be approximately 10% less the difference shown in Figure A.19. The total percentage of VOC was constantly below 1% for the entire growth cycle and did not change significantly based on growth cycle (Figure A.19 inset). From the unaccounted carbon, the greatest product potential from unmeasured carbon corresponds to growth during late stationary and early exponential phase (Figure A.19 inset).

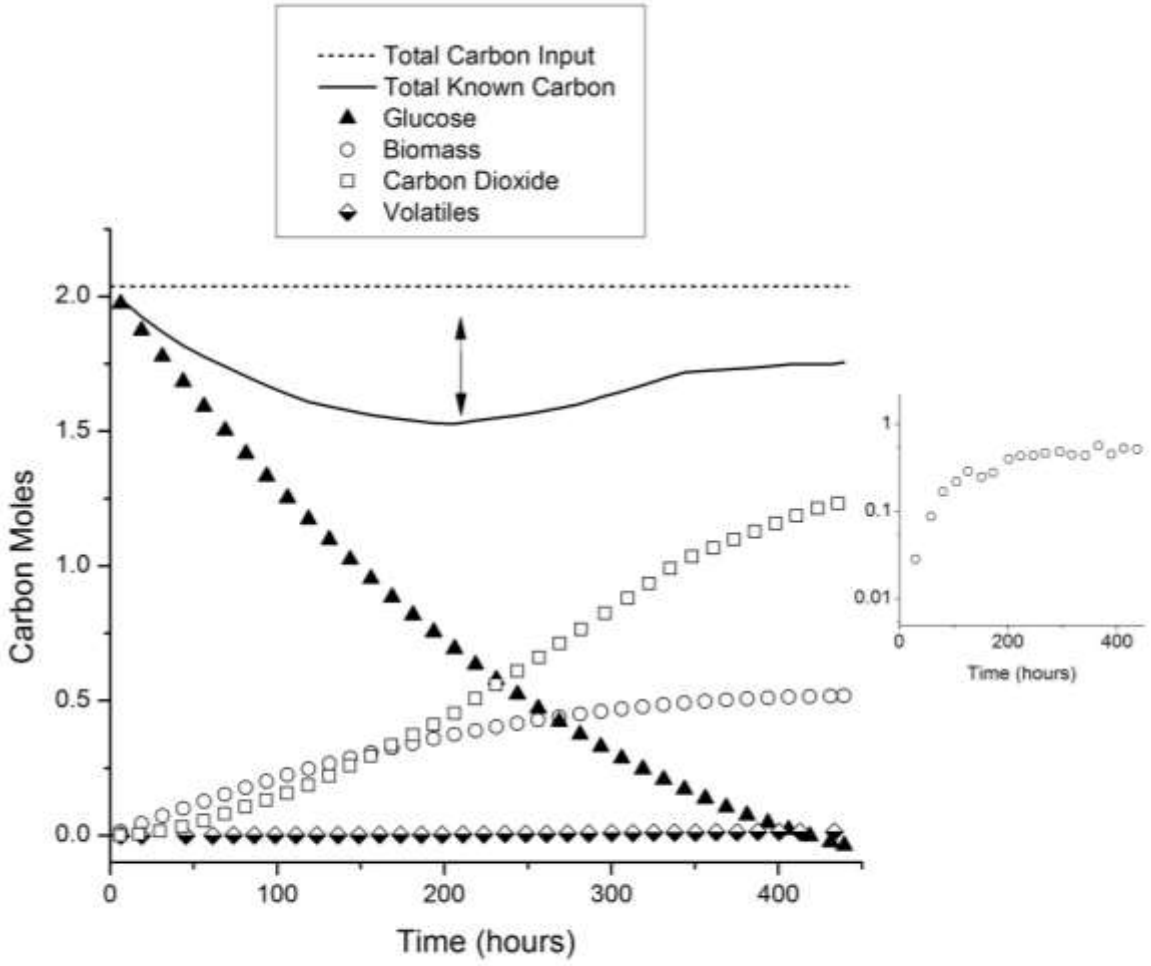

Figure A.19. Completed carbon balance including glucose consumption, biomass, CO_2, and volatile compound production at 23°C, pH 4.5. Difference between total carbon input and known carbon captures the potential of liquid-bound products and volatile alkanes and alkenes not measure.

Conclusions

The results summarized here formed a foundation for future work on this project. A minimal medium recipe was developed for submerged liquid culture work with *A. sarcoides* that used NH_4Cl as the nitrogen source and included micronutrient salts such as

$Ca(NO_3)_2 \cdot 4H_2O$, KCl, KNO_3, $FeCl_3$, $MnCl_2$, $ZnSO_4$, H_3BO_3, and KI. A well-defined medium with trace salts and supplementation with additional phosphate increased biomass accumulation from 0.5 g/L to 4.6 g/L. The culture growth rate and final biomass concentration were improved by altering two system parameters, culture pH and medium nutrient levels.

The maximum specific growth rates of *A. sarcoides* were fastest on glucose at 0.085 ± 0.035 hr^{-1}, and about half that of glucose on CMC at 0.039 ± 0.003 hr^{-1}, and even lower on cellulose microcrystalline powder at 0.014 ± 0.003 hr^{-1}. A significant difference in growth rate based on the starting pH of the culture medium was not seen, though slightly higher rates were seen for sealed batch headspace conditions versus aerobic. Inhibitory growth effects were seen at starting pHs of 3 and 7. In general, *A. sarcoides* behaved as expected: typical growth curve without diauxic growth, respiration rates were higher in exponential phase than stationary phase.

Aerobic respiration by *A. sarcoides* grown on glucose with a steady supply of air was demonstrated with a higher rate of O_2 consumption versus CO_2 production. The highest specific oxygen consumption rates were seen in the pH controlled experiments. The respiratory quotient for batch reactor growth showed less oxygen was needed for respiration in the controlled pH environments which keep the pH at 4.5 or above, indicating stress at the lower pH values. The total VOC measured from growth on glucose were less than 1% of the total consumed carbon.

APPENDIX B

TABLULATED DATA

Chapters 2-4

Table B.1: Data for Figure 2.1 left-hand y-axis PTR-MS (ppbv) is included in the Supplementary File as table is too large for this document.

Table B.2: Data for Figures 2.1 right-hand y-axis & 2.2 y-axis

SPME response in µg/mL

Time (hours)	Acetaldehyde	Benzaldehyde	Ethanol	Nonanal	1-Octen-3-ol	1-Butanol, 3-methyl
0	1.8	1046.5	N/A	49.9	559.1	33.7
1	2.09	1401.5	N/A	25.6	781.2	42.5
2	2.50	1367.4	N/A	16.7	813	38.9
3	2.50	1391	N/A	11.5	762.9	44
6	2.24	1297.3	N/A	13.9	678.3	44.1
12	2.47	1273.6	N/A	2.5	692.1	45.4
24	1.83	976.1	N/A	8.9	432.9	57.8
36	1.84	682.4	N/A	2.4	237.6	72.8
48	2.41	411.55	N/A	1	120.7	78.4

Table B.3: Data for Figure 2.2 x-axis.

	PTR-MS response in ppbv (6 min averages)					
Time (hours)	Acetaldehyde	Benzaldehyde	Ethanol	Nonanal	1-Octen-3-ol	1-Butanol, 3-methyl
0	3075.8	2555.0	351.5	1017.3	1219.5	953.4
1	3222.3	2389.8	288.1	276.3	1108.7	911.8
2	2989.6	2304.4	285.9	102.5	1060.5	887.0
3	2724.8	2195.3	279.9	38.1	1009.1	861.4
6	2028.7	1948.3	261.5	7.1	872.5	776.5
12	1192.2	1593.3	247.6	3.7	647.9	710.7
24	426.7	1066.3	237.5	2.3	372.8	608.6
36	142.7	758.2	205.8	1.9	201.2	484.8
48	50.8	511.0	196.8	1.4	115.8	399.3

Table B.4: Data for Figure 2.3 left-hand y-axis PTR-MS (ppbv) is included in the Supplementary File as table is too large for this document.

Table B.5: Data for Figure 2.3 right-hand axis.

Time (hours)	Biomass Cell Dry Weight (g/L)
0	0.00762
29.4	0.2447
58	0.7682
80.4	1.48563
105.5	1.95176
126.5	2.56747
151.1	2.24728
172.3	2.5133
201.2	3.62342
222.9	3.96071
246.7	4.02025
268.3	4.35338
294.9	4.52264
316.9	4.19602
341.3	4.12937
366.2	5.40462
389.4	4.32044
411.7	5.08155
436.8	5.01869

Table B.6: Data for Figure 2.4 (right-hand y-axis).

	SPME response (µg/mL)						
Time (hours)	benzaldehyde	1-octen-3-ol	acetaldehyde	3-methyl butanol	nonanal	3-methyl butanoic acid	Ethanol
57	0	0	0	14.4	0	0	12.9
125.5	48.92	0.8	0	22.57	0	0	19.67
171.3	54.65	1.27	9.42	37.81	0	0	20.09
221.9	33.69	2.22	0	53.28	0	0	25.09
267.3	61.97	7.15	0	112.83	0.84	0	40.64
315.9	125.64	7.69	0	87.53	6.09	1.28	37.52
410.7	78.34	14.6	0	115.31	8.07	3.5	32.51
460.2	97.29	15.46	0	103.24	5.4	5.16	22.38

Left y-axis PTR-MS data is included in the Supplementary File as table is too large for this document.

Table B.7: Data for Figure 3.3

Chemical Classification	Growth Substrate			
	Cellulose	Cellulose*	PDB	Glucose
Alkane	8	4	6	5
Alkene	2	3	3	3
Aldehyde	1	5	0	0
Ketone	2	4	2	0
Aromatic	6	4	14	2
Alcohol	3	6	2	1
Acid	6	4	1	3
Ester	7	15	9	3

Table B.8 Data for Figure 3.4

Formula of compounds identified in each chemical classification

Alkane	Alkene	Aldehyde	Ketone	Aromatic	Alcohol	Acid	Ester
C11H22	C10H16	C11H20O	C11H22O	C10H14	C10H22O	C2H4O2	C10H12O2
C11H24	C8H14	C5H10O	C7H14O	C10H16	C5H12O	C4H8O2	C10H18O2
C12H26	C8H16	C7H12O	C8H16O	C6H4Cl2	C5H12O	C4H8O2	C10h20O2
C12H26	C9H16	C7H14O	C8H16O	C7H5N	C5H12O	C5H10O2	C10H20O2
C15H32		C9H14O	C9H18O	C7H8O	C6H14O		C10H20O2
C19H40		C9H16O		C8H10	C6H14O		C11H22O2
C5H12				C8H10O	C8H16O		C10H20O2
C6H12				C9H14O			C12H22O2
C7H16				C9H14O			C15H27Cl3O2
							C16H16O2
							C7H14O2
							C7H14O3
							C8H16O2
							C8H16O2
							C9H10O2
							C9H10O2
							C9H18O2

Table B.9 Data for Figure 4.1 Optical Density at 600 nm (n = 9) with standard deviations.

	7% Oxygen		10% Oxygen		21% Oxygen	
Time (hours)	C:N 10	C:N 100	C:N 10	C:N 100	C:N 10	C:N 100
0	0.090±1.7E-17	0.089±0.006	0.090±0.001	0.097±0.001	0.088±0.007	0.088±0.012
16.7	0.104±0.010	0.097±0.009	0.116±0.012	0.115±0.014	0.114±0.009	0.102±0.012
22.7	0.095±0.004	0.092±0.004	0.124±0.007	0.133±0.006	0.127±0.008	0.120±0.009
28.7	0.095±0.008	0.095±0.009	0.139±0.014	0.145±0.011	0.136±0.009	0.144±0.008
40.8	0.097±0.011	0.095±0.009	0.248±0.033	0.201±0.017	0.254±0.016	0.225±0.014
52.8	0.103±0.008	0.097±0.012	0.317±0.035	0.299±0.022	0.401±0.027	0.335±0.035
65.0	0.106±0.013	0.101±0.007	0.444±0.090	0.407±0.057	0.521±0.059	0.477±0.057
76.9	0.109±0.008	0.106±0.006	0.508±0.041	0.511±0.034	0.625±0.055	0.577±0.023
88.8	0.110±0.009	0.108±0.006	0.547±0.027	0.523±0.037	0.637±0.061	0.618±0.038
94.8			0.554±0.070	0.540±0.042	0.622±0.054	0.616±0.056
100.7	0.109±0.008	0.109±0.005	0.523±0.033	0.562±0.066	0.681±0.046	0.625±0.050
111.9	0.113±0.009	0.122±0.011	0.559±0.039	0.555±0.066	0.722±0.050	0.688±0.023

Table B.10 Data for Figure 4.2 (n=3)

Starting O_2 concentration	7%		10%		21%	
Carbon:Nitrogen Ratio	Maximum Specific Growth Rate (hr^{-1})	Standard Deviation	Maximum Specific Growth Rate (hr^{-1})	Standard Deviation	Maximum Specific Growth Rate (hr^{-1})	Standard Deviation
C:N 10	0.00317	0.0017	0.0545	0.00872	0.07487	0.02536
C:N 100	0.0017	0.00101	0.02763	6.51E-04	0.06187	0.01973

Table B.11 Data for Figure 4.3 (n=9)

Starting O_2 Concentration	7%		10%		21%	
Carbon:Nitrogen Ratio	Nitrogen consumption (mM N)	Standard Deviation	Nitrogen consumption (mM N)	Standard Deviation	Nitrogen consumption (mM N)	Standard Deviation
C:N 10	1.71429	0.23853	5.11111	0.65385	2.63492	0.77059
C:N 100	0.57302	0.06442	2.11587	0.06098	1.89683	0.04501

Table B.12 Data for Figure 4.4A (n=3)

Starting O_2 Concentration	7%		10%		21%	
Carbon:Nitrogen Ratio		Standard Deviation	Nitrogen consumption (mM N)	Standard Deviation	Nitrogen consumption (mM N)	Standard Deviation
C:N 10	1.71429	0.23853	5.11111	0.65385	2.63492	0.77059
C:N 100	0.57302	0.06442	2.11587	0.06098	1.89683	0.04501

Table B.13 Data for Figure 4.4B (n=3)

Starting O_2 Concentration	7%		10%		21%	
Carbon:Nitrogen Ratio		Standard Deviation	Nitrogen consumption (mM N)	Standard Deviation	Nitrogen consumption (mM N)	Standard Deviation
C:N 10	1.71429	0.23853	5.11111	0.65385	2.63492	0.77059
C:N 100	0.57302	0.06442	2.11587	0.06098	1.89683	0.04501

Table B.14 Data for Figure 4.5A (n=6)

Starting O_2 Concentration	7%		10%		21%	
Carbon:Nitrogen Ratio	Acetate concentration (mM)	Standard Deviation	Acetate concentration (mM)	Standard Deviation	Acetate concentration (mM)	Standard Deviation
C:N 10	2.00448	0.47895	0.65312	0.54806	0	0
C:N 100	2.23571	0.08971	1.37752	0.45055	0	0

Table B.15 Data for Figure 4.5B (n=6)

Starting O_2 Concentration	7%		10%		21%	
Carbon:Nitrogen Ratio	Ethanol concentration (mM)	Standard Deviation	Ethanol concentration (mM)	Standard Deviation	Ethanol concentration (mM)	Standard Deviation
C:N 10	0.9931	0.30728	0.17407	0.06304	0	0
C:N 100	1.23565	0.09805	0.50846	0.18598	0	0

Table B.16 Data for Figure 4.8A (n=2)

Starting O_2 Concentration	10%		21%	
Carbon:Nitrogen Ratio	Neutral Lipids (w/w biomass)	Standard Deviation	Neutral Lipids (w/w biomass)	Standard Deviation
C:N 10	3.50703	0.68356	2.01683	0.54882
C:N 100	3.9333	0.64601	1.91712	0.41184

Table B.17 Data for Figure 4.8B (n=2)

Starting O_2 Concentration	10%		21%	
Carbon:Nitrogen Ratio	FAME (w/w biomass)	Standard Deviation	FAME (w/w biomass)	Standard Deviation
C:N 10	7.50946	0.93754	4.06271	0.29633
C:N 100	7.41341	1.51843	3.3372	1.12109

Appendix A

Table B.18 Data for Table A.1

Medium (20 g/L carbon source with 0.5g/L YE)	Liquid Growth (OD_{600})
Cellobiose	0.062
Glucose	0.534
Maltose	0.011
Sucrose	0.020
Xylose	0.015

Table B.19: Data for Table A.2

Nitrogen Source	Glucose (OD_{600})	Cellobiose (OD_{600})
Casamino acids	0.550	
Glycine	0.101	
Potassium nitrate	0.068	
Ammonium chloride	0.161	
Ammonium sulfate	0	0
Yeast extract	0.740	0.384

Table B.20: Data for Figure A.4 (n=2).

	A		B		C		D		F	
Time (days)	Cell Dry Weight (g/L)	Standard Deviation	Cell Dry Weight (g/L)	Standard Deviation	Cell Dry Weight (g/L)	Standard Deviation	Cell Dry Weight (g/L)	Standard Deviation	Cell Dry Weight (g/L)	Standard Deviation
8	0.58	0.103	2.73	0.275	0.589	0.013	2.72	0.062	0.58	0.299
14	0.70	0.041	4.65	0.185	0.67	0.027	4.60	0.202	0.70	0.348

Table B.21: Data for Figure A.5 (n=1).

	No buffer	pH 7	pH 4
Time (hours)	Cell Dry Weight (g/L)	Cell Dry Weight (g/L)	Cell Dry Weight (g/L)
0	0.01454	0.0218	0.0218
21	0.0234	0.00735	0.03103
44.7	0.09667	0.00847	0.11748
74.4	0.16353	8E-4	0.1995
94.2	0.18267	0.0047	0.21997
118.2	0.1962	0.00867	0.26143
142.2	0.2096	0.0196	0.2682
166.7	0.24907	0.00843	0.3034
190.95	0.2914	0.00623	0.29787

Table B.22: Data for Figure A.6 (n=3).

	pH 3		pH 4		pH 5		pH 6	
Time (hours)	Cell Dry Weight (g/L)	Standard Deviation	Cell Dry Weight (g/L)	Standard Deviation	Cell Dry Weight (g/L)	Standard Deviation	Cell Dry Weight (g/L)	Standard Deviation
190.95	1.72	0.038	3.00	0.099	2.67	0.073	1.99	0.163

Table B.23: Data for Figure A.8 (n=3).

	pH 3		pH 4		pH 5		pH 6	
Time (days)	pH	Standard Deviation	pH	Standard Deviation	pH	Standard Deviation	pH	Standard Deviation
0	3.1	0	4.1	0	5.06	0	6.05	0
2	3.65	0	4.50	0.0057	5.44	0.0057	6.26	0.0057
4	3.62	0.0057	4.43	0.02	5.35	0.0141	6.22	0.01
7	3.44	0.0144	4.04	0.0519	4.82	0.0353	5.16	0.0608
9	3.32	0.0057	3.77	0.0346	4.38	0	4.41	0.1001
11	3.25	0.01	3.61	0.0208	4.04	0.0283	3.63	0

Table B.24: Data for Figure A.8 (n=1).

	NH_4Cl	NH_4Cl + YE	Amm Tart	Amm Tart + YE
Time (hours)	pH	pH	pH	pH
0	6.15	5.95	6.09	6.09
22.7	6.08	5.6	6.04	6.06
42.2	5.04	5.14	6.04	6.04
72.2	4.74	4.09	5.99	5.96
93.2	4.32	3.77	5.94	5.76
108.7	3.91	3.49	5.88	5.48
138.7	3.73	3.44	5.83	5.41
158.7	3.73	3.36	5.71	5.32
182.5	3.56	3.29	5.62	5.26
209.5	3.52	3.26	5.55	5.21

Table B.25: Data for Figure A.9 (n=3).

	Light (14:10)		Dark	
Time (Days)	Cell Dry Weight (g/L)	Standard Deviation	Cell Dry Weight (g/L)	Standard Deviation
6	1.495	0.032	1.451	0.043
8	2.093	0.048	2.129	0.180

Table B.26: Data for Figure A.11 (n=3).

	CMC			Cellulose	
Time (hours)	Cell Protein (mg/mL)	Standard Deviation	Time (hours)	Cell Protein (mg/mL)	Standard Deviation
0	0.067	0.005	0	0.138	0
16.7	0.087	0.007	23	0.145	0.003
22.7	0.097	0.006	28.5	0.1598	0.007
28.7	0.103	0.007	48.5	0.183	0.012
40.75	0.194	0.012	74.5	0.351	0.046
52.8	0.305	0.020	97.5	0.493	0.006
65.03	0.397	0.045	121.5	0.749	0.038
76.92	0.476	0.042	145.5	0.841	0.065
88.76	0.486	0.046	168.25	0.930	0.017
94.75	0.474	0.0411	216.25	0.962	0.090
100.67	0.519	0.035	243.5	0.756	0.076
111.92	0.550	0.038	266.5	0.699	0.166
144.33	0.546	0.005	290.5	0.751	0.076
168.42	0.584	0.105			
193.17	0.527	0.015			

Table B.27. Data for Figure A.12 (n=3 or more).

13°C	pH 3.5		pH 6.5	
Oxygen Condition	Growth Rate (1/hr)	Standard Deviation	Growth Rate (1/hr)	Standard Deviation
Aerobic	0.05355	0.03514	0.0318	0.00806
Sealed Batch	0.0684	0.02164	0.0593	0.03125
Anoxic	0.0626	0.00905	0.0596	0.01315

Table B.28. Data for Figure A.12 (n=3 or more).

20°C	pH 3.5		pH 5		pH 6.5	
Oxygen Condition	Growth Rate (1/hr)	Standard Deviation	Growth Rate (1/hr)	Standard Deviation	Growth Rate (1/hr)	Cell Dry Weight (g/L)
Aerobic	0.02202	0.01715	0.03727	0.00554	0.03395	0.00679
Sealed Batch	0.075	0.00184	0.0642	0.00622	0.0675	0.01287
Anoxic	0.06275	0.01379	0.06557	0.01	0.05995	0.01266

Table B.29. Data for Figure A.12 (n=3 or more).

28°C	pH 3.5		pH 6.5	
Oxygen Condition	Growth Rate (1/hr)	Standard Deviation	Growth Rate (1/hr)	Standard Deviation
Sealed Batch	0.06835	0.02242	0.06885	0.01973
Anoxic	0.06395	0.01011	0.05845	0.0152

Table B.30 Data for Figure A.14. (See Supplementary File as table is too large for this document.)

Table B.31 Data for Figure A.15. (See Supplementary File as table is too large for this document.)

Table B.32 Data for Figure A.16. (See Supplementary File as table is too large for this document.)

Table B.33 Data for Figure A.17. (See Supplementary File as table is too large for this document.)

Table B.34 Data for Figure A.19. (See Supplementary File as table is too large for this document.)